

## MASTER

### Implementation of distributed generation in the Dutch LV network towards a self-supporting residential area

Mes, M.

*Award date:*  
2008

[Link to publication](#)

#### **Disclaimer**

This document contains a student thesis (bachelor's or master's), as authored by a student at Eindhoven University of Technology. Student theses are made available in the TU/e repository upon obtaining the required degree. The grade received is not published on the document as presented in the repository. The required complexity or quality of research of student theses may vary by program, and the required minimum study period may vary in duration.

#### **General rights**

Copyright and moral rights for the publications made accessible in the public portal are retained by the authors and/or other copyright owners and it is a condition of accessing publications that users recognise and abide by the legal requirements associated with these rights.

- Users may download and print one copy of any publication from the public portal for the purpose of private study or research.
- You may not further distribute the material or use it for any profit-making activity or commercial gain

# Implementation of Distributed Generation in the Dutch LV Network

Towards a Self-Supporting Residential Area

**Date: 30-06-2008**

Prepared by:  
M.Mes

Prepared for:  
Dr. Ir. G.M.A. Vanalme  
Dr. Ir. J.M.A. Myrzik  
Ir. M. Bongaerts  
Dr. Ir. G.J.P. Verbong  
Prof. Ir. W.L. Kling

**Continuon**  
Netbeheer

**TU/e** Technische Universiteit  
Eindhoven  
University of Technology



## Preface

It took four years to get my bachelor degree in Innovation Science. Even though the variety of disciplines and branches of knowledge within the bachelor stage stimulated me, it was time to specialize. The subjects chosen so far had been in line of energy technology and it seemed I was highly interested in this field. The master Sustainable Energy Technology gave me the opportunity to go deep into that subject. Since it is in my nature to take up challenges I switched faculties within the university and started my adventure at the department of Electrical Engineering, Electrical Power Systems to be exact. It turned out that this field of knowledge perfectly matched with the bachelor degree in Innovation Sciences, since next to technical subjects also complex social structures are involved in the electrical infrastructure of today and the future. In the meantime I attended the electrical refresher courses. And finally finished off with a graduation project concerning universal knowledge.

Johanna Myrzik has been very supporting throughout the past years, helping me with the subjects chosen for my graduation, my internship in Brussels and my final graduation project at the network operator Continuon. And there I was, one day a week at Continuon in Arnhem. It was hard getting used to get up at half past six in the morning hoping I was not to be held up by the railways. Sometimes I could already see the building when I looked through the window for half an hour imprisoned by the train. Nonetheless, when I did reach Arnhem, Martijn Bongaerts always gave me a warm welcome. Of course Martijn was a busy man and while listening to Classic fm his telephone rang constantly. Or should I say that the radio was ringing constantly? What an awful noise came out of that little radio, while there wasn't even a peep out of the telephone yet. I could not avoid overhearing the conversations over the phone, but it was even harder not to interfere with the meetings in 'our' office. Talking about the office, we have moved three times. Luckily I didn't get lost, although I always walked the wrong direction after getting a cup of coffee or after I 'powdered my nose'.

It has been a lovely year. I worked very hard. I even used two computers, one I used for calculations and on the other one I wrote my report simultaneously. (This was also because my new computer with Vista was not compatible with the simulation program.) Many people have helped me with this graduation project. Greet Vanalme has been very kind getting me all the information I needed. Jos Blom (Continuon) helped me get heat demand profiles and bothered me with difficult questions, that were of course for my own good. Without Frans Provoost (Nuon) and Jasper Frunt (TU/e) I wouldn't have managed to use the simulation program. They certainly have spent much time on me. It has been a pleasure to work with Michiel van Lumig (Laborelec) again, a former fellow student. Pieter Siekman (Nuon), Bart Verhelst (Howest), Jan Willem Turkstra (Gasunie) and Gerrit Jan Ruijg (ECN) explained me the workings of the combined heat and power, whereas Elena Lomonova (TU/e), Bart Gysen (TU/e), Jan Bozelie (Nuon) and Graham Roberts (Microgen-engine) have tried to explain me the characteristics of the linear generator. Like a preface becomes, I'd like to thank these people and I promise them that I will dedicate the acquired knowledge to a sustainable environment.

For me the graduation-marathon is come to an end. The final bits and pieces have been squeezed out of me, step by step I've come closer to the finish and now you may have the privilege to read my report.

# Content

Preface.....	1
1. Summary .....	4
2. Introduction.....	8
<b>Part A: Background Information</b>	
3. New Scenario of Distributed Generation .....	10
3.1 Opportunities.....	10
3.2 Challenges for the network operator .....	11
3.3 Alternative Operational Approach.....	13
<b>Part B Case Study Approach</b>	
4. The Integrated System.....	15
4.1 The low voltage network.....	16
4.2 The Generators .....	17
4.2.1 Stirling Engine Combined Heat and Power.....	17
4.2.2 Photovoltaic Arrays.....	18
4.3 Battery energy storage.....	18
5. The Scenarios.....	20
6. The Energy Balance .....	23
6.1 Demand-Side .....	23
6.2 Supply-Side .....	23
6.2.1 Heat Supply .....	24
6.2.2 Electricity Supply .....	24
6.3 Battery Energy Storage .....	26
7. The Assessment.....	27
<b>Part C: Case Study Results</b>	
8. The Energy Balance .....	29
8.1 Demand-Side .....	29
8.1.1 Heat Demand.....	29
8.1.2 Electricity Demand.....	34
8.1.3 Heat and Electricity Demand Profiles .....	35
8.2 Supply-Side .....	36
8.2.1 Heat Supply .....	37
8.2.2 Results Heat Supply .....	40
8.2.3 Electricity Supply .....	42
8.2.4 Results Electricity Supply .....	45
8.3 Battery Energy Storage .....	47

8.3.1 Peak Power .....	48
8.3.2 Capacity.....	49
9. The Assessment.....	52
9.1 Reversed power flow .....	53
9.2 System Losses .....	54
9.3 Voltage levels .....	55
9.4 Transformer loads.....	57
10. Discussion .....	58
10.1 Generator Control.....	58
10.2 Storage Control .....	59
10.3 Increase photovoltaic power.....	60
10.4 Question Marks .....	61
11. Conclusion .....	62
12. Recommendations.....	64
References.....	65
Nomenclature.....	67
Appendices	
Appendix A Demand-Side .....	68
Appendix A1 Heat Demand .....	68
Appendix A2. Electricity Demand .....	68
Appendix A3. Sources Demand Surveys .....	69
Appendix B (Heat-)Power Balance.....	69
Appendix C. Electrical Power Profiles Detached House.....	70
Appendix D Vision Macro .....	73
Appendix E Battery Energy Storage .....	76
Appendix E.1 Average scenario in January.....	76
Appendix E2 Average scenario in April.....	77
Appendix E3 Average scenario in July .....	78
Appendix E4 Average scenario in October .....	79
Appendix F Reverse Power flow .....	80
Appendix G Voltage levels .....	80



# 1. Summary

The self-supporting residential area is seen as an alternative operational approach of the power supply system. The intention of the new approach is to exploit the advantages of distributed generation and avoid the problems, that come with distributed generation when implemented in the distribution network, by balancing power supply and demand efficiently in close proximity to each other in the low voltage network so that it can easily be controlled and isolated from the upper grid. This case study verifies statements about the alternative operational approach by calculating reversed power flows; voltage levels, system losses, cable and transformer loads of a well-designed self-supporting residential area in the low voltage (LV) network containing combined heat and power (CHP), photovoltaic (PV) arrays and storage devices with a simulation program called ‘Vision Network Analysis’

Part A: The new scenario of distributed generation

- *Section 3.1: The Opportunities*

The architecture of the electrical network developed over the past century is based on the concept that the power supply is based on very large central power plants [16]. Over the last years, the attention towards distributed generation as an alternative to centralized generation has increased [17]. The most important reasons for an increase of distributed generation in the near future are the following assumed advantages assigned to distributed generation in literature: low-cost entry into a competitive market, the exploitation of renewable energy sources, increased efficiency through using waste heat, efficient use of the demographic environment, low transmission and distribution losses, stabilised voltage levels, increased reliability of the power supply, reduced cable loads and transformer loads [12][19][20][21].

- *Section 3.2: Challenges for the Network Operator*

The efficacy of distributed generation can vary considerably depending on how it is deployed [20]. From studies on distributed generation it appears that the issues that arise with the implementation of distributed generation are often contradictory to the advantages assigned in literature. Furthermore, the issues that arise with the generators are the concern of the network operators [16]. A few important induced technical challenges for the network operator are: reversed power flow, increased short-circuit power, unintentional islanding, selectivity of protections, stability problems and power quality problems as harmonic distortion [11][22].

- *Section 3.3: Alternative Operational Approach*

The implementation of distributed generation changes the operation conditions of the distribution network [23]. Therefore, network operators are investigating alternative operational approaches that allow a higher level of distributed generation capacity [18]. A popular proposition has been the self-supporting residential area supplied by a mixture of distributed generators and storage devices that is sufficient to supply the entire local loads within the LV network with intelligent control systems or otherwise. A self-supporting residential area deviates from an arbitrary decentralized power supply, since it organises distributed generation and storage in a way that maximises the value of distributed generation to customers as well as the network operators. The values of distributed generators is maximized by balancing power supply and demand efficiently in close proximity in the LV network so it can easily be controlled and isolated from the upper grid [12][13][20]. The main issue that remains to be considered is whether this new operational approach can live up to the expectations. The following case study will contribute to this issue.

Part B: Case Study - Approach

- *Section 4: The Integrated System*

When the LV network of the residential area is to offer reliable power supply, a mixture of different energy sources that are complementary to each other as well as storage devices are needed [13]. The LV network considered entails 40 detached and 200 terraced houses that all have  $1\text{kW}_{\text{peak}}$  Photovoltaic (PV) power and a free-piston Stirling CHP with a linear generator (alternator) supplying  $1\text{kW}_e$  and  $4\text{kW}_{\text{th}}$ . The houses are divided over six 150 A1 feeders connected to a 400 kVA transformer (10.25kV:400V) [31]. Seven storage devices are integrated; at the transformer node and at the end of each feeder.

The spring-mass system of the Stirling engine is balanced at 50 Hz, causing the linear generator to alternate at a fixed frequency of 50 Hz, suitable for direct grid-connection [34]. PV power is shaped by the inverter. Both generators are not capable of controlling active (P), reactive power (Q), voltage (U) and frequency (f) as the synchronous generators with P/f and U/Q control [26]. As a consequence, the power output of the generators are regarded as constants with a constant power factor of 0.95. In island mode of the LV network the control is taken over by flow-batteries that can be tailored to the required storage capacity and maximum power separately [38].

- *Section 5: The Scenarios*

Because PV and CHP are complementary it is important to generate power profiles throughout the year. A total of 10 scenarios are specified containing a week in which the self-supporting residential area is evaluated; 3 overload scenarios (in January, April and July), 3 shortage scenarios (in January, July and October) and 4 average scenarios (in January, April, July and October). The overload scenarios have high electricity generation compared to the demand, attributed to low outside temperatures and much solar radiation. For the shortage scenarios this is the other way around. January and July are the months that rely on only CHP or PV respectively. In these months all three scenarios (average, overload and shortage) are investigated to keep all options open. During spring low outside temperatures and high sun power occur compared to autumn [39], so spring is more convenient for an overload scenario than autumn. April, a cold month in spring, will represent the overload scenario during spring, as the shortage scenario should be during autumn where the weather involves higher temperatures, like October. To cut back on the amount of power demand and supply profiles, only two kind of consumers are taken into account (the terraced house and the detached house).

- *Section 6: The Energy Balance*

The amount of power and operation time of the energy supply needed from the distributed generators combined with on-site heat production are determined by flexible balancing actual demand and supply as required. The overall balance of the energy yield (kWh and MJ) and the real-time balance in power output ( $kW_e$  and  $kW_{th}$ ) must assure that in general the heat and electrical consumption are met. This requires accurate load and generator (heat-) power profiles at least throughout a week for every defined scenario. The power demand profiles of this case study are generated by the yearly energy consumption from [4] and temperature dependent hourly gas demand fractions and 15-minute-mean electricity demand fractions from [41].

The CHP is heat controlled. The CHP operation time is therefore determined by the heat demand and the size of the heat storage vessel attached to the CHP. The CHP heat power output is used to determine the CHP electrical power output from which the CHP electricity yield is calculated. The electricity yield of the CHP is on its turn used to calculate the installed PV power from which the real-time PV power output profiles are confined. PV power output has three variables that distinguish the scenarios: seasonally-adjusted amount of sun hours, the seasonally- and daily-adjusted sun irradiance and the possibility to include weather conditions, such as a cloudy or clear sky. From the resulting lack of simultaneity between the generators and the loads, the capacity and peak power needed from the storage devices are determined with the help of load-flow calculations.

- *Section 7: The Assessment*

The self-supporting residential area is in charge of its own power supply. To comply with challenges of the network operator, the self-supporting residential area needs to meet an extensive list of technical issues. It is important to quantify the technical issues and then select the parameters that serve the purpose of assessing the self-supporting residential area of this case study. The main quantifiable parameters that can be used to assess the alternative operational approach are: magnitude and direction of the power flow (1), cable and transformer loads (2), voltage levels (3), system losses (4), variety of power quality parameters (dips, harmonics, flicker, etc.) (5) and reliability and security indices (short-circuit current, failure calculations, stability, selectivity of protections) (6). This case study is restricted to the calculation of the first four parameters in steady-state. The load-flow function of the simulation program 'Vision Network Analysis', that makes use of the Newton-Raphson method [44], is used to assess these parameters.

The generated 15-minute-mean power profiles throughout a week require several calculations in quick succession changing the input data each time. 'Vision' made this possible with a programming editor provided for writing macros. Within the macro also the operational control of the storage devices is programmed. Vision load-flow calculations treat synchronous generators with power factor control as negative loads of constant power. Also the loads behave as constant power, which means that the rated power of the load will always remain constant, independently of the calculated node voltage. Consequently, if the node voltage increases, load current decreases and the other way around, so the loads will have maximum effect on the grid [44].



- *Section 8.1: Demand Side*

The demand profiles are deduced from the absolute yearly energy consumption of [4] and hourly or 15-minute fractions of the yearly energy demand from [41]. Extra effort is done to check the validity of the data that is used to form the profiles. The yearly demand for 2010 [4] matches with the demand fractions from [41] and are representative for the detached and terraced houses in this case study. Though, it should be noted that the generated 15-minute-mean electricity profiles are averaged. For that reason the simultaneity of all the peaks for every household within the LV network will be 100% during the load-flow calculations.

The yearly electricity demand amounts to 4084 kWh per household, the yearly heat demand of a detached house is 47.3 GJ and that of the terraced house comes to 38.6 GJ. The hourly gas demand fractions [41] separate the Temperature Dependent Profile (TDP) and Temperature Independent Profile (TIP). Adding up both values gives the fraction of the total gas demand that is consumed within that hour. The TDP reacts according to the effective temperature, which is the actual temperature minus the wind speed divided by 1.5. The TDP is valid until the heating point is crossed, when space heating is redundant. This approach is applied for the predefined scenarios. The daily and seasonal differences are already integrated in the gas- and electricity profiles and can not be changed [42][43].

- *Section 8.2: Supply Side*

The main task of the heat power output profiles is to deduce the operation-time of the CHP. The CHP heating system consists of a CHP, storage vessel and supplementary heater. Every hour it is investigated whether the heat is supplied directly by the CHP, indirectly with the help of the heat storage vessel or by the supplementary heater. Of course, the CHP must operate as much as possible, since only the CHP itself produces electricity as well. The heat power output profiles are determined in excel spreadsheets. In case of a vessel temperature of 90 °C, the maximum energy is reached in the vessel (200 litres), since it is not advisable to reach temperatures closer to the boiling point. Energy will not be extracted from the vessel at a vessel temperature below 65 °C, since this is not desirable for health considerations. Furthermore, the CHP can only be turned on twice a day, otherwise the CHP system might wear out. The operation time is also applicable to the electricity supply, after which it is transformed into the same time-scale as the electricity demand profiles and switching effects on the electricity power output are integrated.

From the balance between the CHP electricity yield and electricity demand throughout a week in the predefined scenarios it is immediately clear that the PV arrays can either improve or worsen the electricity balance per scenario. The highest reduction of power shortcomings compared to the increase in surplus appear at a 1 kW<sub>peak</sub> installed PV power. With the help of the Photovoltaic Geographical Information System (PVGIS) PV estimation utility of the European Commission, the crystalline PV electricity yield is calculated and daily profiles are formed for the load-flow calculations.

- *Section 8.3: Battery Energy Storage*

The storage devices operate on the basis of local measurements. The storage devices at the end of the feeders change their power output until the voltage set-point of the connection node is reached. The set-point is based on the turning point when supply equals demand. The storage device at the transformer node imitates the active and reactive power flow through that node. The simulation happens in small step changes in rotation, because when the voltage of one node changes it might effect the voltage levels within the entire LV network.

The maximum peak power during the average scenarios occurred in April with a total of 235 kW<sub>e</sub> that is almost 1 kW<sub>e</sub> per household. The required storage capacity is limited. In situations with general excess electricity yield, storage has to bridge the moments of shortage. Conversely, the scenarios in which the electricity generation is more scarce, the moments of excess power supply throughout a week determine the storage capacity. The total storage capacity installed in the self-supporting neighbourhood is 937 kWh, almost 4 kWh per household. The capacity and peak power requirement of the transformer node storage device is mainly 4 to 5 times bigger than the requirement of each end-feeder device. The peak power and capacity limits as well as storage losses (16% [37]) are integrated in the 'Vision' macro for further load-flow calculations to assess the design of the power supply and Battery Energy Storage (BES).

## Part C: Case Study Results - Assessment

- *Section 9.1: Reverse Power Flow*

Distributed generation reduces power extracted from the grid. In January and April overload scenarios much power is transported back to the grid, but not more than is required in the average scenarios without distributed generation. The maximum effect of BES is achieved, although this is rather limited in January/April overload scenarios and July/October shortage scenarios.

- *Section 9.2: System Losses*

The LV network losses of the self-supporting residential area include LV cable and transformer losses calculated with the 'Vision' macro. The transport losses over the rest of the medium voltage (MV) and high voltage (HV) network are estimated by the network operator. A considerable amount of the transport losses is reduced when distributed generators and BES are implemented, except for the overload scenarios. Unfortunately, storage losses are higher than the reduced transport losses. It is useless to put more effort in the siting of the storage devices, since the LV network losses are minimal.

- *Section 9.3: Voltage Levels*

Distributed generation increases the 15-minute-mean voltage levels but they stay within the range of +9% and -2% of the nominal 230 (V) voltage level. At scenarios with a good energy balance, storage converges the voltage levels. At shortage scenarios the peaks are covered, while during overload scenarios the minima are covered instead.

- *Section 9.4: Transformer Loads*

Cable loads do not reach 32%, whereas the transformer loads reach 78%. The transformer is therefore further specified. In general the transformer loads decrease by distributed generation, though the periods of excess power supply have much effect on the transformer loads. At the lowest amount of 15-minute-mean power demand of 200 W per household and the highest 15-minute-mean power output of 1.8 kW, the transformer load increases to 99% and the voltage level would increase to 252 V. Just below the upper limit of 100% and 253 V respectively.

### Conclusions and Recommendations

This research is only based on the assessment of 15-minute-mean steady-state parameters, that have averaged out the demand profiles. The question is whether more specific demand profiles are useful for steady-state calculations, since the main problems are caused by excess power supply of the distributed generators. The generator's (maximum) power output is limited and occurs also during the 15-minute-mean profiles.

The distributed generation in the self-supporting LV network implies the need for peak load shaving. The peak power, the capacity and operational control of the storage devices succeeded in minimizing the reverse power flow and transport losses. Unfortunately, storage losses are higher than the transport losses. During scenarios that contend with excess electricity yield, storage devices are on overall fully charged and fail to serve peak load shaving, i.e. limit voltage peaks and transformer loads. This indicates the need for a different solution. A different operational control on the storage devices, such as a higher voltage set-point, increases the charge-limit, but will decrease storage efficiency. Shutting down the generators is also an option, though it would be a shame not to take advantage of the generator's power output since three out of four average scenarios are not completely self-supporting yet.



## 2. Introduction

Changes in the regulatory and operational environment of the current power supply system and the emergence of smaller generating systems such as micro-turbines have opened up new opportunities for on-site power generation by electricity users. In this context, distributed generators are small power generators typically located at users' sites where the energy generated (both electricity and heat) is used in close proximity. This report suggests that the potential of distributed generation can be best captured by organizing these generators into a self-supporting residential area [19]. The definition applied in this report reads as follows: the self-supporting residential area is formed by small modular generators, i.e. changeable types of distributed generation with limited (e.g. renewable) energy sources, and storage devices that are connected in close proximity to each other in a small area within the low voltage (LV) network in order to supply the local loads [11]. The alternative operational approach of distributed generation has the potential to resolve the problems concerning future power systems that comprise distributed generation. Section 3 of this report examines the opportunities and challenges of distributed generation and explains the potential of the self-supporting residential area.

The setting of the self-supporting residential area includes generators, energy storage devices, and, for certain systems, load control and advanced power electronic interfaces between the generators and the distribution network [19]. Provided that the self-supporting residential area is well-designed it can be controlled as a solitary changeable load that overcomes the problems experienced by the upper grid or the other way around [14]. Network operators noticed the importance of this concept and started to do research on mainly the control possibilities to realize this idea into an intelligent control-system called the 'Virtual Power Plant', 'Smartgrid' or 'Microgrid'. In this study, however, the real-time amount of power available and direct effects on the LV network without the intelligent control systems will be investigated to finally evaluate the potential of such systems for the network operators for future research. The main question is thereby:

- *'To what extent will a self-supporting residential area in the Dutch LV network meet the challenges of the network operator?'*

The goal of this research is to find out whether the self-supporting residential area will operate satisfactorily in respect to the advantages assigned to the new approach concerning distributed generators as it turns out from literature, such as improving reliability, safety and voltage profiles, decreasing transmission losses and increasing efficiency [14]. Analysis must be done for a variety of time-varying and uncontrollable load and generator conditions to find out what will exactly happen when distributed generators are organized into a self-supporting residential area [11].

The first step that enables the investigation of the main question is to design the power supply system within the LV network in a way it approximates a self-supporting residential area as far as possible. Therefore the following essential sub-questions enable the investigation of the main question:

1. *What will be the most favourable design of the power supply system within the self-supporting residential area for a typical Dutch case, concerning the number (i), size (ii), positioning (iii) and kind of (iv) distributed generators (with on-site heat production) as well as storage devices?*
2. *How closely and over what time-scale will the power supply system (both electricity and heat) eventually satisfy the local loads within the self-supporting residential area?*

These questions are investigated by hands of a case study, that starts in section 4 with the definition of the LV network, generators, storage devices and loads, i.e. the components of the resulting self-supporting residential area. Section 5 confines the environment in which the self-supporting residential area is created and evaluated, such as outside temperature, solar radiation and other weather conditions. Section 6 explains how the final configuration of the power supply system within the self-supporting residential area is formed. The design of the power supply system within the self-supporting residential area is determined by the overall 'energy balance' (MJ and kWh) during a week and a real-time 'power balance' ( $\text{kW}_{\text{th}}$  and  $\text{kW}_{\text{e}}$ ) throughout a week that take a close look at the power profiles from the generators as well as the consumers. The 'energy balance' (MJ and kWh) matches the weekly demand and supply so it is possible that the total figure in heat and electricity demand can be met throughout a week. The real-time 'power balance' ( $\text{kW}_{\text{e}}$  and  $\text{kW}_{\text{th}}$ ) calculates the required storage power and capacity to overcome time differences in supply and demand throughout that week by means of load-flow calculations with the computer simulation program 'Vision Network analysis' from Phase to Phase.



The input for the load-flow calculations that are treated in this case study is:

- A variety of load levels (active and reactive power),
- installed power, operation time and the operating characteristics of the distributed generators,
- number, size and location of the storage devices,
- the characteristics of the LV network configuration,
- and the connection mode to the grid.

Section 8 figures how closely the power supply system (both electricity and heat) eventually satisfies the local loads within the self-supporting residential area.

The performance of the designed power supply system and storage devices concerning the effects on the LV network, which is interesting for the network operators, is assessed by means of the same load-flow calculations for a variety of situations concerning seasonal differences and daily load fluctuations. Section 7 discusses to what criteria the power supply system is assessed and this section also specifies the assessment tool. The next sub-question that will be investigated in section 9 is thereby:

3. *What are the effects on the LV network concerning magnitude and direction of real and reactive power, system losses, voltage levels, cable and transformer loads?*

Concluding, the case study objective proposed in this report is to verify statements about the alternative operational approach by calculating reverse power flow, voltage levels, system losses, cable and transformer loads of a well-designed self-supporting residential area in the LV network containing combined heat and power (CHP), photovoltaic (PV) arrays and storage devices.

The higher goal of the new alternative approach is to support the transition into a more sustainable and competitive energy market by encouraging the implementation of distributed generation. The generators in question mostly make use of renewable energy sources and efficient conversion technologies through used waste heat. The close proximity of demand and supply, the self-supporting residential area has the opportunity to utilize the waste heat from conversion of primary fuel to electricity. Unlike electricity, heat can not be easily transported long distances, so typically half to three-quarters of the primary energy consumed in power generation is in the end unutilized. The potential gains from using this heat productively are significant [19]. Moreover, the close proximity of generation to the loads enhances efficient use of the demographic environment and reduces transport losses. Less energy will be wasted, since the idea of the self-supporting residential area is to gear generation and consumption efficiently to one another [15]. Concluding, the self-supporting residential area implies possibilities to support the sustainable environment [12], since it encourages consumers' as well as network operators' participation to the transition into a sustainable environment by the use of renewable energy sources, waste heat and by decreasing transport losses, while offering a power supply that meets the challenges of the network operator and consumers' contemporary needs as explained above.

# Part A Background Information

---

From literature it can be concluded that there are high expectations from distributed generation implemented in the distribution network. Other studies think the opposite and point at the difficulties that come with distributed generation. Clearly, the statements about distributed generation need to be verified. The self-supporting residential area is seen as an alternative operational approach that satisfies both sides of the matter by exploiting the advantages of distributed generation and avoiding the difficulties that come with distributed generation when implemented in the distribution network. Part A explains the issues of the changing power supply and the need for profound research on the potential of the self-supporting residential area.

## 3. New Scenario of Distributed Generation

The architecture of the electrical system developed over the past century is based on the concept that very large central power plants at strategic places with respect to primary energy resources, costs and safety provide the entire power supply. The electricity networks assimilate with the centralized power generation by transporting electrical power from the source to the end-user unidirectional from higher voltage levels to lower voltage levels in a hierarchical network structure of high voltage transmission networks, medium voltage distribution networks to low voltage networks. The centralized power supply has proven its effectiveness, consumers connected to the Dutch electricity network are accustomed to gas and electrical power available on demand [16].

Over the last years, the attention towards distributed generation as alternatives to centralized generation has increased, because of a variety of either economical, environmental and social advantages assigned to the distributed generators [17], which will be explained in section 3.1. A distributed generator is a small generator typically ranging from less than a kW to tens of MW that is not a part of a large central power station, located close to the load. Distributed generation includes for instance combustion based generators, photovoltaic (PV) systems, fuel cells, wind turbines, micro turbines and small hydro plants. Distributed generators are direct grid-connected or connected through power electronics. Those connected to the grid are interfaced at the distribution system, and thus dispersed across the electricity network rather than concentrated as a central power plant [16]. Section 3.2 discusses the technical issues associated with distributed generation and deals with the technical matters that come along with the incorporation of small distributed generators into the distribution network, i.e. the low voltage (LV) and medium voltage (MV) network [12]. In section 3.3 an alternative operational approach that allows a higher level of distributed generation capacity within the MV and LV networks is outlined that is used for further research in this report [18].

### 3.1 Opportunities

A well-known advantage assigned to distributed generation in literature is that it exploits a variety of renewable energy sources as well as primary energy sources. Renewable generators and cogeneration with high efficiencies imply possible environmental and economical benefits. Some renewable energy sources have large power outputs, like hydropower or geothermal power, but the power output of the mainstream is relatively little. This indicates that many of these renewable sources will be adopted by consumers themselves and connected in the form of distributed generators at lower voltage levels in the distribution system. Also the efficient exploitation of primary energy sources through cogeneration is seen as one of the important ways to create a sustainable environment [12]. Cogeneration utilizes waste heat resulted from conversion of primary fuel to electricity [19]. The improved exploitation of the primary energy sources should thereby increase overall energy efficiency [23]. The conventional power supply is based on centralised large fossil fuel or nuclear power stations, that produce large quantities of waste heat [12]. A variety of distributed generators, like many small-sized combined heat and power systems, are based on the principle of cogeneration, that uses both electricity and waste heat permitted by the close proximity of the generator to the user [20].

Other supposed environmental benefits (sometimes also referred as economical benefits) assigned to distributed generation are the reduction of transmission and distribution losses. A reduction in transmission and distribution losses increases the efficiency of the power supply. Furthermore, some studies expect that the implementation of small-scale distributed generation has less environmental impacts than large-scale central power plants. Distributed generators in the built environment, such as the installation of solar photovoltaic arrays on a roof top, are therefore referred to as embedded generators that point at efficient use of existing building land [20]. Existing building land already needs or contains an electricity infrastructure, so no extension of the existing infrastructure is required.



Moreover, evaded degradation of the electricity infrastructure is also expected to reduce future investments costs. By situating generation closer to the loads, the lifetime of both the distribution and transmission network increases, attributed to improved voltage levels and reduced cable and transformer loads. For example, the International Energy Agency (IEA) estimated a 30% lower total costs by mitigating transmission and distribution loads and displacing expensive infrastructure through distributed generation [20].

Also social advantages of distributed generation are suggested. A relatively large number of small generators spread over the network closer to the loads might improve the reliability. The proximity of the generators to the loads decreases the length of the power transport. The increased number of dispersed generators might limit the areas effected by a failure of one of the network elements [12].

Concluding, the assumed advantages assigned to distributed generation in literature are;

1. to enable low-cost entry into a competitive market,
2. to decrease household's use of fossil fuels and emissions by the exploitation of renewable energy sources and by increased efficiency through the use of waste heat,
3. to increase energy efficiency by reducing transmission and distribution losses,
4. to unburden the demographic environment by the use of existing building land,
5. to evade investments in a new extended network infrastructure,
6. to avert depreciation of the electricity infrastructure by reduced cable- and transformer loads,
7. to improve the quality of voltage levels,
8. and to increase reliability of the power supply.

### 3.2 Challenges for the network operator

The generators of special interest for future developments in the power supply are distributed generators [12]. In the United Kingdom (UK) for example it is perceived that by 2010 each distribution network operator has to deal with around 300 distributed generators connected to each of their substations compared to the existing 300 distributed generators over the whole UK network [21]. Most important reasons to think that the implementation of distributed generation will increase in the near future are the liberalization of electricity markets allowing for the participation of private generators, the growing concern around climate change and the depletion of fossil fuels [20]. Moreover, it is believed that new innovations in distributed generation technologies, can also bring economical and social advantages such as a reduction of energy costs and increase in reliability of the power supply, as is explained in section 3.1. However, from studies on technical challenges of the implementation of distributed generation it appears that the issues that arise with the implementation of distributed generation are mainly contradictory to the advantages assigned in section 3.1. Inappropriately connected distributed generation can compromise the advantages assigned to the generators [16]. So, the efficacy summed up in section 3.1 is the half truth, since it can vary considerably depending on how distributed generation is deployed [20].

The issues that arise with the implementation of distributed generation are mainly the concern of the network operators [16]. Some important induced technical challenges for the network operator are complex, uncontrollable or unpredictable reversed power flow, increased short-circuit power, unintentional islanding, selectivity of protections, stability problems and power quality problems as harmonic distortion [11][22].

The implementation of distributed generators will result in a shift towards less centralized generation [20], yet the existing MV and LV network are designed for centralized power supply. Because of the increasing bidirectional flow in the distribution system, the operation must be distinguished from the current operation of the centralised power supply. It seems that this is hardly touched in the studies that allocate advantages to distributed generation. For instance, the voltage level in the distribution grid is controlled by the transformer tap change. In the centralized power supply with unidirectional power flow the setting of the transformer tap ensures that the voltage levels along the outgoing feeders remain within the specified limits, Figure 1. In case of reverse power flow this operational approach is far from ideal and can violate protection schemes [16]. As a consequence from bidirectional power flow in the LV cables with a considerably large resistive component, primary concerns are maintaining the voltage profile and prevention from cable overloads [24]. Earlier, the voltage levels were expected to improve through distributed generation. Apparently there are studies that claim the opposite.

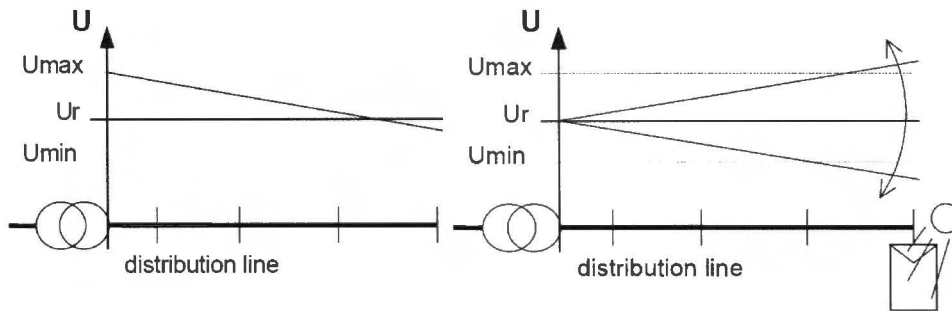


Figure 1: Voltage control transformer tap without DG (left) and with DG (right) [24].

The characteristics of the current distributed generators make the reverse power flow even more complicated; the installed power (number and size) of the generators is arbitrary (1), implemented at dispersed places anywhere in the network (2), supplying an unpredictable and uncontrollable amount of power (3) interconnected to the distribution network with a variety of power, voltage, and frequency control systems (4). This proves the variety of considerations that play an important role in the effectiveness or either harmfulness of distributed generation in the distribution network [20].

The amount of power supplied by the distributed generators is often unpredictable and uncontrollable for the network operator. Many generators exploit intermittent and unpredictable renewable energy sources, such as wind and solar power and are in private ownership of the consumers [13]. The main purpose of private owned generators is to optimize profits and energy efficiency and not to serve the power flow, voltage level or frequency of the public electricity network. Moreover, the distributed generators operate at quite different operational modes [25]. Some generators exploit direct current (dc) sources, such as photovoltaic arrays and fuel-cells, and others generate variable frequency or high frequency alternating current (ac), such as micro-turbines. The non-50 Hz sources are not fit for direct grid-connection and need to be interfaced to the grid through power electronics [13][23]. So, the power supply becomes increasingly complex by the implementation of distributed generators and changes the operation conditions of the distribution network, like control and safety issues that must be addressed [19]. Network operators have to deal with active operational controls instead of the current passive network operation.

Currently, most network operators rely on commonly used connection standards. Many of those standards are based on recommendations by ANSI and IEEE. The connection of a generator is conform these standards to prevent that utility equipment and other users connected to the network are effected. However, the distribution network operators often disagree regarding the appropriate connection standards [26] from which the applicability is limited to a power rating of 10 MVA, which is larger than the ratings expected for the total installed power within the self-supporting residential area [19]. The standards still do not overcome all problems, such as the issue of unintentional islanding. Islanding happens when the power to a local area of the electricity network maintains live by a distributed generator electrifying an unidentified area of the electricity network, while the main supply is switched-off during a fault [12]. This situation endangers not only generators and the distribution system, but also utility workers performing repairs [20].

Concluding, even if a generator conforms to the relevant codes of practice and engineering recommendations, the implementation of distributed generation will still bring problems to the network operation and some technical limits will occur when connecting a lot of distributed generators [15]. Therefore, the power supply of distributed generation will change the philosophy of operation of the power supply with which the network operators have to deal [27]. Network operators remain responsible for the grid, its operation, maintenance and investment plans [16]. A new plan for the energy system is suggested in the next section, that is expected to solve the challenges induced by distributed generation and enhance the advantages assigned to distributed generation.



### 3.3 Alternative Operational Approach

In the changing landscape of the power supply the MV and LV network will become active, challenging the network operators. The need for a reliable and controlled energy system are the network operator's driving forces which makes the advantages as well as the challenges assigned to the distributed generators in previous sections important issues for the network operators, Figure 2. Network operators are investigating alternative operational approaches that allow a higher level of distribution generation capacity within the MV and LV networks than at present [18].

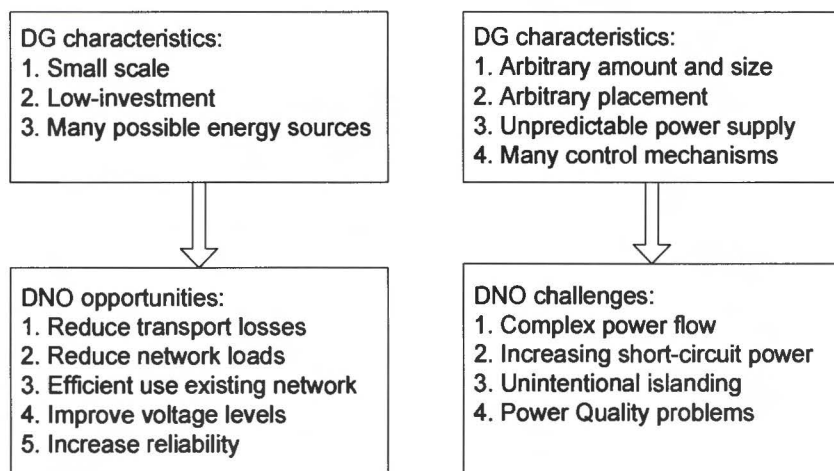


Figure 2: Opportunities and challenges of Distributed Generation (DG) for the Distribution Network Operators (DNO).

Many studies investigated how to deploy distributed generators in a way that is compatible with the current power system. These studies mostly aim at a self-supporting small community as an alternative operational approach of the implementation of distributed generation. This alternative approach knows a large diversity of interpretations in literature called by different terms such as a Smartgrid, Microgrid or Virtual Power Plant. These terms usually aim at a self-supporting small community in the MV or LV network through distributed generators with intelligent control systems and decentralised monitoring or otherwise. The term 'small community' can refer to a housing estate, isolated rural community, commercial area or industrial site. The control strategies mentioned are energy storage, load management and demand-side management [28]. The self-supporting residential area, as it is called in this report, refers to a radial LV network with 240 households connected to a MV/LV transformer. The self-supporting residential area contains a mixture of decentralised electricity generators merged with on-site production of heat and storage devices that will be sufficient to supply most or the entire local loads within the LV network [12][13].

This alternative operational approach in question is expected to serve the advantages mentioned in section 3.1 and to overcome the challenges of section 3.2, Figure 2. The distributed generators of a self-supporting residential area are installed in the LV network, situated near the loads and are of comparable size as the loads within the same LV network of the residential area in question [12]. There is no better place to serve the advantages assigned to distributed generation of Figure 2 than in the nearest proximity of the loads in the LV network. One can see the advantages of close proximity of demand and supply through the following Dutch figures; 85% of the electricity fall-out time is the result of power failures in the HV and MV network [8][29], centralised coal fired power plants convert approximately 39% of the fuel into electricity, whereas the gas-fired power plants have an efficiency of about 44 to 55% [30] and thirdly HV and MV network losses reach 3% of the provided electricity.

The design of a self-supporting residential area makes an extra effort to link energy generation and consumption efficiently to prevent excess power supply that will undo the advantages of distributed generation and will enhance the challenges of the implementation of distributed generation [15]. Excess power supply of distributed generators could have a substantial influence on grid reliability. Exces power supply could cause heavily loaded distribution lines to trip, even more if the generators are installed at arbitrary places. Transport of excess power through the distribution system is expected to be less in the self-supporting residential area, since the generators and storage devices of the self-supporting residential area are designed to satisfy their predetermined local load and no more [19].

To increase reliability of the power supply, the self-supporting residential area must be able to isolate from the upper grid [12]. The infrastructure of the self-supporting network is suitable for disconnection of the upper grid. With a switch at the transformer the LV network is isolated from the upper grid and proceeds as an autonomous network. In addition this infrastructure gains a clear view of the reverse power flow that facilitates the network operators to take effective measures against induced power quality problems and undesirable islanding of the distributed generators.

The isolated LV network can not live on its own straightforwardly. The distributed generators and storage devices within the self-supporting residential area must be able to balance the active and reactive power output while keeping voltage and frequency levels within limits. An important design criteria of the self-supporting residential area is therefore the control mechanisms of the generators or storage devices that supply the required active and reactive power at the fundamental frequency and voltage level [12].

Concluding, the self-supporting residential area deviates from an arbitrary decentralised power supply since it has a higher potential to exploit the benefits of distributed generation and it is able to resolve the problems concerning future power systems that comprise distributed generation by balancing power supply and demand efficiently within a small area that can locally be controlled and isolated from the upper grid (Figure 3) [12][13].

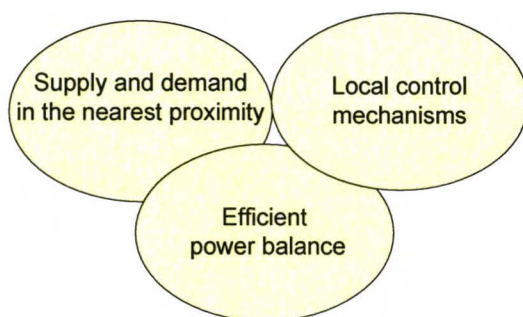


Figure 3: The focus of the self-supporting residential area.



# Part B: Case Study - Approach

From part A it can be concluded that in theory the implementation of distributed generators in the low voltage (LV) network might improve the future energy supply. Moreover, a self-supporting residential area is regarded as a method of organising decentralised generation and storage in a way that maximises the value of distributed generation to customers as well as the network operators [20]. Unfortunately, the main issue that remains to be seen is whether the expectations of this new operational approach are achievable. This case study will contribute to this issue, but since the case is rather comprehensive, it must be confined.

The self-supporting residential area engages a complex integrated system that involves the LV network configuration, the distributed generators, storage systems and the local loads within the LV network. The characteristics of the generators, storage systems and LV network of this case study are defined in section 4. Section 5 confines the positions in which the LV network will be assessed, like the surrounding factors as outside temperature and solar radiation. The design of the generator and storage devices within the self-supporting residential area are determined by the overall energy (MJ and kWh) and real-time power balance ( $kW_e$  and  $kW_{th}$ ) in section 6, that takes a close look at the load profiles on the demand-side as well as on the supply-side. Finally, section 7 discusses to what criteria and with what kind of assessment tool the design is to be evaluated. Figure 4 illustrates how these sections come together.

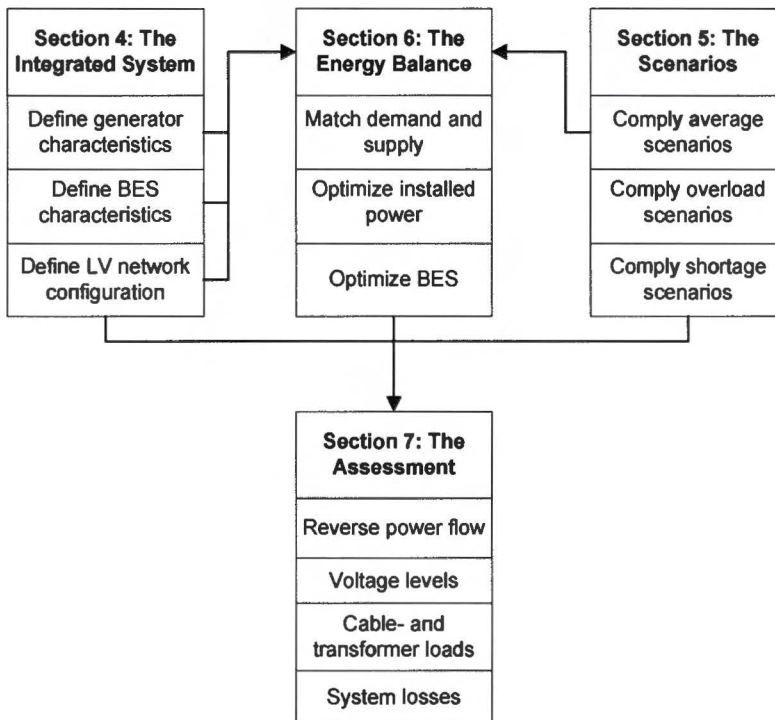


Figure 4: The form and content of part B .

## 4. The Integrated System

Section 4.1 entails the first step, namely the definition of the low voltage (LV) network, the distributed generators and the battery energy storage (BES) devices. When the LV network of the residential area is to offer reliable power supply, a mixture of different energy sources that are complementary to each other as well as storage devices are recommended [13]. Section 4.2 explains the characteristics of the power supply system. The LV network entails 40 detached and 200 terraced houses that all have  $1kW_{peak}$  photovoltaic (PV) power and a free-piston Stirling combined heat and power (CHP) with a linear generator (alternator) supplying  $1kW_e$  and  $4 kW_{th}$ . The houses are divided over six 150 Al cables connected to a 400 kVA transformer (10.25kV:400V) [31]. Seven BES devices are integrated at the transformer node and at the end of each cable. The operating characteristics of the BES devices follow from section 4.3.

The LV network that is utilized in this case study is part of the development programme entitled ‘Smart Power Systems’ that researches the management of decentralised energy systems into a ‘Virtual Power Plant’ concept as part of the Energy Valley initiative, including Continuum, ECN, Eneco Netbeheer BV, Essent Netwerk B.V., Gasunie Engineering & Technology, GasTerra, ICT Automatisering, Kema, N.V. NOM, TietoEnator and TNO ICT.

The composition of the generators is inspired by the HERMES DG project [31]. At stage 1 of this project the 6 most probable future energy systems with distributed generators are described. The energy systems had to be technically realizable anno 2007 and economically profitable anno 2020. In the further phases of the HERMES DG project the 6 systems are computed with special attention to the energy infrastructures.

### 4.1 The low voltage network

The LV network entails 40 detached and 200 terraced houses that all have their own PV and CHP system. The loads in Figure 5 are represented by the red arrows. The inverse arrows in green are the PV and CHP generators. The cables from the transformer to the first node of connection vary between 80 and 200 meters. The cables representing the feeders in this LV network are 150 Al cables with a resistance of 49 milliohm per meter and a reactance of 19 milliohm per meter. The transformer’s nominal power is 400 kVA and the voltage step is 10.25 kV to 400 V nominal voltage three phase. The distance between the houses varies between 8 and 20 meters. The distance between detached houses is generally bigger than between terraced houses. Node C is the 1 phase connection of the consumer’s home to the copper service line that runs to the 3 phase feeder at node C41. ‘Vision Network Analysis’ does not allow the inclusion of 1 phase connections, so the cable length in ‘Vision’, that represents the service line, is multiplied by 9 to imitate the transport losses over the 1 phase service line<sup>1</sup> [31].

Seven BES devices are integrated; at node A, B, C41, X, E, F and at the transformer node, representing the taller black arrows in Figure 5. These nodes, including node D, G and all 41 nodes at the feeder of node C, contribute in the ‘Vision’ macro to picture the voltage levels throughout the LV network.

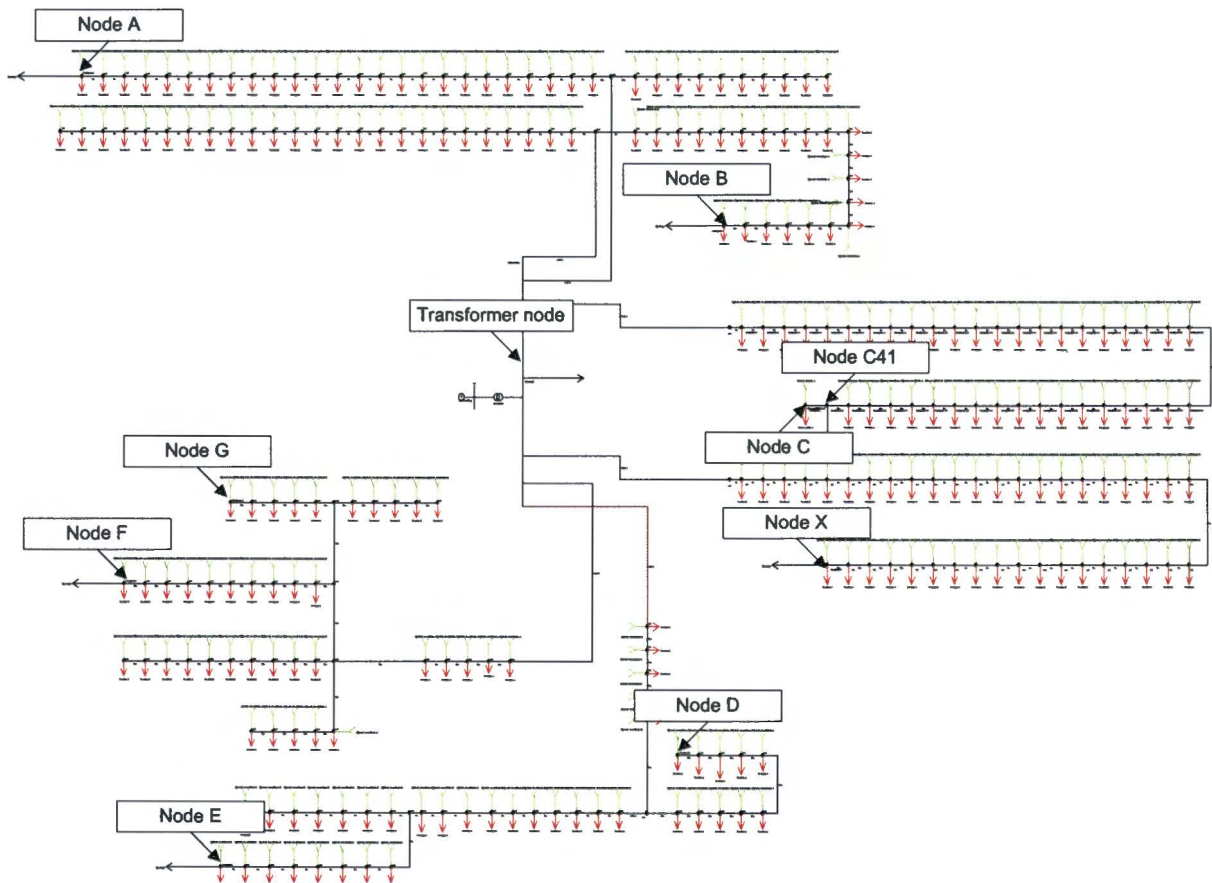


Figure 5: The LV network in ‘Vision Network Analysis’ including loads, generators and BES devices.

<sup>1</sup>  $P_{Loss,1ph} = (3 \times I_{3ph})^2 \times R = 9 \times P_{Loss,3ph}$



## 4.2 The Generators

The generators are selected from a case study on 6 scenarios of future distributed generators [31]. One scenario is depicted that will be specified and further developed in this case study into a self-supporting residential area. When the LV network of the residential area is to offer reliable power supply, a mixture of different energy sources that are complementary to each other is recommended as well as storage devices [13]. With the knowledge that a self-supporting residential area in the near future must make use of a diversity of developed technologies that are also complementary to each other, the combination of Stirling micro CHP and polycrystalline PV arrays is chosen to further develop into a self-supporting residential area.

The internal control systems of the distributed generators are important components influencing the LV network. The control of distributed generation technologies are considerably different from conventional centralised power generation technologies. The conventional large power generators are synchronous generators which are able to control the power factor, i.e. the reactive power output, frequency and voltage level [26]. The distributed generators in this case study include direct current generators, like PV arrays, and fixed frequency generators, like the CHP. The spring-mass system of the Stirling engine is balanced at 50 Hz, causing the linear generator to alternate at a fixed-frequency of 50 Hz, suitable for direct grid-connection [34]. PV power is formed by the inverter. Both generators are not capable of controlling active (P), reactive power (Q), voltage (U) and frequency (f) as the synchronous generators with P/f and U/Q control. [26]. As a consequence, the power output of the generators are regarded as constants with a constant power factor of 0.95 [32]. In islanding mode of the LV network the control is taken over by flow batteries that can be tailored to the required storage capacity and power separately [39].

### 4.2.1 Stirling Engine Combined Heat and Power

There exist several types of Stirling CHP systems. The Microgen will serve as an example in this case study, since it has proven its feasibility. Moreover, it is perceived that the Microgen will have the highest economical potential and efficacy for low heat demand, because the small heat to power ratio ( $1\text{kW}_e:4\text{kW}_{th}$ ) of the Microgen results in a high operation time.

The Microgen CHP, Figure 6 and Figure 7 makes use of the Sunpower free-piston Stirling engine of  $1\text{kW}_e$ , and  $4\text{kW}_{th}$  and a power factor of 0.95 or higher [32]. The displacer is attached to a planar spring forming a simple resonant spring-mass system. The addition of heat at the acceptor to the working fluid increases the gas pressure in the engine. Conversely, the rejection of heat at the rejecter causes a corresponding decrease in gas pressure. The oscillating motion of the displacer moves the gas back and forth from between regions where heat is accepted or rejected by the working fluid. The resulting pressure wave acts upon the face of the piston, causing the piston and attached ring of magnets to swing through the coil of wire within the linear alternator, producing an alternating current (ac) from the engine [34]. The spring-mass system is balanced at 50 Hz, causing the linear generator to alternate at a fixed frequency of 50 Hz. The harmonic frequency of the linear alternator has a stabilizing effect, tests showed no variance of frequency [32].

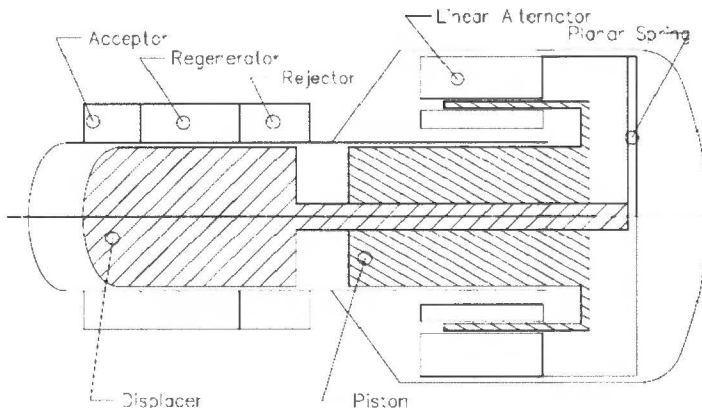


Figure 6: Sunpower's beta type free-piston Stirling Engine [33]



Figure 7: The Microgen [33]

The Microgen has a fuel-to-electric conversion efficiency of 30% [33]. The heat rejected from the engine is recovered to hot water for space heating, resulting in an overall fuel-to-combined heat and electric power conversion efficiency of 90% (Lower Heating Value) and 110% (Higher Heating Value) [34].

A 200 litre hot water storage vessel is included to the heating system. The 200 litre vessel is most commonly used in household applications, since the dimensions of a 200 litre storage vessel are compact compared to the energy storage capacity and easily concealed in the building.

### 4.2.2 Photovoltaic Arrays

PV arrays are non-controllable systems, because the power output is dependent on the solar radiation and outside temperature. The power output of the Philips crystalline solar cell (PSM 125) is taken as an example in this case study, which delivers 125  $W_{peak}$  per panel with a surface of 1  $m^2$ . The reactive power output is mainly formed by the inverter capacitance [36]. Electronic converters have a power factor of 0.95 or higher. The optimum inclination angle in a Dutch case is 36° and south-oriented. The monthly and yearly potential electricity generation E (kWh) of a crystalline PV configuration with defined module-inclination and orientation can be calculated with the following formula:  $E = n \times P_k \times r_p \times H_{h,i}$ .

Where n is the number of days in a month or year,  $P_k$  ( $kW_{peak}$ ) is the peak power installed,  $r_p$  is the system performance ratio (typical value for roof mounted system with modules from mono- or polycrystalline silicon is 0.75) and  $H_{h,i}$  is the monthly or yearly average of daily global irradiation on the horizontal or inclined surface. Further aspects that influence PV yield are:

- Estimated losses due to temperature: 7.0% (using local ambient temperature)
- Estimated loss due to angular reflectance effects: 3.0%
- Other losses (cables, inverter etc.): 14.0%

Above values are estimated by the Photovoltaic Information System (PVGIS), a research, demonstration and policy support instrument of the European Commission.

### 4.3 Battery energy storage

Since the small generators of this case study can not respond to sudden changes of load, BES is needed to cope with the fluctuations in power demand [12]. BES has three operation modes: to assure the continuity of power quality (1), to assure continuity of service by bridging power for seconds to minutes (2) or even to manage the energy supply by decoupling the timing of generation and consumption of electric energy for many hours (3). Both power ( $kW_e$ ) and energy (kWh) management are important issues for a self-supporting residential area, since the intermittent generators, that do not supply on demand, can cause long-term energy imbalances for hours and real-time power imbalances on the short-term. Therefore BES capacity as well as the reloading and discharging peak power are important issues. Figure 8 show the batteries able to fulfil these requirements.

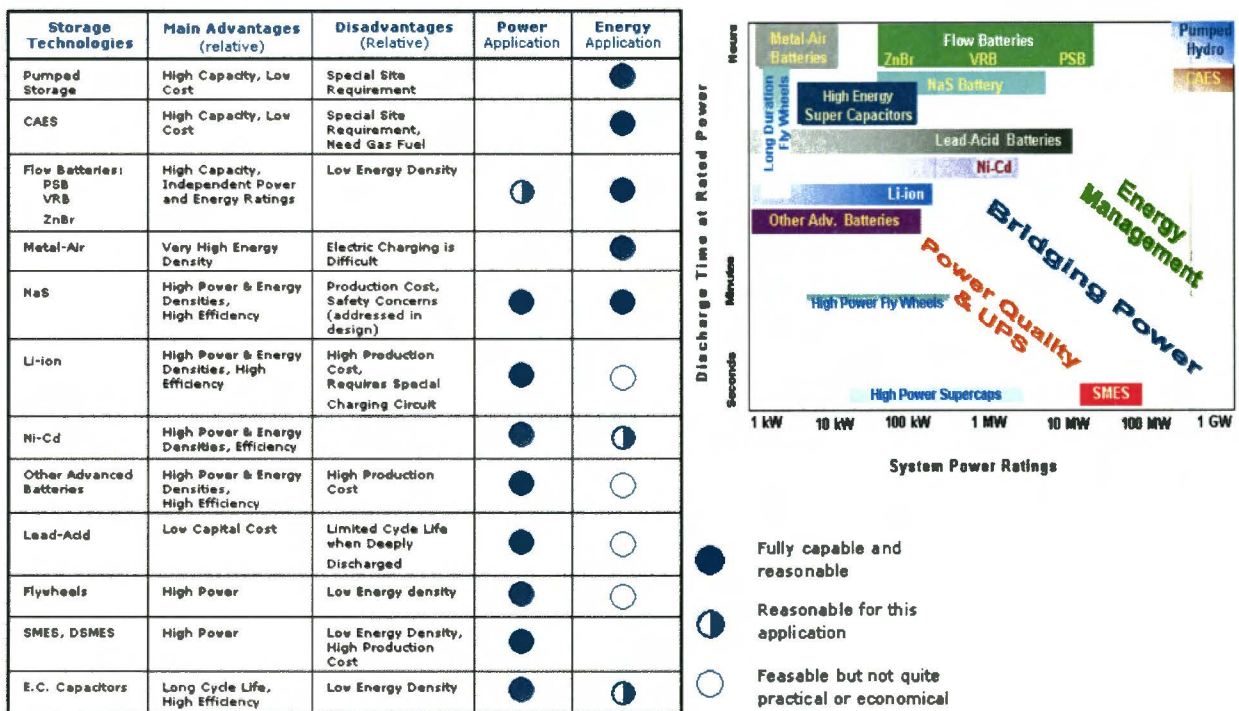


Figure 8: BES applications [37]



Flow batteries are best designable for the required capacity as well as power output. A flow battery, Figure 9, is an electrochemical system which allows energy to be stored in two solutions containing different redox couples with electrochemical potentials separated from each other to provide an electromotive force that drives the reactions needed to charge and discharge the cell. In normal accumulator systems power conversion and energy storage are in the same component. Because power and capacity are separated within the flow battery, the peak power output becomes independent from capacity and vice versa. The size of the electrolyte tanks determines the capacity of the system, while the system power is determined by the size of the cell stacks. The size of the flow batteries can therefore tailor to the storage capacity and peak power required in the self-supporting residential area [38].

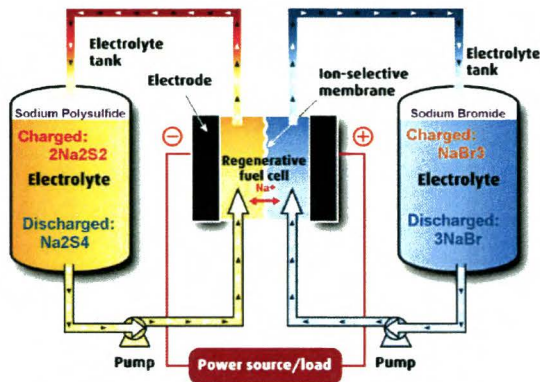


Figure 9: Polysulfide Bromide flow-battery (PSB) [37]

Island mode of the self-supporting residential area means that the power system within the residential area continues to operate when it is disconnected from the upper grid [12]. Only synchronous generators with frequency control (power to frequency droop) and voltage control (voltage to reactive power static) can participate to the regulation in island mode. Synchronous generators with a fixed power factor control, as the generators in this case study, are considered as constant power generators and do not contribute to the frequency and voltage control [44]. So, especially in island mode BES is essential to respond quickly to load variations in order to preserve the power balance at all times, i.e. controlling the real and reactive power output, system frequency and voltage without upper grid support [23]. The basic inputs of the BES controller in this case study are steady-state set-points for output power  $P$  and  $Q$  or the local bus voltage  $V$  [14]. The BES devices are placed at the end of every cable and at the beginning near the transformer, so the loads within the LV network are equipped with a storage device on both sides when grid connected as well as in island mode.

## 5. The Scenarios

This section discusses in what circumstances the self-supporting residential area is evaluated and what (heat-) power profiles on the demand-side as well as on the supply-side have to be created. The (heat-) power profiles are needed to calculate the total energy yield from the generators and to assess the self-supporting residential area with the help of load-flow calculations. Figure 10 shows the variety of (heat-) power profiles used in this case study. In this case study  $960^2$  profiles are generated, when the combined heat and power (CHP) heat and electricity supply are regarded as two different profiles.

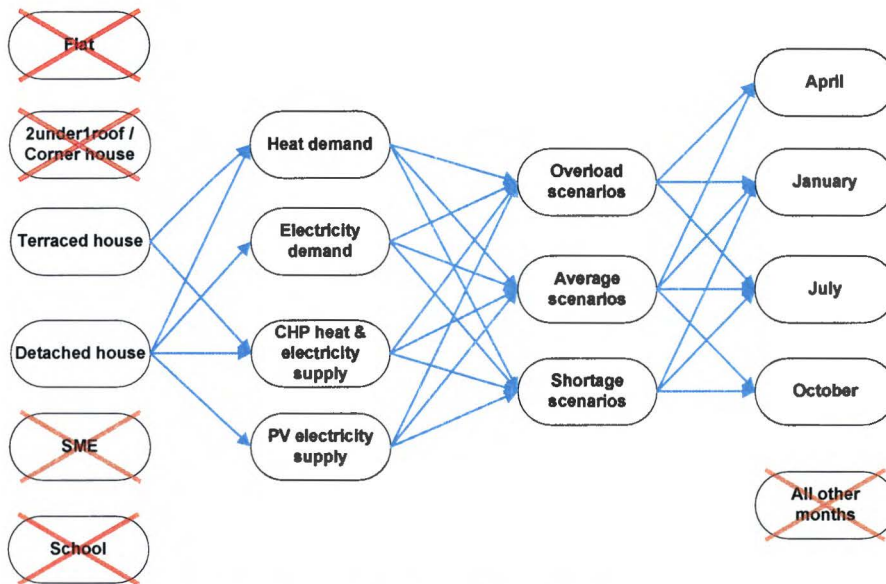


Figure 10: The variety of profiles used in this case study.

In the low voltage (LV) network different actors are connected to one another; like flats, corner houses, terraced houses, detached houses, small medium-sized enterprises (SME) and schools. To cut back on the amount of load and power output profiles, only two actors are taken into account: the terraced house and the detached house. One should remark that the links between the terraced house and the electricity demand as well as the terraced house and the photovoltaic (PV) electricity supply is left out in Figure 10. This is because the PV electricity supply and electricity demand will not distinguish between the detached and terraced house. The two different actors and their power supply systems generate 8 profiles: two heat demand profiles, only one electricity demand profile, two CHP heat power output profiles, two CHP electrical power output profiles and one PV power output profile.

For each of these profiles three kind of scenarios are generated, called the average, overload, and shortage scenario, resulting in 96 profiles. Figure 11 illustrates the generation of the overload and shortage scenarios. The overload scenarios take place at high electricity generation compared to the electricity demand. In these scenarios it is tried to create an overload by means of excess power supply. For the shortage scenarios this is the other way around. The most PV electricity yield will be in summer, when there is a lot of sun. CHP generates most electricity at high heat demand, i.e. at cold winter days. Because the generators are complementary, the self-supporting residential area needs to be assessed throughout the year and the profiles need to cover the seasonal differences. Figure 12 and Figure 13 show the KNMI wind velocity, outside temperature data, global irradiance and sun hours throughout the year [39]. These four weather characteristics determine the power output of PV and CHP. Because of the high sun power in July and the cold outside temperature in January, July will represent summer and January represents winter. The average, shortage as well as the overload scenarios will be assessed in these months. The average scenarios are also computed during spring and autumn to find out whether heat and electrical consumption are met as much as possible throughout the year.

<sup>2</sup> From Figure 10: 8 arrows x 12 arrows x 10 arrows = 960 profiles

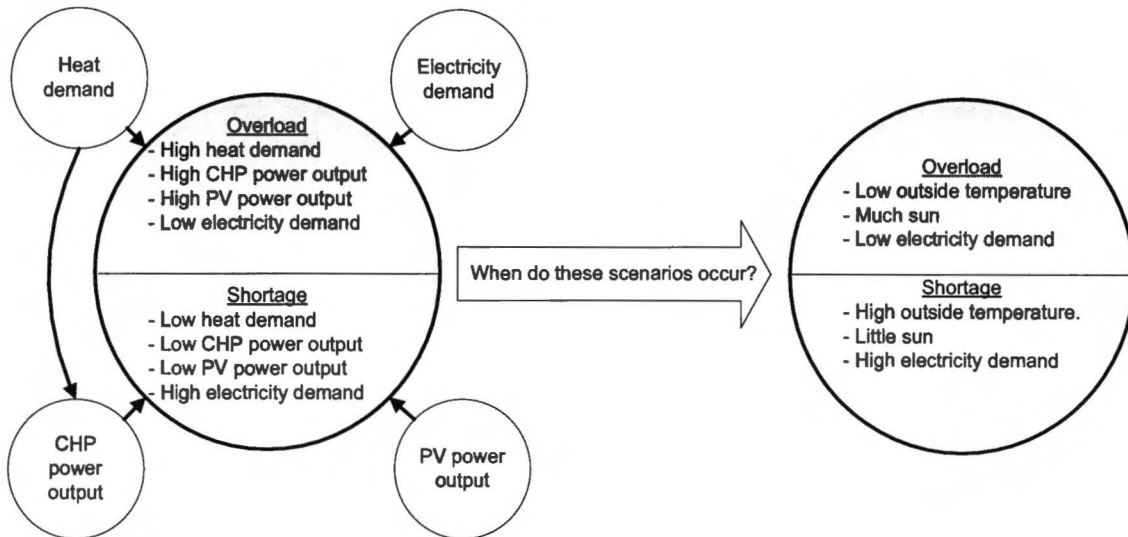


Figure 11: The generation of the overload and shortage scenarios.

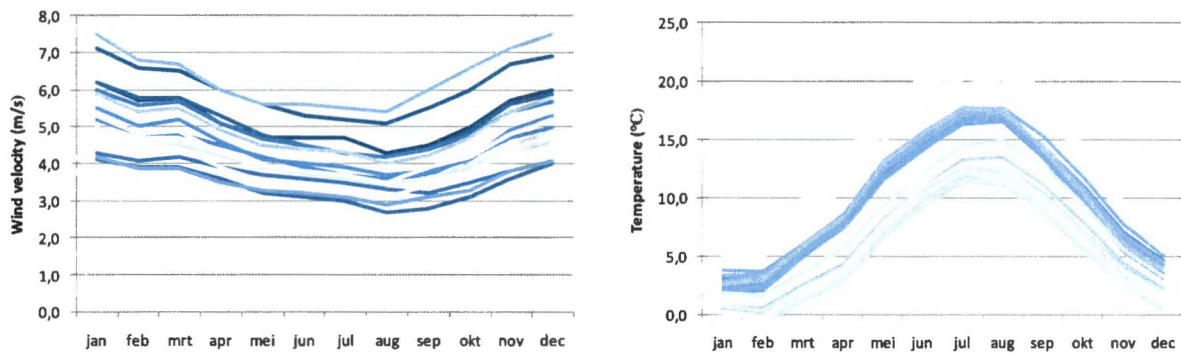


Figure 12: Wind velocity (left) and maximum, minimum and average temperatures (right) [39].

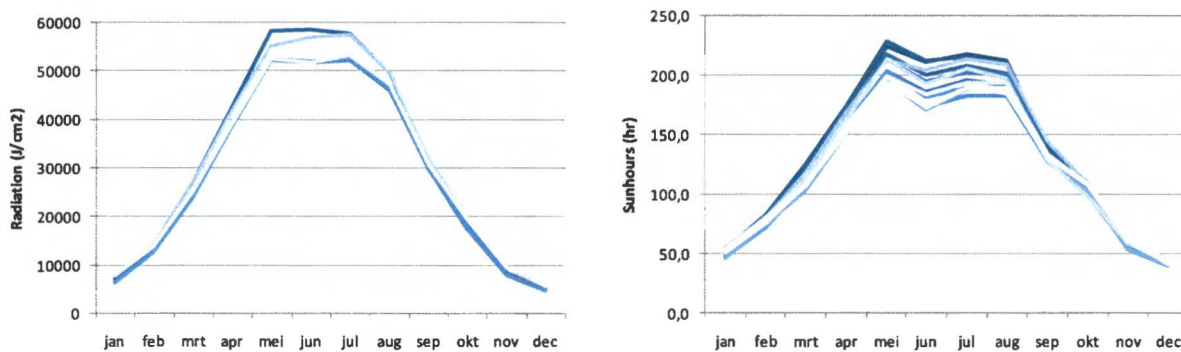


Figure 13: Global solar radiation (left) and sun hours (right) of the KNMI weather stations [39].

A shortage and an overload scenario will be included either during spring or autumn. From Figure 12 and Figure 13 it is concluded that during spring the outside temperature is low (high CHP power output) and more sun hours and solar radiation (high PV output) occur compared to autumn. Moreover, the electricity demand from

Figure 14 is also bigger during autumn than during spring. From this it is concluded that during spring the overload scenario will always exceed the autumn overload scenario and for the shortage scenario this is the other way around. A shortage scenario in spring is redundant, because the shortage scenario in autumn will be much worse. This is made clear in Figure 15. Since CHP is the main power source, the outside temperature is the deciding factor of what months to assess. The coldest month April will represent the overload and average scenario during spring (B) and as the shortage scenario should be during autumn where the weather involves higher temperatures (E), like October.



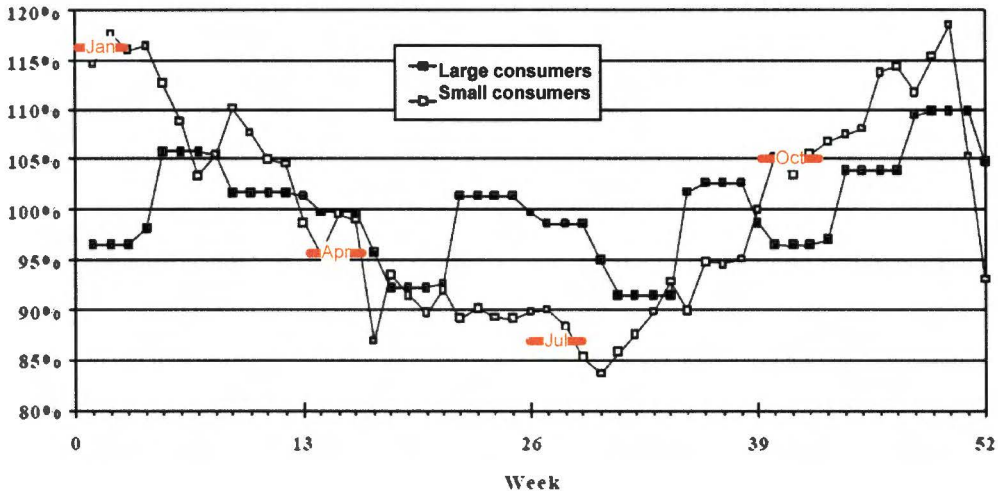


Figure 14: Daily electricity consumption throughout a year [22].

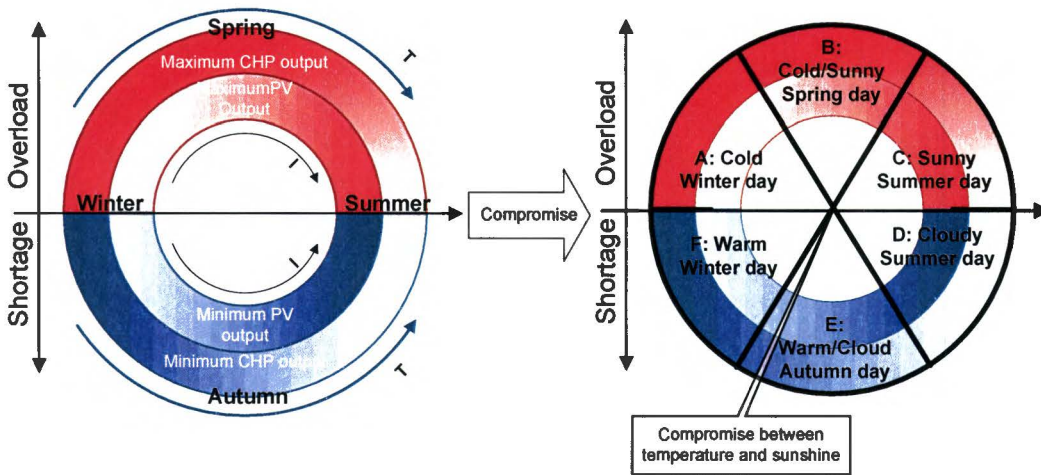


Figure 15: The generation of the overload and shortage scenarios with temperature  $T$  and sun hours  $I$ .

Concluding, a total of 10 scenarios are specified (Table 1) containing a week in which the self-supporting residential area is evaluated; 3 overload scenarios (in January, April and July), 3 shortage scenarios (in January, July and October) and 4 average scenarios (in January, April, July and October). The overload scenarios have high electricity generation compared to the demand, attributed to low outside temperature and much solar radiation. For the shortage scenarios this is the other way around. Because PV and CHP are complementary it is important to generate power profiles throughout the year. January and July are the months that rely on only CHP or PV respectively. In these months all three scenarios (average, overload and shortage) are investigated to keep all options open. Spring is most convenient for an overload scenario than autumn. During spring low outside temperatures and high sun power occur compared to autumn [39]; April, a cold month in Spring, will represent the overload scenario during spring, as the shortage scenario should be during autumn where the weather involves higher temperatures, like October. To cut back on the amount of power demand and supply profiles, only two actors are taken into account (the terraced house and the detached house). Nevertheless, total profiles run to 960. The average scenarios will be used for the design of the generators and storage devices, whereas all scenarios are used to assess the final design by load-flow calculations.

Scenarios	January	April	July	October
Overload	✓	✓	✓	✗
Average	✓	✓	✓	✓
Shortage	✓	✗	✓	✓

Table 1 The scenarios investigated in this case study.

## 6. The Energy Balance

The power and operation time of the energy supply needed from the distributed generators combined with on-site heat production are determined by balancing demand and supply as good as possible. The overall balance in the energy yield (kWh and MJ) and the real-time balance in power output ( $\text{kW}_e$  and  $\text{kW}_{th}$ ) must assure that in general the heat and electrical consumption are met as good as possible. This requires accurate demand and generator (heat-) power profiles at least throughout a week for every defined average scenario. The power demand profiles of this case study are obtained by the yearly energy consumption from [4] in combination with the temperature dependent hourly gas demand fractions and 15-minute-mean electricity demand fractions from [41] as is explained in section 6.1.

Section 6.2 gives the details of the formation of the generators' power output profiles. The combined heat and power (CHP) is heat controlled. The CHP operation time is therefore determined by the heat demand and the size of the heat storage vessel attached to the CHP. The CHP heat power output is used to determine the CHP electrical power output from which the CHP electricity yield is calculated. The electricity yield of the CHP is on its turn used to calculate the installed photovoltaic (PV) power from which the real-time PV power output profiles are confined. PV power output uses three variables to distinguish the scenarios: seasonally-adjusted amount of sun hours, the seasonally- and daily-adjusted sun irradiance and the possibility to include weather conditions, such as a cloudy or clear sky. From the resulting lack of simultaneity between the generators and the loads, the capacity and peak power needed from the storage devices are determined with the help of load-flow calculations. Section 6.3 clarifies this.

### 6.1 Demand-Side

The intention is to design a self-supporting residential area for the year 2010. In [4] the amount of yearly heat and electricity demand of the year 2010 is defined and used to form the heat and electricity demand profiles in this case study. To have an idea whether the forecasting yearly consumption from [4] for the year 2010 are good estimates, several outcomes from different studies are compared. Together with the yearly consumption [4], the gas and electricity demand fractions [41] form hourly heat demand profiles and 15-minute-mean electricity demand profiles throughout a week.

The heat demand profiles are generated from the hourly gas demand fractions from [41] of consumers that use less than  $5000 \text{ m}^3$  a year. The gas demand fractions are fractions of the total gas demand that will be consumed in one hour for every hour in the year 2007 based on measurements in the years before 2007. The gas demand fractions [41] include a temperature dependency. So, the fractions [41] will be used to form temperature dependent hourly profiles of the heat demand.

The electricity demand profiles are generated from the electricity demand fractions from [41] of consumers with at the most a 3x25 Ampere connection single tariff. The electricity demand fractions [41] contain fractions of 15 minutes throughout the year 2007 based on the years before 2007. It will be investigated whether the hourly and 15-minute fractions from 2007 are good estimates and whether the gas demand fractions are conform the heat demand fractions. The first step is described in Figure 16.

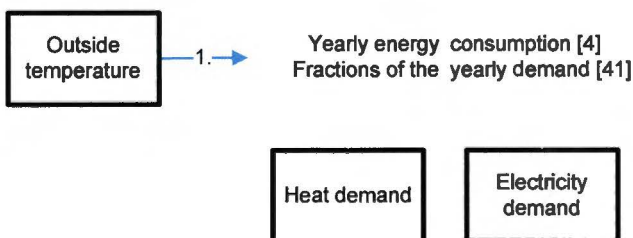


Figure 16: Step 1, the formation of demand profiles.

### 6.2 Supply-Side

The technical characteristics of the generators and storage devices are described in section 4.2. This report will also explain how the weekly (heat-) power output profiles of the CHP generators are formed, that is necessary to size the PV arrays and afterwards the battery energy storage (BES) devices, whereupon the load-flow calculations are able to evaluate the effects on the low voltage (LV) network.

To overcome misunderstandings in the interpretation of energy related terms used in this case study, an overview is presented in Table 2.



	Energy	Heat	Electricity
Balance	Energy supply and demand (MJ, kWh, kW)	Heat supply and demand (MJ, kW)	Electricity supply and demand (kWh, kW)
Supply	Energy supply (MJ, kWh, kW)	Heat supply (MJ, kW)	Electricity supply (kWh, kW)
Yield	Energy yield (MJ, kWh)	Heat yield (MJ)	Electricity yield (kWh)
Output	(Heat-)Power output (kW)	Heat-power output (kW)	Power output (kW)

Table 2: Overview of the energy related terms.

### 6.2.1 Heat Supply

The heat system comprises a CHP, a storage vessel and a supplementary heater. Since the heat demand profiles are hourly data, the heat balance is set for every hour. Every hour throughout a week it is determined whether the CHP operates, what part of the CHP heat yield is directly consumed, what part is stored in the heat storage vessel for later use and what is the contribution of the supplementary heater. The only designable factors of the CHP heat system are the kind of CHP and the size of the heat storage vessel. The supplementary heater is capable of supplying total heat demand if necessary.

The CHP will always produce heat and electricity at the same time, causing an abundance of either heat or electricity. It is not efficient to have an overshoot in heat supply, since it is difficult to dispose an overshoot in heat within the energy structure of this case study, while an overshoot in electrical power can easily be transported through the LV network to the upper grid. A heat overshoot endangers the CHP, therefore the CHP will be heat controlled. Meaning, the CHP will only operate if it is able to throw out the heat without overheating the system, that happens when the total of possible heat storage and heat demand is less than the CHP produces. So, the heat demand controls the operation time of the CHP in a way the system is not overheated. This heat control already proved its practicability.

The size of the heat storage vessel is an important decision. If the storage vessel is too large, the CHP produces an overall heat overload, devastating the energy efficiency of the CHP through heat losses. If the storage vessel is too small, the operation time of the CHP collapses which also effects the electricity yield. Therefore, it is stated that heat produced by the CHP must be consumed within a day, to have a reasonable operation time while heat losses are kept limited.

The resulting heat power output profiles will not participate in the load-flow calculations directly. Though, the heat supply will effect the electricity supply of the CHP by determining the heat controlled operation time of the CHP. Moreover, since the real-time (heat-) power output of the Microgen is fixed, the operation time only determines the electricity yield and power output profiles. Concluding, the operation time of the CHP is related to the heat demand and the size of the storage vessel and the CHP heat supply is the base of further calculations.

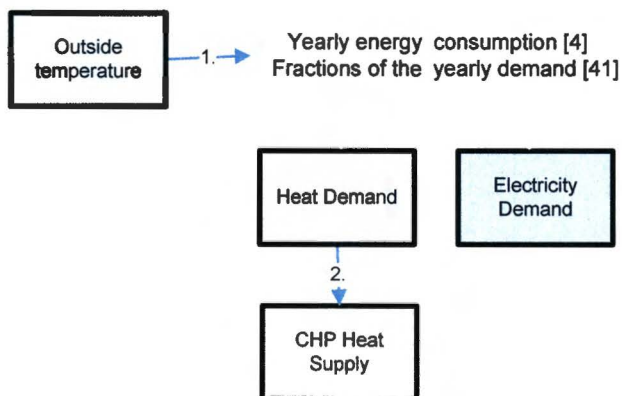


Figure 17: Step 2, determination of the CHP heat supply.

### 6.2.2 Electricity Supply

The electricity supply makes a distinction between the weekly electricity yield (kWh) and the real-time power output throughout a week ( $kW_e$ ). The CHP heat power output is used to determine the CHP electrical power output from which the CHP electricity yield is calculated. The electricity yield of the CHP is on its turn used to calculate the installed PV power from which the real-time PV power output profiles are confined. When both power profiles are finished the load-flow calculations of the average scenarios investigate the power and the capacity of the BES devices. The power output profiles must contain 15-minute-means, just like the electricity demand profiles.



### 6.2.2.1 Combined heat and power

The fixed heat and power output ( $1 \text{ kW}_e$  and  $4 \text{ kW}_{th}$ ) together with the real-time heat demand profiles determine the operation time of the CHP. These facts bring about an on-off power output profile of  $1 \text{ kW}_e$ . Since the CHP electricity supply is determined by the CHP heat supply (arrow 3 in Figure 18) that is of course caused by the heat demand (arrow 2 in Figure 18), the CHP power supply is dependent on the outside temperature (arrow 1 in Figure 18). The dependency between outside temperature and CHP electricity supply makes good shortage and overload scenarios in which the self-supporting residential area will be assessed in the next section.

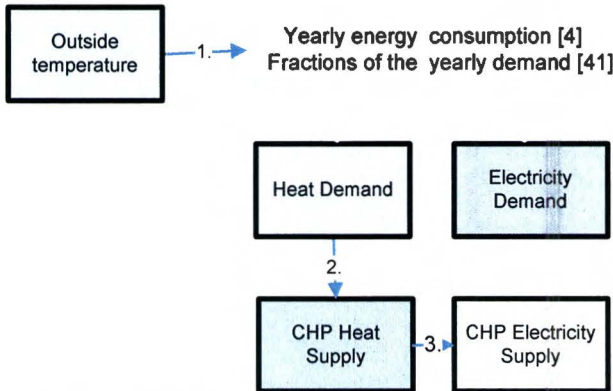


Figure 18: Step 3, determination of the CHP electricity supply.

### 6.2.2.2 Photovoltaic Arrays

The required installed PV power is determined by the electricity demand (arrow 6 in Figure 19) and the CHP electricity yield that already supplies a part of the electricity demand (arrow 4 in Figure 19) in the average scenarios throughout a week. After the installed PV power is optimized the PV power output profiles throughout a week need to be formed for the load-flow calculations. In case of PV, next to the operation-time, that changes for every season due to the amount of sun hours, also the sun-irradiance ( $\text{W/m}^2$ ) is an important factor for the power output. The amount of sun-irradiance changes during a day as well as along seasons. So, unlike the constant CHP power output of  $1 \text{ kW}_e$ , the PV power output is variable during the day and between seasons. Moreover, within each season the average, shortage and overload scenarios can be distinguished due to an average solar radiation profile (average-scenario), a solar-radiation profile under a cloudy sky (shortage-scenario) and a solar-radiation profile under a clear sky (overload scenario) that comes at hand when evaluating the self-supporting residential area in the overload and shortage scenario.

Concluding, solar radiation and amount of sun hours confine the daily profile of the PV power supply (arrow 5 in Figure 19) among the different scenarios. Therefore the PV power output has three factors to distinguish the scenarios: the seasonally-adjusted amount of sun hours, the seasonally- and daily-adjusted sun irradiance, and the possibility to include weather conditions.

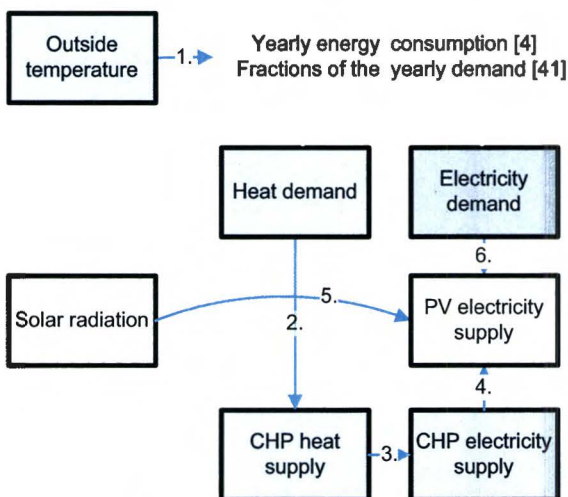


Figure 19: Step 4, determination of the PV electricity supply.

### 6.3 Battery Energy Storage

BES is to overcome the difference between demand and supply (kWh and kW) resulting from the lack of simultaneity (arrows 7, 8 and 9 in Figure 20). BES must fix the real-time power ( $kW_e$ ) imbalances as well as the overall electricity (kWh) imbalance within a week. BES can also service voltage levels, reduce system losses, cable and transformer loads. Nevertheless, the design of the BES in this case study is based on the target to bridge supply and demand that creates a self-supporting residential area. The BES characteristics need to be conform to the required peak power during reloading and discharging (1), storage capacity (2) and charge/discharge frequency (3). In load-flow calculations of Figure 20 the average scenarios are simulated in grid connected and island mode to find out this capacity and power needed from the BES in both situations. Afterwards, it is checked whether BES also has positive effects on the voltage levels, system losses, cable and transformer loads.

The operational mode of the BES has to be programmed in a macro of the computer simulation program 'Vision Network Analysis'. Next section explains more about this computer simulation program. The operational mode of the BES makes sure that only electricity from the distributed generators within the self-supporting residential area is stored. If the upper grid would feed the BES devices as well, unnecessary storage losses result when grid connected, and the effects of BES will become counterproductive. The upper grid would charge the BES and the loads simultaneously when the generators' power output is insufficient. When the generators' power output becomes sufficient afterwards, the BES would already be fully charged by the upper grid.

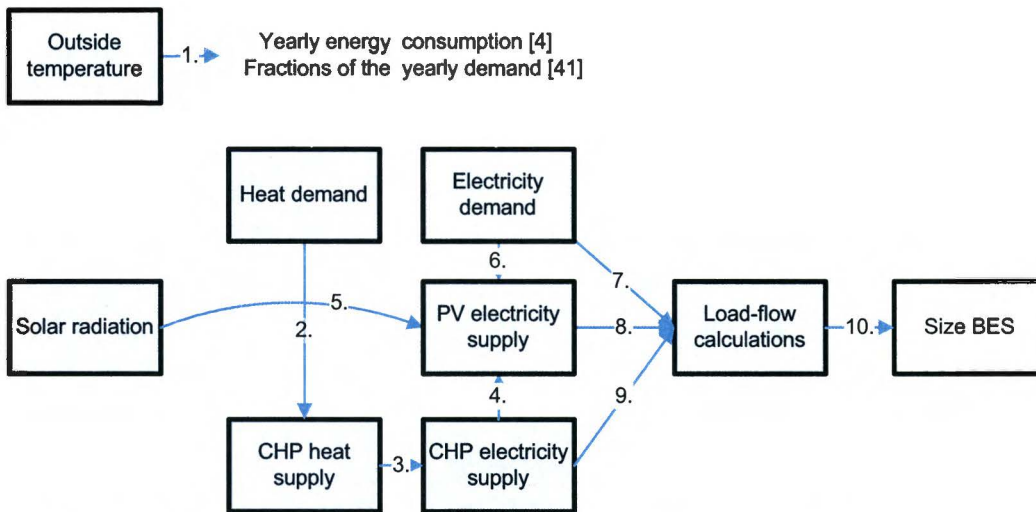


Figure 20: Step 5, determination of the capacity and power needed from the BES devices.

## 7. The Assessment

In the previous section it is explained how the power supply of the self-supporting residential area for a typical Dutch case is designed by the generation of load profiles during the average scenarios. The final goal of this case study is to find out whether the self-supporting residential area will be satisfactory in respect to the advantages assigned to the new alternative approach. Therefore, the effects on the low voltage (LV) network need to be assessed. In this section it will be explained how the effects of the implementation of distributed generation within a self-supporting residential area on the LV network are evaluated. This time the installed photovoltaic (PV) power and battery energy storage (BES) parameters are fixed and the overload and shortage scenarios are included. The same approach is used to form the overload and shortage load profiles as in the previous section, Figure 21.

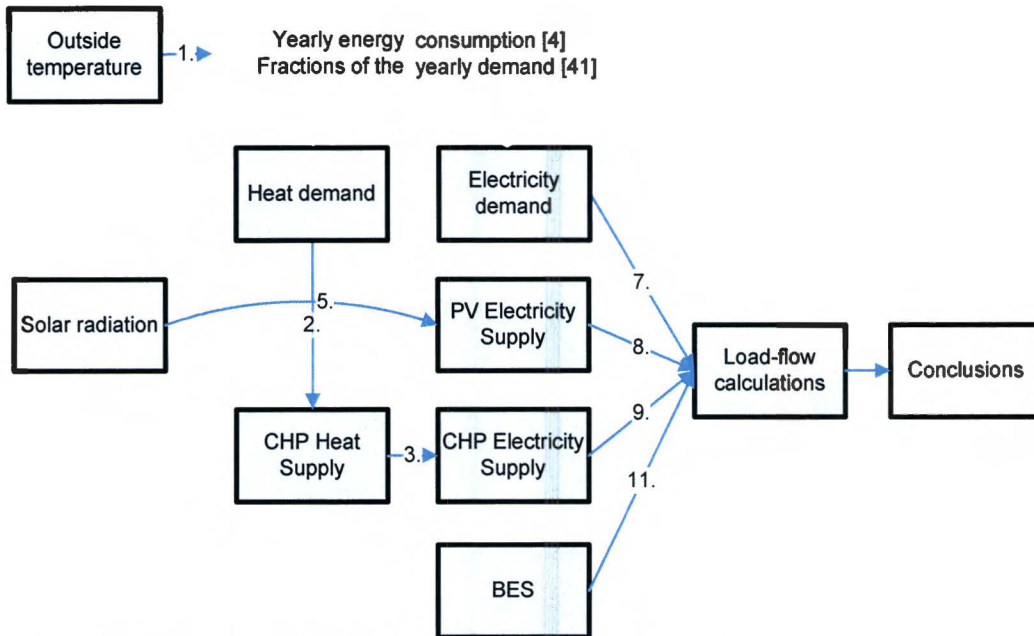


Figure 21: Step 6, Assessment of the self-supporting residential area.

The self-supporting residential area is in charge of its own power supply, that must not be inferior to the power supply as it is today. To comply with consumers' and network operator's needs, the self-supporting residential area needs to meet an extensive list of technical issues. It is important to quantify the technical issues and then select the parameters that serve the purpose of assessing the self-supporting residential area of this case study. The main quantifiable parameters that can be used to assess the alternative operational approach, copied from section 3, are:

1. the magnitude and direction of the power flows,
2. cable- and transformer loads,
3. steady-state voltage levels,
4. system losses,
5. a variety of power quality parameters (dips, harmonics, flicker, etc.),
6. and reliability and security indices (short-circuit current, failure-calculations, stability, selectivity of protections).

This case study will be restricted to steady-state situations, that include calculations of the first four parameters. Load-flow calculations are suitable for calculating the defined parameters stated above in steady-state; the magnitude and direction of real and reactive power, voltage levels, cable loads, transformer loads and system losses. Therefore, the load-flow function of the simulation program 'Vision Network Analysis', that makes use of the Newton-Raphson method [44], is used to assess these parameters. Total input from previous sections will be:

1. independent characteristics of the LV network; cables, source and transformer,
2. the loads (15-minute-mean demand profiles),
3. the generators (15-minute-mean power output profiles),
4. BES devices (capacity, power, number and location of the BES devices),
5. and the connection mode to the grid.



In this case study the power profiles require particular calculations several times in quick succession, changing the input data each time. 'Vision' made this possible with a programming editor provided for writing macros. Results can be automatically reported in Excel, with the user determining what data is included in the excel spreadsheet, like the quantifiable parameters that can be used to assess the alternative operational approach in this case study [44].

'Vision Network Analysis' from the company Phase to Phase makes use of the Newton-Raphson method. The load-flow calculations are based on solving the nodal voltage levels with network equations. Each system is modelled using as many network equations as there are nodes in the LV network. The solution process for this set of equations requires the complex voltage on one node as a reference. This reference node is connected to the source (swing bus). The voltage at the connection node of the source is fixed, both in magnitude and angle of  $0^\circ$ . The source (swing bus) supplies the difference between generation and load, including the network losses. The source can thus also be considered as a connection with the upper grid [44].

In the 'Vision' load-flow calculations cables are represented in accordance with the pi model, with resistance (R), inductive reactance (X) and capacitance reactance ( $X_C$ ), Figure 22. The transformer is modelled in accordance with Figure 23, in which R is principally determined by the short circuit loss, and the reactance (X) principally by the relative short-circuit power [44].

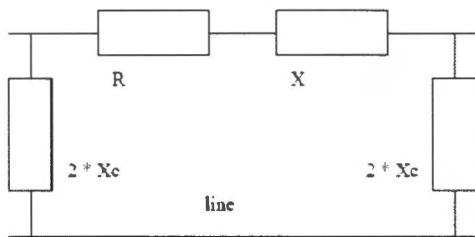


Figure 22: Vision model for cables [44]

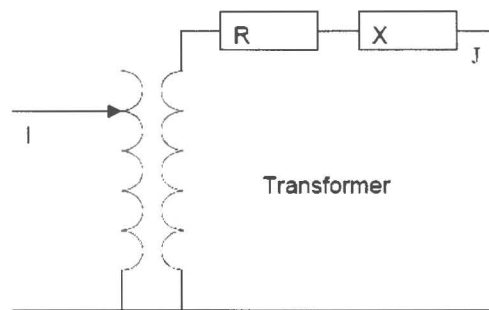


Figure 23: Vision model for the transformer [44]

At each node the loads extract a fixed apparent (S) power while the generators inject a fixed apparent power. The loads and generators present at each node are multiplied by a simultaneousness factor. Simultaneousness defines the fraction of the total connected load expected to occur simultaneously at each node [44]. The case-study's power profiles are levelled of, so a 100% simultaneity seems appropriate.

Moreover, the choice of a load behaviour is used to establish the voltage dependence of the load [44]:

1. 0% constant active and reactive power: constant admittance behaviour
2. 50% constant active and reactive power: constant current behaviour
3. 100% constant active and reactive power: constant power behaviour

At constant power, the rated power of the load will always remain constant, independently of the calculated node voltage level. Conversely, if the node voltage level increases, load current decreases and the other way around. The constant power load behaviour is applied in this case study, since constant power loads have noticeable effects on the grid [44].

'Vision' load-flow calculations treat synchronous generators with power factor control as negative loads of constant power. 'Vision' enables to change the input data for the load elements better than for synchronous generators, so the generators are represented by negative loads instead [44].

Concluding, the generated 15-minute-mean power profiles throughout a week require calculations several times in quick succession changing the input data each time. 'Vision' made this possible with a programming editor provided for writing macros. Within the macro also the operational control of the storage devices is programmed. 'Vision' load-flow calculations treat synchronous generators with power factor control as negative loads of constant power. Also the loads behave as constant power, which means that the rated power of the load will always remain constant, independently of the calculated node voltage. Consequently, if the node voltage increases, load current decreases and the other way around, so the loads will have maximum effect on the grid [44].

# Part C Case Study - Results

---

Section 8 expounds the design, defined by the electricity demand profiles, heat demand profiles and the (heat-) power output profiles. At first the demand profiles, composed by the yearly energy consumption from [4] and the electricity and gas demand fractions from [41], are checked on their usability and validity. From there, the power output profiles are determined by an overall balance of the energy demand and supply. The real-time power balance will complete the design by determining the peak power and capacity required from the battery energy storage (BES). The generated profiles and BES size are used in section 9, where the results of the load-flow calculations are computed for the different scenarios, including the overload and shortage scenarios, to assess the effects on the low voltage (LV) network.

## 8. The Energy Balance

In section 8.1 the demand profiles are formed that will be used to determine the combined heat and power (CHP) supply, as well as the installed photovoltaic (PV) power in section 8.2. Afterwards, the profiles serve as direct data input for the load-flow calculations used to size the storage devices in section 8.3. The demand profiles are formed by the yearly energy consumption [4] and fractions of the yearly energy consumption [41]. Extra effort is done to check the validity of the data that is used to form the profiles.

The design of the amount of PV and BES is based on the balance between demand and supply. This section scrutinizes the demand-side as well as the supply-side of the self-supporting residential area. Figure 12 showed the amount of profiles that have to be formed in this section. The completed electrical power profiles are found in Appendix C. The design is finished off by sizing battery energy storage (BES). In previous sections it is explained that the heat demand is the base for further calculations and will be discussed at first.

### 8.1 Demand-Side

The demand profiles are formed by the absolute yearly energy consumption [4] and fractions of the yearly energy consumption [41]. Extra effort is done to check the validity of the data that is used to form the profiles. The yearly demand data for 2010 from [4] seem good matches with the demand fractions throughout the year [41] and are representative for the detached and terraced houses in this case study. Though, it figures that the generated 15-minute-mean electricity profiles are quite levelled off. For that reason the simultaneity of all the peaks for every household within the LV network will be 100% during the load-flow calculations.

The yearly electricity demand amounts to 4084 kWh, the yearly heat demand of a detached house is 47.3 GJ and that of the terraced house comes to 38.6 GJ. The gas demand fractions separate the Temperature Dependent Profile (TDP) and Temperature Independent Profile (TIP). Adding up both values will give the fraction of the total gas demand that is consumed within that hour. The TDP reacts according to the effective temperature, which is the actual temperature minus the wind speed divided by 1.5. The TDP is valid until the heating point is crossed, when space heating is redundant. This approach is applied for the predefined scenarios in section 5. The daily and seasonal differences are already integrated in the gas and electricity fractions [41] and can not be changed [42][43].

#### 8.1.1 Heat Demand

It has proved very difficult to compare the data from different studies to the yearly heat consumption from [4], because it remains regularly ambiguous what parameters are taken into account in the heat demand calculations and measurements. There are four possibilities to obtain the heat demand, defined in Figure 24:

1. gas consumption,
2. primary gas demand,
3. primary heat demand,
4. and secondary heat demand.



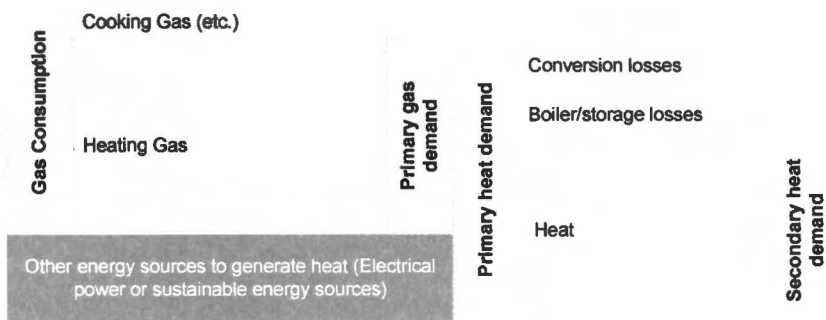


Figure 24: The definitions of households' heat demand in different studies.

In appendix A3 a short description of the case studies used in Figure 25 and Figure 26 is given. More than likely most of the case studies calculate secondary heat demand from the gas consumption (with or without cooking gas) with the help of average conversion efficiencies. Other case studies measured secondary heat demand of houses connected to residential area heating or by means of a survey. Unfortunately it is not always clear how the heat demand is specified in the literature references and therefore speculated. The yearly heat consumption from [4], used for this case study, is based on educated guesses of the secondary heat demand, meaning that the heat demand is defined as measured gas consumption corrected for cooking gas, other heat sources, conversion losses and future improvements in isolation.

The yearly heat demand of a detached house will be different from the terraced house. In Figure 25 the heat demand of the average households is presented and the home-specific heat demands are compared in Figure 26. The absolute data are encountered in Appendix A1. The source 2010 [4] on the x-axis that is used as the yearly heat consumption in this case study. If the linear graph connecting the bars is simply regarded as the reference, the heat consumption in [4] might be a little overestimated.

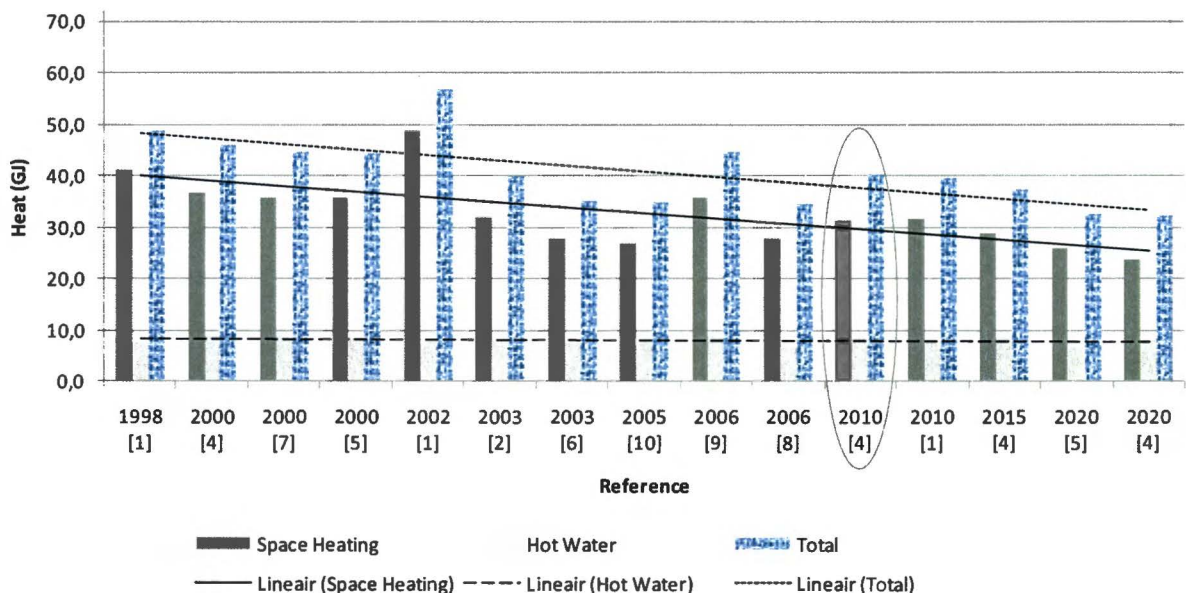


Figure 25: Yearly average heat demand (GJ)

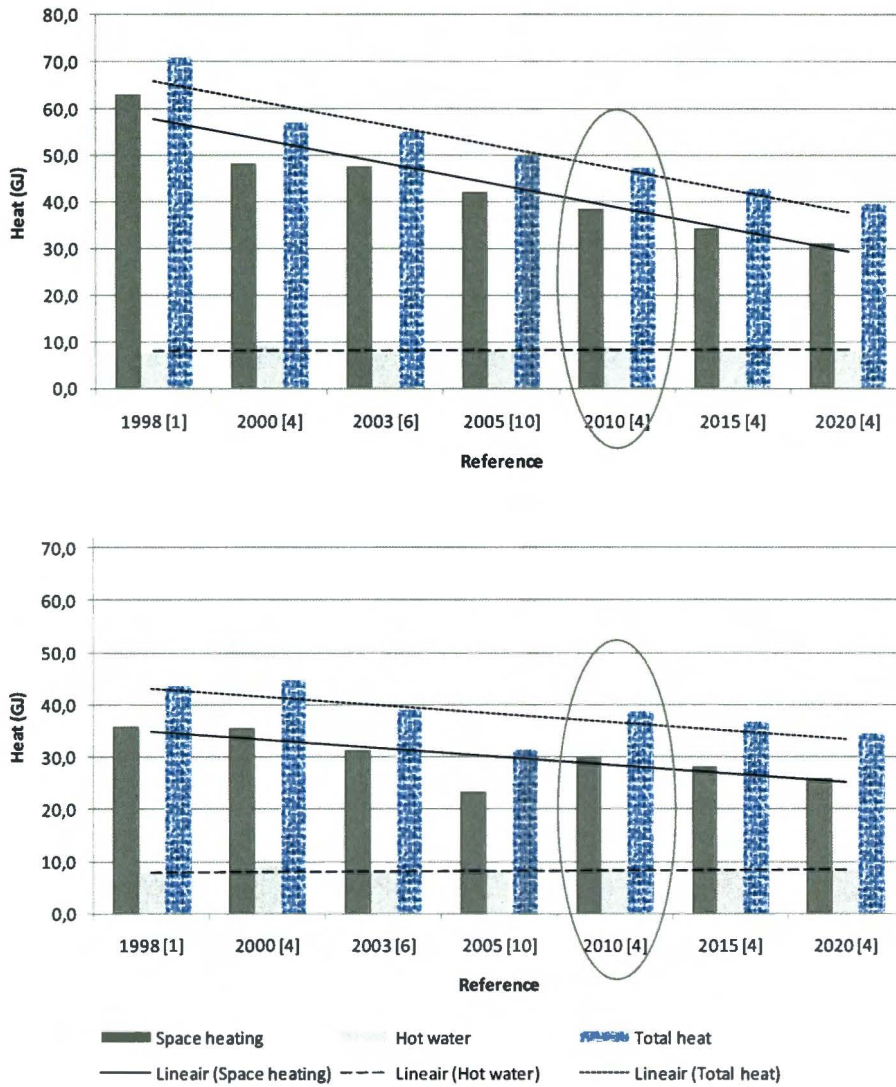


Figure 26: Yearly average heat demand (GJ) of a detached house (above) and a terraced house (below).

The gas demand fractions from [41] are used to form the final heat demand profiles throughout a week. The gas demand fractions [41] separate the TDP (generally space heating) and TIP (mostly hot water and cooking gas). Adding up both values will give the fraction of the total gas demand that is consumed within that hour. Figure 27 illustrates the calculation model per hour. The TDP reacts according to the effective temperature, which is the actual temperature ( $^{\circ}\text{C}$ ) minus the wind speed (m/s) divided by 1.5. The TDP is valid until the heating point is crossed, when space heating is redundant. The same approach is applied for the predefined scenarios of section 3 in Table 3. The daily and seasonal differences are already absorbed in the fractions throughout the year [41] and can not be changed [42].

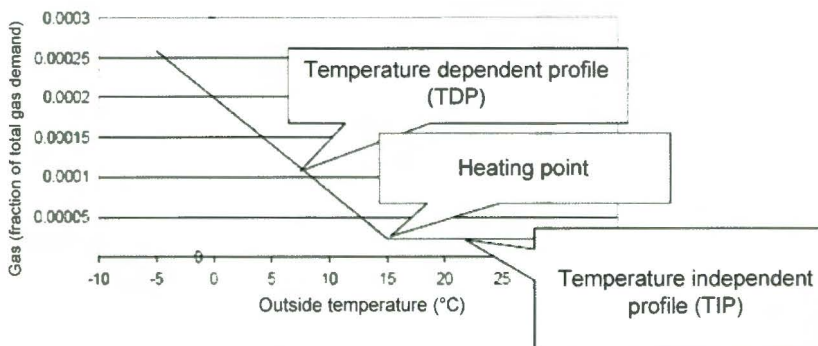


Figure 27: Calculation model for the gas demand of one hour. [42]



	Actual temperature (°C)			Wind speed (m/s)			Effective temperature (°C)		
	average	overload	shortage	average	overload	shortage	average	overload	shortage
January	4,1	-1	6,5	5	7,1	5	0,8	-5,7	3,2
April	9,3	2,5	-	4,2	6	-	6,5	-1,5	-
July	15,9	11	23,1	4,8	5,5	3	12,7	7,3	21,1
October	10,4	-	15	4,4	-	3,1	7,5	-	12,9

Table 3: The effective temperatures for the heat-power profiles. [Figure 12 and Figure 13]

Total hourly fractions of the gas demand throughout the year corresponds to one. The ratio of the total TDP to the total TIP in a year is comparable to the ratio of space heating and hot water. It is expected that the ratio of hot water is increasing compared to the space heating demand. The reason for this is the expected decrease of space heating in general because of better insulated houses. The change in contribution of hot water and space heating to the total heat demand is not changing in a way it is effecting the usability of the gas demand fractions [41] in the year 2007 for the heat demand profiles in 2010 as can be seen in Figure 28.

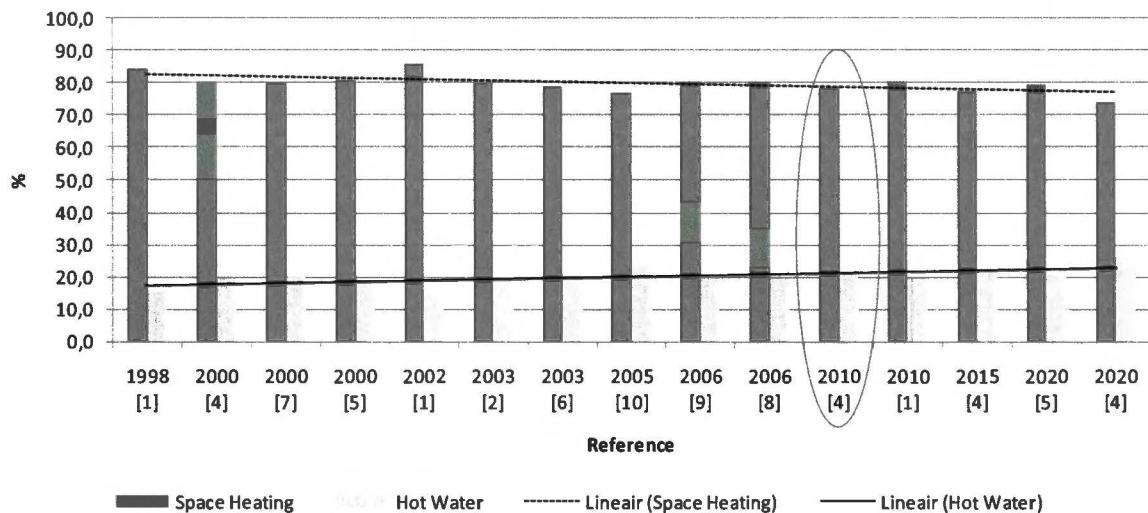


Figure 28: Yearly contribution to the total heat demand.

Heat demand of a household shows periodic fluctuations. The gas demand fractions [41] encompass hourly fluctuations throughout a year in 2007. A study on the fluctuations in heat demand [1] investigated with what power and frequency the heat demand for space heating in general fluctuates. On the whole, the dominant frequency is twice a day, in the evening and in the morning. During winter the dominant frequency changed to a dominant fluctuation per period of twenty-four hours. Nevertheless, the 12 hour frequency gave only a 60% accurate reproduction of the fluctuations in heat demand. The smallest less dominant frequency is 3.4 hours, meaning that with this interval the accuracy is optimal. Obviously following [1], the supposed hourly fractions of the gas demand [41] are very specific representatives for the space heating demand.

Though, the fluctuations in hot water demand are generally small. In 80% of the cases hot water demand takes less than half a minute [1]. According to the NEN standard 5128 the hot water supply must be capable to supply hot water demand as is shown in Figure 29. Because of the heat storage vessel in this case study, CHP (direct or via the storage vessel) meets the demand peaks up to 15 kW. This means that the supply of the demand peaks above 15 kW might be wrongly assigned to the CHP. This only happens roughly 1%<sup>3</sup> of the cases. Because the inclusion of this hot water profile only gains a little extra accuracy, it is better not to fiddle with the gas profiles as they are.

<sup>3</sup> Contribution hot water to total heat demand: 20%  
Percentage of peaks higher than 15 kW a day: 6% With CHP contribution of: 40%  
Amount of power output wrongly assigned to the CHP:  $0.20 \times 0.06 \times 0.60 = 0.008$



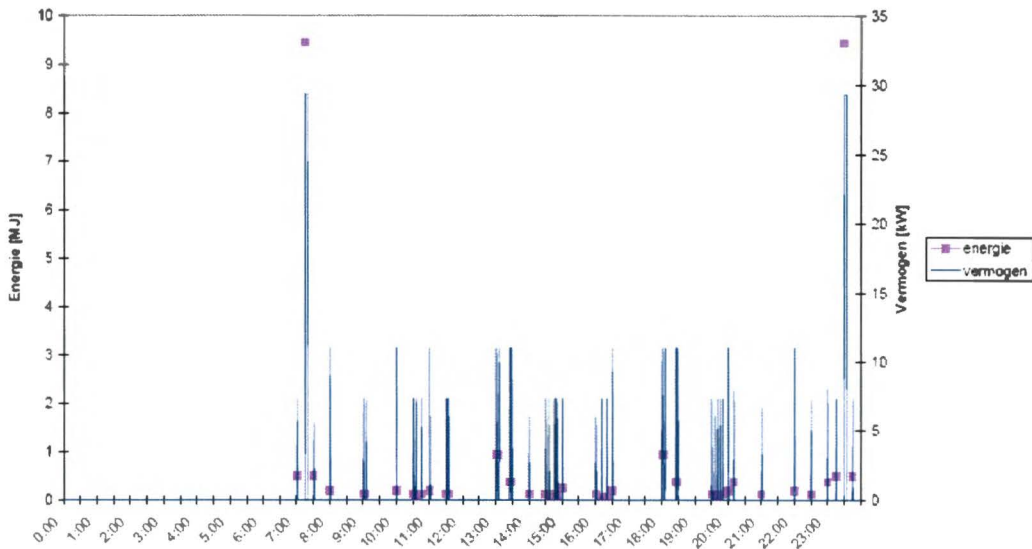


Figure 29: The standard hot water profile, according NEN 5128 [1].

Next to the space heating / hot water ratio and the hourly fluctuations, another issue of the gas demand fractions [41] have to be checked on its validity. The fractions used in this case study are gas demand instead of heat demand fractions. The difference between gas demand and heat demand is that gas demand is the primary heat consumption including conversion efficiencies and cooking gas and excluding other heat sources, such as solar panels and electric heating systems, as was already explained in Figure 24. Below it is investigated whether this effects the usability of hourly gas demand instead of hourly heat demand fractions in this case study.

#### 1. Exclusion of other heat sources:

In 2010 only a maximum of 2% of the space heating and a maximum of 1% of the hot water demand is supplied by distributed heat generators as solar panels. The electrical heat generators, like an electrical boiler, will provide a maximum of 2% of the hot water demand [5]. Since the space heating as well as the hot water exclude almost the same percentage, it is almost certain it does not distort the ratio between the TDP and TIP, i.e. the usability of hourly gas demand fractions as fractions of the heat demand.

#### 2. Exclusion of conversion losses:

According to literature the conversion and boiler losses are considerable. The average efficiency for space heating is 80-90% and for hot water 60-70%. In appendix A1 it is shown how many different values for the efficiencies are used in literature. Besides, it is again uncertain what is taken into account when calculating the efficiencies. Next to conversion losses also boiler/storage losses and transmission losses might join in the efficiencies. Only the conversion and boiler losses are important in this study to form heat demand profiles, since the CHP heating system deals with the same transmission losses as the conventional heat systems. Unfortunately, it is complicated to form these efficiencies from literature, so the correction for efficiencies can either generate or solve problems in the usability of gas fractions.

#### 3. Inclusion of cooking gas:

Only 3% of the gas is used for cooking [8]. But since this is only effecting the TIP, this might result in a distortion of the ratio between TIP and TDP when translating the gas demand fractions into heat demand fractions.

The total TDP in the gas demand fractions [41] throughout a year corresponds to 79.1% for space heating and total TIP matches 20.9% for hot water and cooking gas. If the gas demand fractions [41] are corrected by cooking gas and conversion efficiencies found in literature, this would result in 85% space heating and 15% hot water. The ratio between space heating and hot water in the corrected heat demand fractions diverge from the ratio between the absolute yearly space heating and hot water consumption in [4]. So the corrected heat demand profiles, will only induce false accuracy, and is therefore omitted with this marginal note. Concluding, the yearly heat consumption data of 2010 from [4] is a good match with the gas demand fractions in [41] and are both representative for the detached and terraced house heat demand in this case study.

Contribution	Space heating	Hot water
Original gas demand fractions [41]	79%	21%
Corrected heat demand fractions	85%	15%
Yearly heat consumption average house [4]	79%	21%
Yearly heat consumption detached house [4]	82%	18%
Yearly heat consumption terraced house [4]	78%	22%

Table 4: Contribution of space heating and hot water on the total demand.

### 8.1.2 Electricity Demand

The electrical power demand profiles are formed by the same sources as the heat demand. This time no distinction is made between the electricity demand of the detached house and the terraced house. The 4084 kWh a year in 2010 from [4] is a good estimate for the electricity demand by an average household, Figure 30.

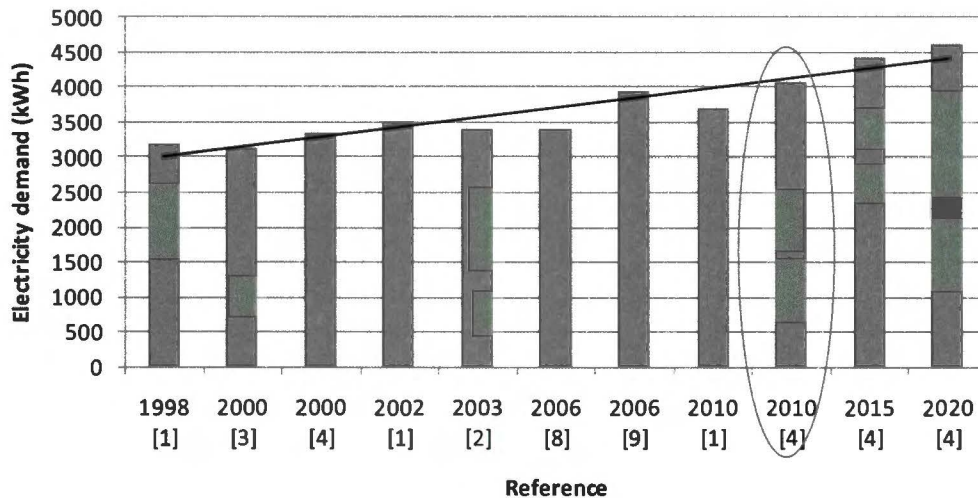


Figure 30: Yearly average electricity demand of a household.

The electricity demand profiles that are used in this case study are also constructed by the electricity demand fractions from [41]. The electricity demand fractions [41] are fractions of the yearly electricity demand that will be consumed in 15 minutes throughout the year. Total fractions in a year sum up to 1. The electricity demand fractions are not constructible like the gas demand fractions by changing the effective temperature. Therefore only small contrasts are possible between the eventual electrical power demand profiles in the overload, average and shortage scenarios. The daily and seasonal effects on the power demand are already admitted in the 15-minute-mean electricity demand fractions [41] throughout the year.

From [1] it appears that an interval of 2.4-minute-mean fractions give a 95% accurate reproduction of the fluctuations in electricity demand. This study also measured the power demand per minute of one household, Figure 31. It appears that 90% of the time the power demand is below 1 kW<sub>e</sub>. The yearly electricity consumption of 4084 kWh a year in combination with the 15-minute-mean fractions of the electricity demand [41], the power demand in this case study will be for 99.9% below 1 kW<sub>e</sub>. Disregarding the small sample size of [1], it can be concluded that this case study is missing out on 10% of the peaks exceeding 1 kW<sub>e</sub>. However, the steady-state voltage standards of the NetCode are based on 10-minute-means, meaning that the standards already allow missing out on about 7% of the peaks.



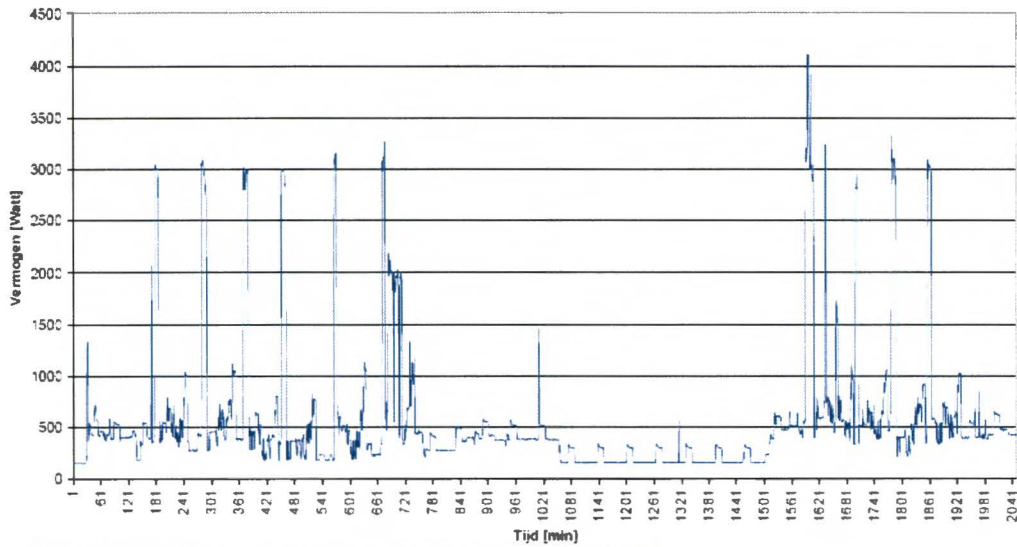


Figure 31: the power demand per minute of one household [1].

Anyway, it figures that the 15-minute-means together with the average of a large sample has levelled of the power demand profile. For that reason the simultaneity of all the peaks for every household within the low voltage (LV) network will be 100% during the load-flow calculations.

### 8.1.3 Heat and Electricity Demand Profiles

The generated demand profiles from the yearly energy consumption [4] and demand fraction [41], are shown in Appendix C and Figure 32 to Figure 34. Appendix C shows the real-time power profiles throughout the week. In Figure 32 to Figure 34 the range of the heat and electricity demand is displayed. The boxes represent 68% of the data. The projections give the maximum and the minimum. In July and October the differences in heat demand between the detached and terraced houses are negligible. In January and April the heat demand is very high compared to July and October. In January and April the biggest difference in heat demand are obtained between the detached and the terraced house, but also between the scenarios. This is attributed to the temperature dependency of the heat demand and the respectively cold months January and April.

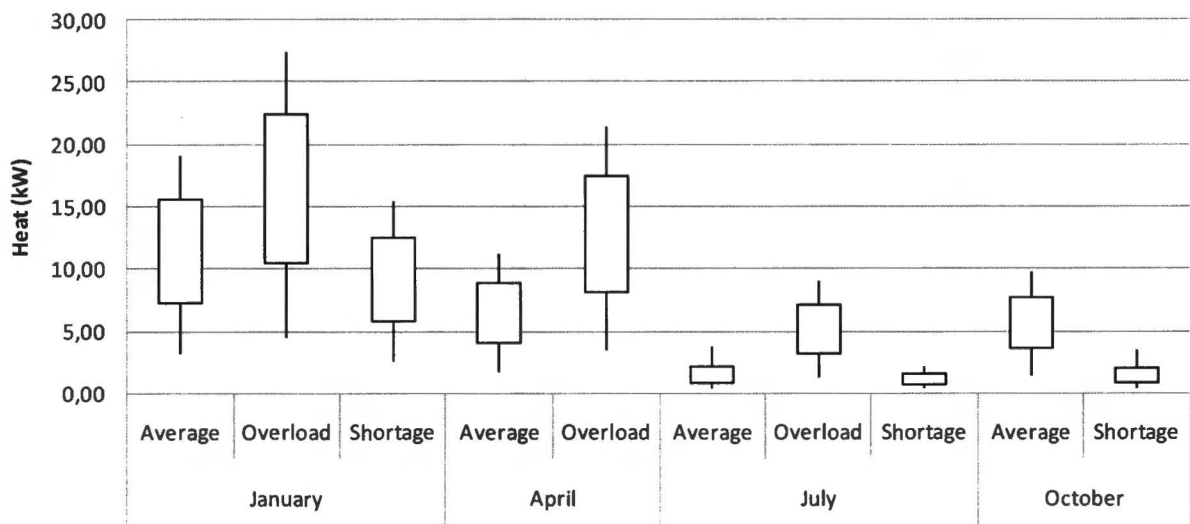


Figure 32: Range of the hourly heat demand of a detached house for different scenarios.

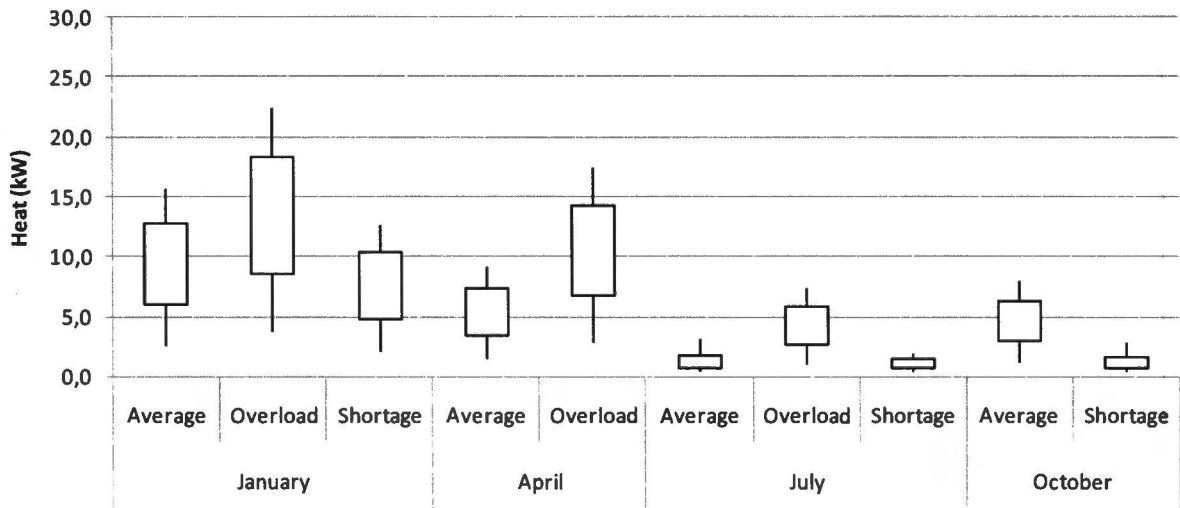


Figure 33: Range of the hourly heat demand of a terraced house for different scenarios.

In case of the power demand no distinction is made between the detached and the terraced houses. The difference in power demand between the average, overload and shortage scenarios are insignificant, because the lack of dependent changeable variable like temperature. Though, the difference between January, April, July and October is clearly shown in Figure 34. The electricity demand fractions [41] bring about seasonal differences

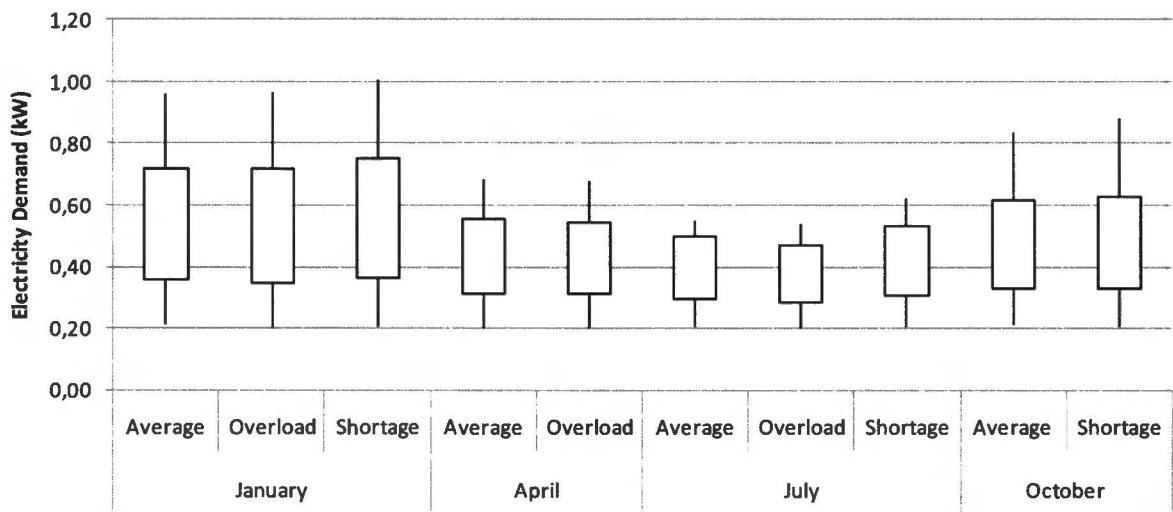


Figure 34: 15-minute-mean power demand per household for the different scenarios.

## 8.2 Supply-Side

The main task of the heat power output profiles is to deduce the operation time of the CHP. The CHP heating system consists of a CHP, storage vessel and supplementary heater. Every hour it is investigated whether the heat is supplied directly by the CHP, indirectly with the help of the heat storage vessel or by the supplementary heater. Of course, the CHP must operate as much as possible, since only the CHP itself produces electricity as well. The heat power output profiles are determined in excel spreadsheets. In case of a vessel temperature of 90 °C, the maximum energy is reached in the vessel (200 litres), since it is not advisable to reach temperatures closer to the boiling point. Energy will not be extracted from the vessel at a vessel temperature below 65 °C, since this is not desirable for health considerations. Furthermore, the CHP can only be turned on twice a day, otherwise the CHP system might wear out.



### 8.2.1 Heat Supply

The Microgen (with a 4 kW<sub>th</sub> heat power) ejects the lowest heat power of all Stirling CHPs on the market within two years, without being inferior to the electrical power output. Figure 35 shows a time-delay between the eventual heat power output and the actual running of the CHP before and after the CHP switches on or of. There are three reasons why the switching effect is not expected to be of great importance for the heat power output profiles. Firstly, during the start-up the Microgen needs to heat up, decreasing the real-time heat power output. However, when the CHP shuts down, the heat is yet rejected, eventually supplying the households. Secondly, the hourly averages level off the few minutes that the CHP operates at half speed. These two reasons indicate that the operation time of the CHP does not change because of the switching effect. Since the main task of the heat power profiles is to deduce the operation time of the CHP, the switching effect is not taken into account when generating the heat power output profiles. Concluding, the CHP heat power output immediately delivers heat and the heat power remains stable during the operation time delivering 14.4 MJ an hour.

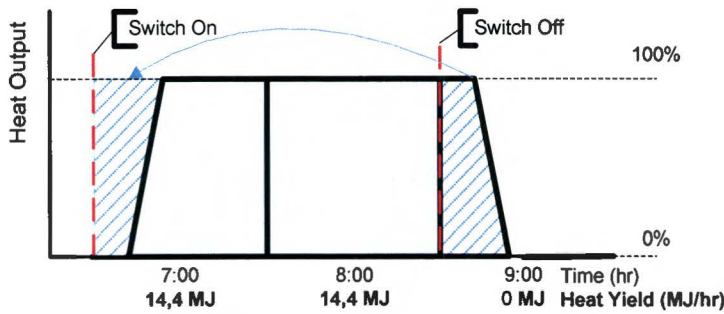


Figure 35: Start- and stop effects on the CHP heat-power.

The heating system consists of a CHP, storage vessel and supplementary heater. This heating system is always able to supply the heat demand. It is investigated whether the heat is supplied directly by the CHP, indirectly with the help of the heat storage vessel or by the supplementary heater. Of course, the CHP must operate as much as possible, since only the CHP itself produces electricity as well. The heat power output profiles are determined in excel spreadsheets. Table 5 gives an example of a heat output profile of a detached house throughout an average October day when the effective temperature is 7.5 °C.

Heat Balance - average October week - freestanding house (MJ)									
	Column A	Column B	Column C	Column D	Column E	Column F	Column G	Column H	Column I
	Time of day	Heat-demand	Heat yield CHP	Discrepancy	Energy content vessel	Available energy vessel	Direct use CHP	Heat used vessel	Supplementary heat supply
Day 1	0:00	1,8		-1,8	34,8	0,0	0,0	0,0	1,8
	1:00	1,4		-1,4	34,1	0,0	0,0	0,0	1,4
	2:00	1,4		-1,4	33,5	0,0	0,0	0,0	1,4
	3:00	1,5		-1,5	32,8	0,0	0,0	0,0	1,5
	4:00	1,7		-1,7	32,1	0,0	0,0	0,0	1,7
	5:00	2,4		-2,4	31,5	0,0	0,0	0,0	2,4
	6:00	6,1		-6,1	30,9	0,0	0,0	0,0	6,1
	7:00	8,2	14,4	6,2	42,1	5,3	8,2	-6,2	0,0
	8:00	8,1	14,4	6,3	47,4	10,6	8,1	-6,3	0,0
	9:00	6,7	14,4	7,7	54,0	17,2	6,7	-7,7	0,0
	10:00	5,9		-5,9	47,1	10,3	0,0	5,9	0,0
	11:00	5,4		-5,4	40,9	4,1	0,0	5,4	0,0
	12:00	5,2		-5,2	36,1	0,0	0,0	4,1	1,1
	13:00	5,0		-5,0	35,4	0,0	0,0	0,0	5,0
	14:00	4,9		-4,9	34,7	0,0	0,0	0,0	4,9
	15:00	5,4		-5,4	34,0	0,0	0,0	0,0	5,4
	16:00	6,4		-6,4	33,3	0,0	0,0	0,0	6,4
	17:00	7,7	14,4	6,7	39,2	2,4	7,7	-6,7	0,0
	18:00	7,6	14,4	6,8	45,1	8,2	7,6	-6,8	0,0
	19:00	7,3	14,4	7,1	51,2	14,3	7,3	-7,1	0,0
	20:00	6,9	14,4	7,5	57,5	20,7	6,9	-7,5	0,0
	21:00	6,1		-6,1	50,4	13,6	0,0	6,1	0,0
	22:00	4,7		-4,7	44,8	7,9	0,0	4,7	0,0
	23:00	2,8		-2,8	41,1	4,3	0,0	2,8	0,0
Day 2	0:00	etc.	etc.	etc.	etc.	etc.	etc.	etc.	etc.
	1:00	...	...	...	...	...	...	...	...

Table 5: Excel spreadsheet to determine the CHP heat power output profile.

Column A represents the time of day throughout the week from which the hourly heat power output profiles are determined. Column B is the hourly average heat demand (MJ) of a detached or terraced house specifically for every hour throughout a week. The third column contains the CHP input that is filled in by hand to discover the operation time of the CHP. When the CHP operates throughout an hour, the hourly average heat yield (MJ) in column C is filled in. In column D the discrepancy between the CHP heat yield and the heat demand is calculated (MJ). This amount of heat (positive or negative) is rectified by the storage vessel, if possible, otherwise by the supplementary heater. Column E keeps the energy content of the heat storage vessel up to date from which it is decided, whether it is possible to extract or put heat into the vessel. Column E takes into consideration the capacity and the hourly heat losses of the heat storage vessel (2%)<sup>4</sup>. The maximum energy stored in the vessel (200 litres) is 57.8 MJ<sup>4</sup>, because in that case the vessel temperature is 90 °C and it is not advisable to reach temperatures closer to the boiling point. To survey the situation clearly, column F determines the extractable energy from the vessel (MJ). Energy will not be extracted from the vessel when the energy contain is 36.8 MJ or lower, since a vessel temperature below 65 °C is not desirable for health considerations. The eventual results are reproduced in the last three columns, representing the direct heat yield of the CHP (Column G), the heat supplied by the storage vessel indirectly by the CHP (Column H) and by the supplementary heater (Column I). The total of the positive values in the last three columns equal to the heat demand. The operation time of CHP is construed from column C.

Figure 36 gives a detailed description of the excel spreadsheet method per hour. The CHP is turned on at the hours with the highest heat demand of that day. The start / stop violation is the first restriction on the CHP. The CHP turns on only twice a day to prevent wastage [32]. Secondly the vessel temperatures must not be violated. If it does violate the maximum temperature, the CHP is turned off again and it is seen what happens if the CHP operates at the second-best hour of the demand. When this happens, the storage vessel and supplementary heater take over the heat supply.

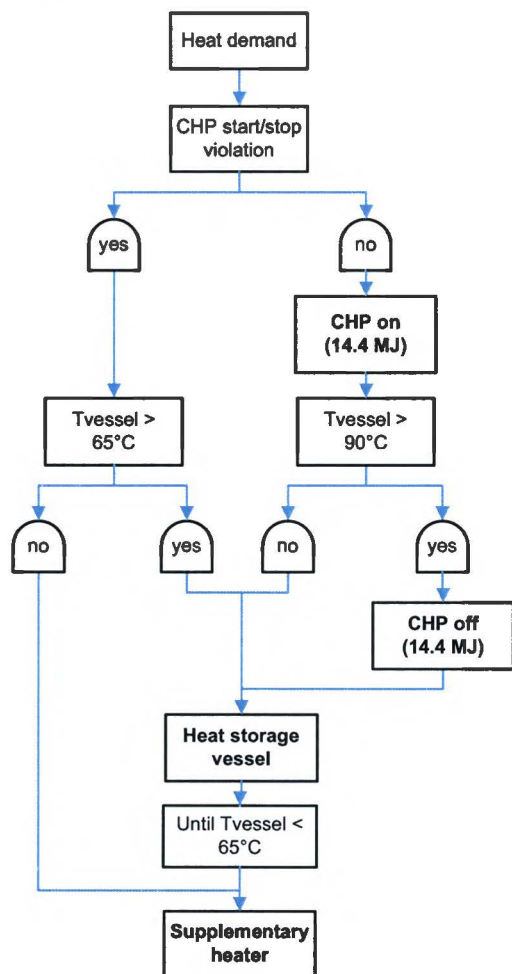


Figure 36: Graphical model of the excel-spreadsheet in Table 5 for every row representing one hour.

4 Energy-content vessel (E<sub>vessel</sub>) = V<sub>vessel</sub> x c<sub>water</sub> x (T<sub>vessel</sub>-T<sub>outside</sub>)  
 Storage loss (S<sub>l</sub>) range from 9 to 24 kJ/hr/°C  
 Efficiency = 1 - [ S<sub>l</sub>(T<sub>vessel</sub>-T<sub>outside</sub>) / E<sub>vessel</sub> ]  
 Hourly storage efficiency ranges from 97 to 99%



In Figure 37 the operation time curve of the heat power demand (detached house) is visualized by the continuous black line. The continuous grey line represents the operation time curve of the Microgen (4 kW<sub>th</sub>) CHP with the 200 litre vessel, as is calculated above and applied in this case study. The Microgen operation time with a storage vessel is compared to the Microgen operation time without a storage vessel from which the operation time is determined by the fact that the horizontal dark dotted line can not cross the heat demand. If the dotted line crosses the heat demand, supply is higher than demand which overheats the system by increasing the working fluid temperature. When this happens, the Microgen shuts down automatically. It appears that the storage vessel increases the Microgen operation time from a few hundred hours to 3000 hours.

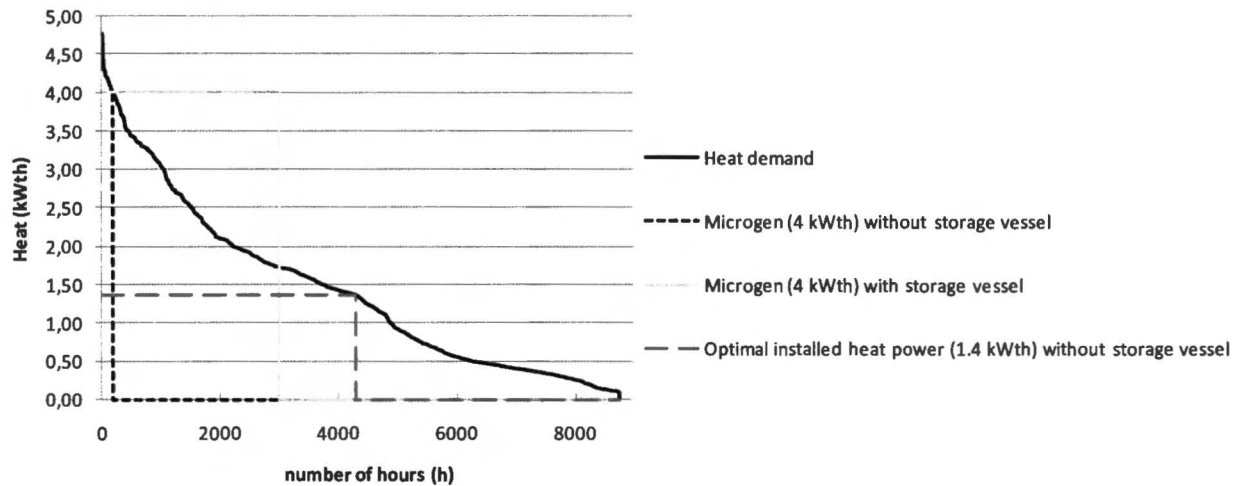


Figure 37: Operation time curve of the heat power throughout a year. Detached house.

To compare the heat yield of both situations the x-axis is multiplied with the y-axis from Figure 37 into Figure 38. The Microgen heat yield (including heat storage losses) is 7 times higher with storage vessel. The Microgen with storage vessel almost reaches the maximum possible energy yield, which endorses the early choice of the 200 litre storage vessel. The optimal installed heat power output that obtains the highest heat yield without a storage vessel, is also deduced from this graph. The optimal installed heat power amounts to 1.4 kW<sub>th</sub>, which is even lower than the Microgen heat power output. The operation time of a 1.4 kW<sub>th</sub> installed CHP without storage vessel is 40% higher than the operation time of the Microgen with storage vessel (Figure 37). Nevertheless, Figure 39 shows that the effects on total energy yield is limited. Figure 39 sums up the electricity yield (the operation time times 1 kW<sub>e</sub>) and the heat yield. However, the fixed electrical power output of 1 kW<sub>e</sub> aims too high for a 1.4 kW<sub>th</sub> installed CHP. Sophisticated technologies are needed to get a power to heat ratio of 1 : 1.4, if even possible. Concluding, the power output of the Microgen is quite good if it includes a storage vessel, but yet a lower or changeable heat power output increases operation time instantly.

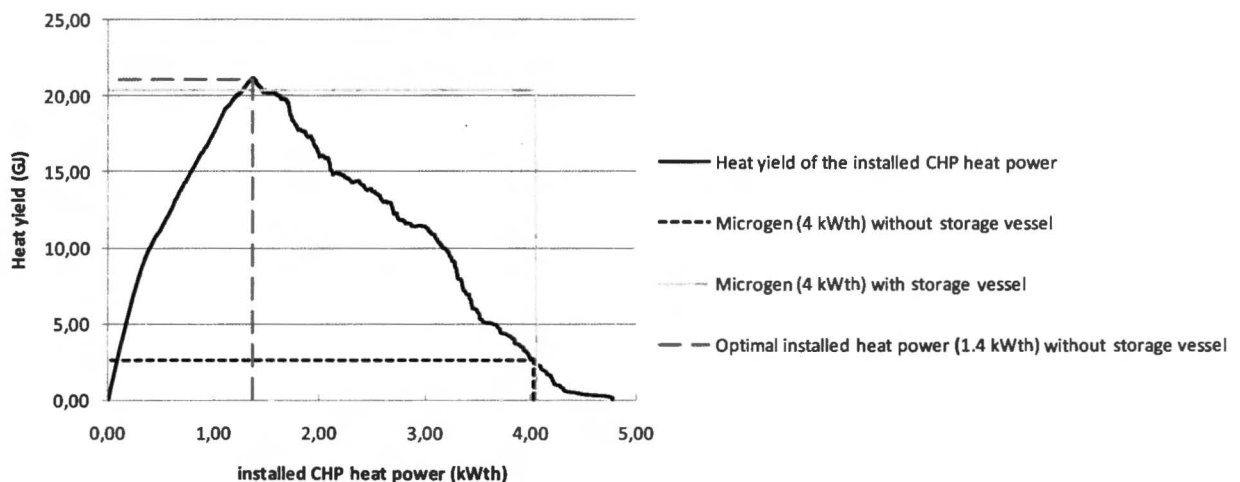


Figure 38: Yearly heat yield per kW<sub>th</sub> installed for a detached house.

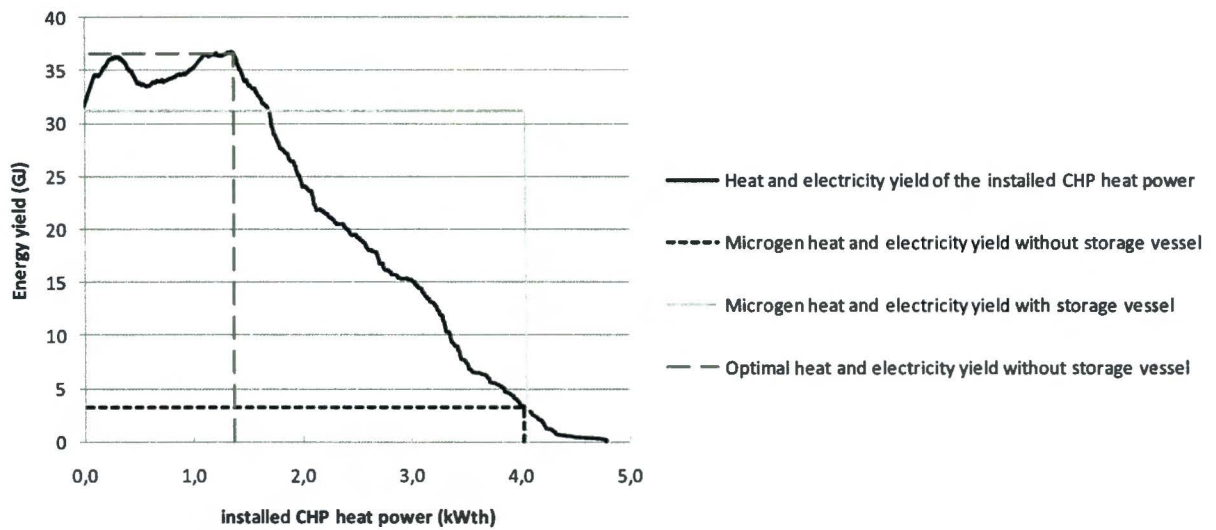


Figure 39: Yearly energy yield per kW<sub>th</sub> installed for a detached house, assumed fixed power output of 1 kW<sub>e</sub>.

### 8.2.2 Results Heat Supply

Figure 40 and Figure 41 show the absolute heat yield of the different elements of the heating system. The absolute heat values per week are encountered in Appendix B. In January and April much more heat is required. The biggest difference is seen in the direct CHP heat yield as an immediate result of the heat demand. The absolute participation of the heat vessel (indirect CHP) does not change much between scenarios, as well as the storage losses. The supplementary heater is turned on when the CHP heat power output is too low (January overload) or too high. The supplementary heater takes over the heat supply when the CHP power output is too high compared to the heat demand, because in that case the heat storage vessel is immediately overheated. This explains the difference in the supplementary heater participation between the average January scenario and the other scenarios with lower heat demand. Figure 42 and Figure 43 will clarify this.

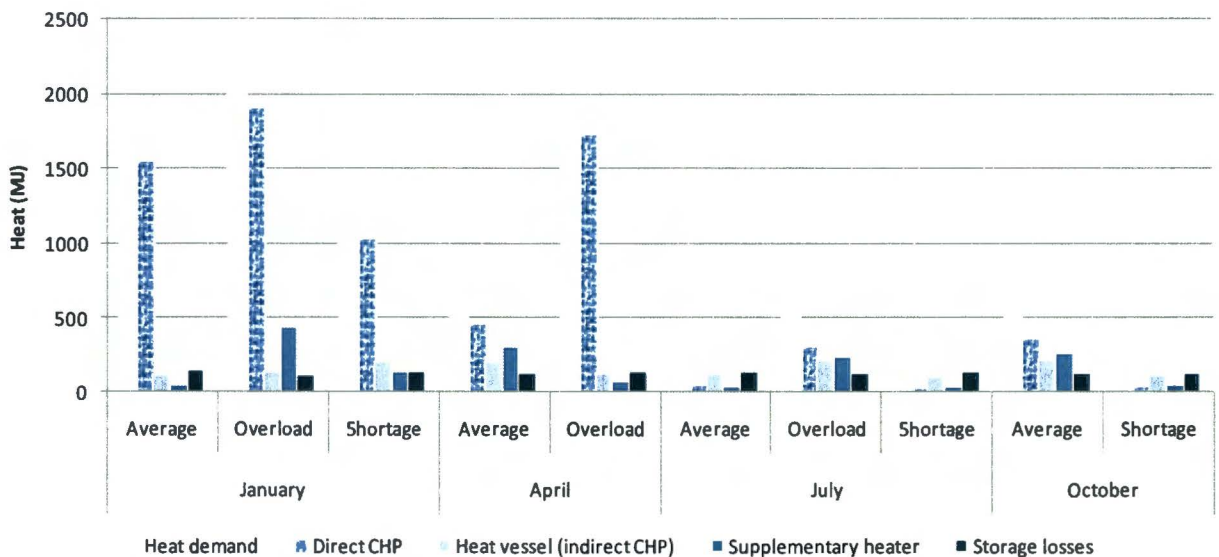


Figure 40: Absolute heat yield and demand within a week of a detached house for different scenarios.



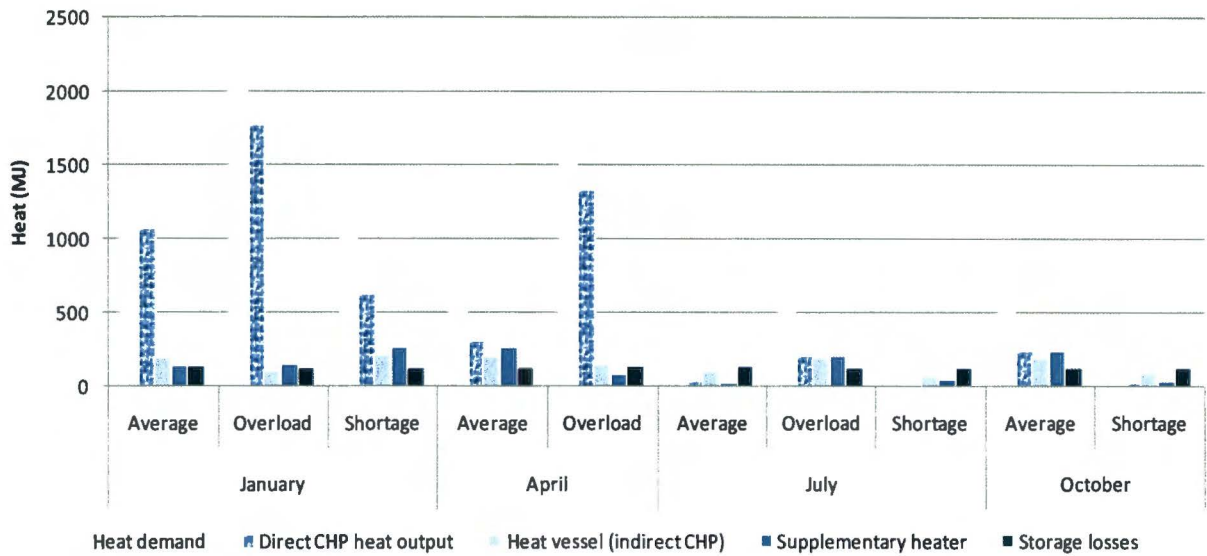


Figure 41: Absolute heat yield and demand within a week of a terraced house for different scenarios.

The average scenarios of Figure 40 and Figure 41 are reordered in Figure 42, so it is feasible to assess the proportions between the elements of the heat system for every month. Clockwise the direct CHP, heat storage vessel, supplementary heater and storage losses are illustrated. Every slice represents the heat yield or losses in MJ throughout a week. CHP supplies at least three quarters of the total heat yield (exclusive of the heat storage losses) that is consumed in the four average weeks; directly or with the help of the storage vessel. The participation of the CHP in July is nil. Remarkable is the extreme low participation of the supplementary heater in January again. Because of the high heat demand in January, the operation time of the CHP increases and the supplementary heater is redundant. In short, the  $4 \text{ kW}_{th}$  is a perfect fit in January. The storage losses are high, almost as high as what the vessel supplies. Though, before one queries the profitability of the storage vessel, one should still take in the extension of the operation time that is advantageous for the electricity supply.

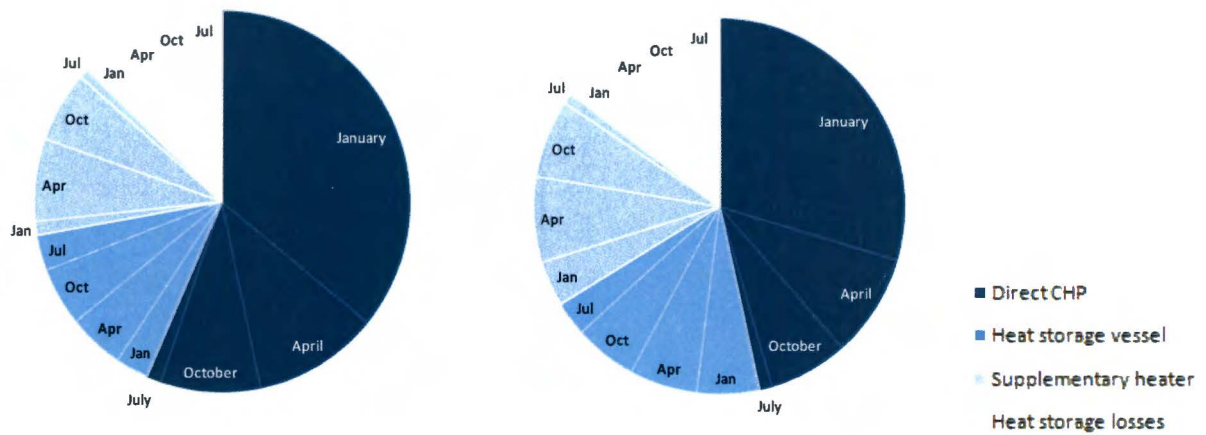


Figure 42: Reordering of the average scenarios in figure 42/43. Left detached house, right terraced house.

In Figure 43 the proportions of the total heat demand are shown per scenario. For each scenario the hundred percent represents the total heat demand within a week of that scenario. In these graphs it is very clear that the installed heat power of the CHP is too high in July and October, that causes big storage losses and participation of the supplementary heater.

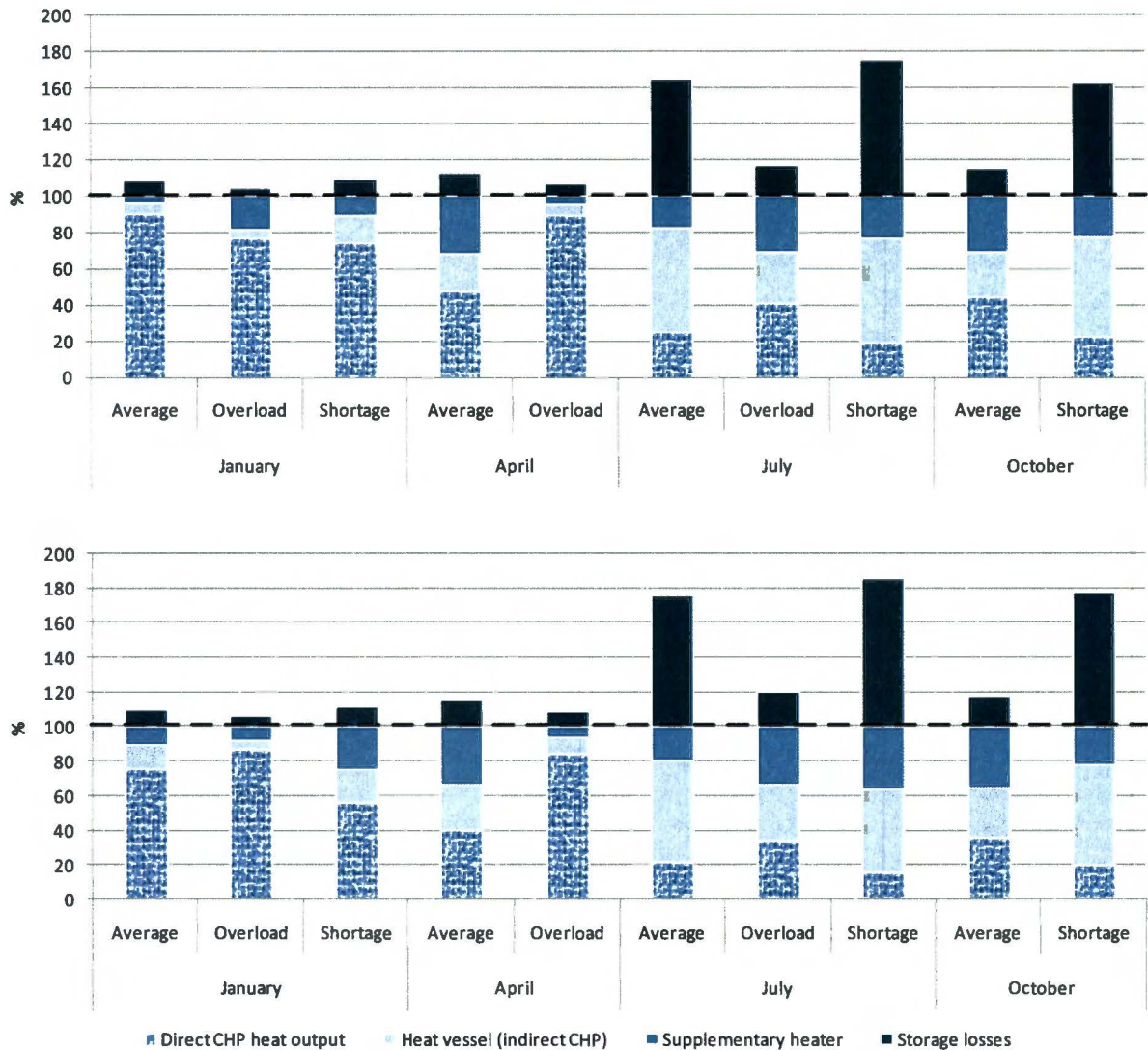


Figure 43: Percentage of the total heat demand within a week of a detached (above) and a terraced house (below) for different scenarios.

### 8.2.3 Electricity Supply

The operation time is also applicable to the Microgen electricity supply, yet it is transformed into the same time-scale as the electricity demand profiles. Switching effects on the electricity power output are integrated. From the balance between the CHP electricity yield and electricity demand throughout a week in the predefined scenarios it is immediately clear that the PV arrays can either improve or worsen the electricity balance per scenario. The highest reduction of power shortcomings compared to the increase in surplus appear at a  $1 \text{ kW}_{\text{peak}}$  installed PV power. With the help of the Photovoltaic Geographical Information System (PVGIS) PV estimation utility of the European Commission, the crystalline PV electricity yield is calculated and daily profiles are formed for the load-flow calculations.



### 8.2.3.1 Combined heat and power

Section 8.2.1 determined the operation time. The operation time is also applicable to the electricity supply. Though, since the electricity profiles are 15-minute-means, the operation time is transformed into the same time-scale. The CHP heat power output is fixed (4 kW<sub>th</sub>), also during (de-)activating the CHP, because the heat thrown out by the system after deactivation equals the heat that was ‘lost’ at the start-up. Moreover, during the hourly means the switching effect was negligible. In Figure 35 the shaded part is therefore shifted from the right to the left, squaring off the profile completely, which is also shown in Figure 44. The CHP electrical power output represents 15-minute-means instead of hourly means. Furthermore, the start-up losses are not recovered after deactivating the CHP as is the case for the heat supply. Concluding, the electricity power output diverges from 1 kW<sub>e</sub> after (de-)activating the CHP pursuing the green coloured path.

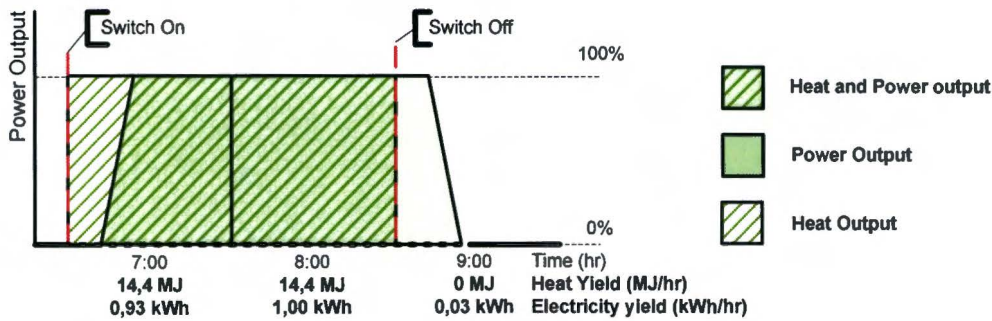


Figure 44: Start- and stop effect on CHP (heat-)power.

In Figure 45 the (de-)activation of the CHP is measured. After turning on the Microgen, it takes 2 minutes for the generator to supply electricity to the grid. After that, the power output raises slowly to full capacity. The 15-minute-mean electricity supply of a start-up delivers 71%<sup>5</sup> of the nominal 15-minute-mean electricity supply, corresponding to an average electricity yield of 0.18 kWh in 15 minutes and a continuous average power output of 0.72 kW<sub>e</sub> after start-up. When the Microgen is deactivated, it takes 3.5 minutes before the generator completely stops delivering power. In the 15 minutes *after* the CHP is deactivated the CHP electricity supply is 12%<sup>6</sup> of the nominal electricity supply, corresponding to an average electricity yield of 0.03 kWh in 15 minutes and a continuous power output of 0.12 kW<sub>e</sub> after the CHP is turned down. Concluding, the CHP power profile starts with 0.72 kW<sub>e</sub> for the first 15 minutes and remains 1 kW<sub>e</sub> until the CHP is switched off. The power profile finishes off with 0.12 kW<sub>e</sub> along the 15 minutes after the CHP has been turned off. The profiles of the detached house can be found in the Appendix C.

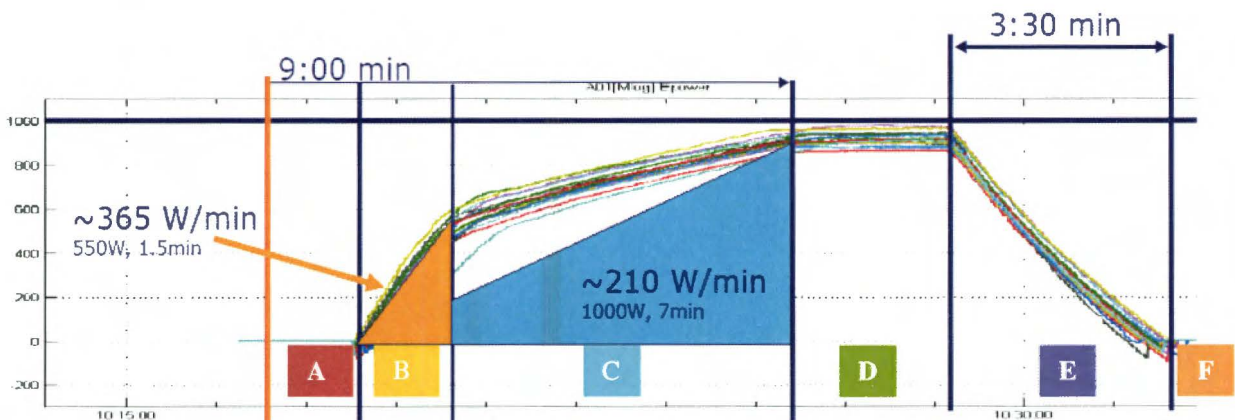


Figure 45: Measured start- and stop of the Microgen [32]. The graph plots power output (W<sub>e</sub>) over time.

<sup>5</sup> Average start-up power output:  $[(t_A \times P_A) + (t_B \times P_B) + (t_C \times P_C) + ((15 - t_A - t_B - t_C) \times P_D)] / 15$ , where  $P_x$  is averaged over  $t_x$ .  $[(2 \times 0kW_e) + (1.5 \times 275W_e) + (5.5 \times 775W_e) + (6 \times 1kW_e)] / 15 = 711W_e$ . And  $(711/1000) \times 100\% = 71.1\%$

<sup>6</sup> Average shut-down power output:  $[(t_E \times P_E) + ((15 - t_E) \times P_F)] / 15$ , where  $P_x$  is averaged over  $t_x$ .  $[(3.5 \times 500W_e) + (11.5 \times 0W_e)] / 15 = 116W_e$ . And  $(116/1000) \times 100\% = 11.6\%$ .

### 8.2.3.2 Solar cells

The PV electricity yield is supposed to overrule the weekly discrepancy of the electricity demand and the CHP electricity yield in the average scenarios. From ‘From grid 1’ in Table 6 it is immediately clear that this is difficult, since the CHP already created excess electricity yield in January. So, the installation of the PV panels can either improve or worsen the electricity balance.

Weekly yield (kWh)	Demand	CHP	From grid 1	1 kW PV	From grid 2	<i>kWp optimal</i>
January	90,4	126,7	-36,2	5,5	-41,8	-6,6 kW
April	72,8	55,4	17,4	23,0	-5,6	0,8 kW
July	66,7	22,4	44,3	25,4	18,9	1,7 kW
October	79,3	44,4	34,9	12,7	22,2	2,8 kW

Table 6: Electricity balance of a detached house with and without PV electricity yield.

The power output of the Philips crystalline solar cells (PSM 125) is determined at the optimum inclination angle of 36° all south-oriented with the help of the Photovoltaic Geographical Information System (PVGIS). PVGIS is a research, demonstration and policy support instrument for geographical assessment of the solar energy resource in the context of integrated management of distributed energy generation. PVGIS combines expertise from laboratory research, monitoring and testing with geographical knowledge to analyse technical, environmental and socio-economic factors of solar electricity generation. This application is firstly employed to calculate the weekly average electricity generation (kWh) of 1kW<sub>peak</sub> crystalline PV power with defined module-inclination and orientation. From this average electricity generation the optimal kW<sub>peak</sub> PV power is calculated in the last column of Table 6 for each average week. The optimal installed PV power per household varies from -6.6 kW<sub>peak</sub> in January to 2.8 kW<sub>peak</sub> in October. Taking into account the variation in seasonal electricity yield per kW<sub>peak</sub> installed, the optimal installed PV power approximates 0.9 kW<sub>peak</sub><sup>7</sup>.

The eventual installed PV power will be limited by manufactured PV installations. The PSM 125 of Philips is taken as an example. Every panel contains an area of 1 m<sup>2</sup> and are sold in sets of 2 panels. An area of 8 m<sup>2</sup> produces 1 kW<sub>peak</sub> which is closest to 0.9 kW<sub>peak</sub>. The need of PV power installed is much bigger in July and October, but 8 panels on a roof top area (all south-oriented and at the optimal inclination angle) is difficult to exceed. In ‘From grid 2’ (Table 6) the new electricity balance of the average weeks are calculated when PV is included. When the PV electricity yield is included in the average scenarios, all average scenarios improve except in January. There is 11.2<sup>8</sup> kWh more excess electricity yield, but on the other hand 55.5<sup>9</sup> kWh less shortage in those four weeks. Moreover, the adverse effects of the installed PV power during moments of excess power supply are solvable by turning off the CHP and let the supplementary heater take over the heat supply, whereas a shortage will be definite.



Figure 46: Example of a roof top area covered by 8 m<sup>2</sup> crystalline PV arrays [45]

$${}^7 \text{ month} \Sigma[(kW_e / kW_{\text{peak}})_{\text{month}} \times (\text{Optimal } kW_{\text{peak}})_{\text{month}}] / \text{month} \Sigma[(\text{Optimal } kW_{\text{peak}})_{\text{month}}] = \text{Optimal } kW_{\text{peak}}$$

$$(5.5 \times -6.6 + 23.0 \times 0.8 + 25.4 \times 1.7 + 12.7 \times 2.8) / (5.5 + 23.0 + 25.4 + 12.7) = 0.91 \text{ kW}_{\text{peak}}$$

<sup>8</sup> A = “from grid 1” and B = “from grid 2”.

Increase in overload =  $\text{month} \Sigma[A_{\text{month}} - B_{\text{month}}]$ , (1) only if B < 0 and (2) if A > 0, than take A = 0.  
 $(41.6 - 36.2) + (5.6 - 0) = 11.2 \text{ kWh}$

<sup>9</sup> Decrease in shortage =  $\text{month} \Sigma[A_{\text{month}} - B_{\text{month}}]$ , (1) only if A > 0 and (2) if B < 0, than take B = 0.  
 $17.4 + (44.3 - 18.9) + (34.9 - 22.2) = 55.5 \text{ kWh}$



Secondly, PVGIS can get daily profiles of clear-sky and real-sky irradiances for a chosen month for a selected module inclination and orientation. The calculator takes into account also the shadowing by local terrain features. In excel spreadsheets the daily electricity power output profiles are formed. The reactive power output is mainly formed by the inverter capacitance [36]. Electronic converters have a power factor of mainly 0.95 or higher. Every month three scenarios can be generated; global irradiance, diffuse irradiance and global clear-sky irradiance. The profiles can be found in the Appendix C.

### 8.2.4 Results Electricity Supply

The absolute values of the results in electricity supply are presented in Appendix B. Figure 47 demonstrates the difference between the CHP electricity yield of the detached and terraced house. The biggest difference is shown in the scenarios with high heat demand, like January, where the CHP supplies most of the electricity and heat.

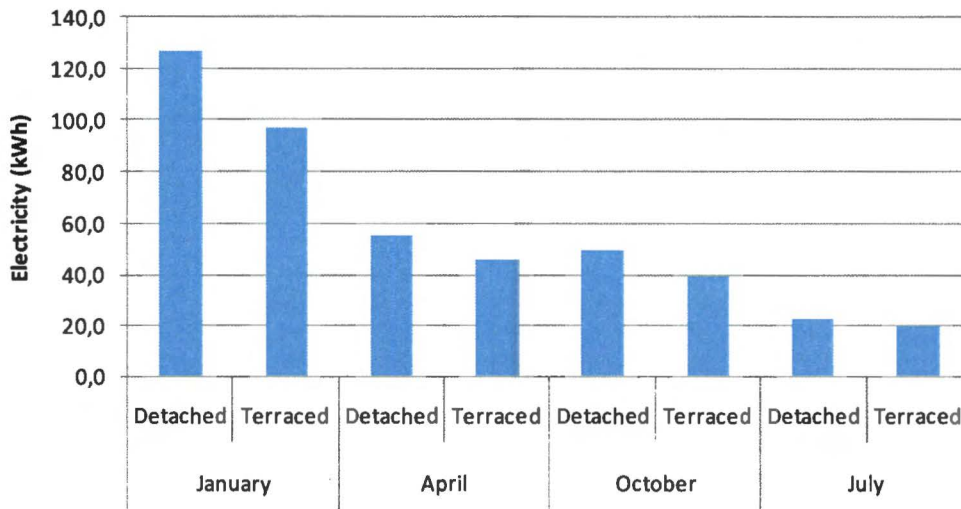


Figure 47: CHP electricity yield of the detached and terraced house within a week for different scenarios.

The PV power output varies between the different seasons and scenarios, Figure 48. It is remarkable that the  $1 \text{ kW}_{\text{peak}}$  is not reached. The 15 minute-means might be the cause. Apparently the maximum is reached in April instead of July. In April the 15-minute-mean maximum is  $0.78 \text{ kW}_e$  during clear-sky (overload scenario). In July during clear-sky (overload scenario) the maximum is only  $0.72 \text{ kW}_e$ . After all, the efficiency is temperature dependent and in April it is relatively cold compared to July. Also the radiation angle can be counterproductive in July. Nevertheless, in Figure 49 July contains the highest total electricity yield, because July includes always the highest amount of sun hours. Only in the July average scenario the PV electricity yield exceeds the CHP electricity yield.

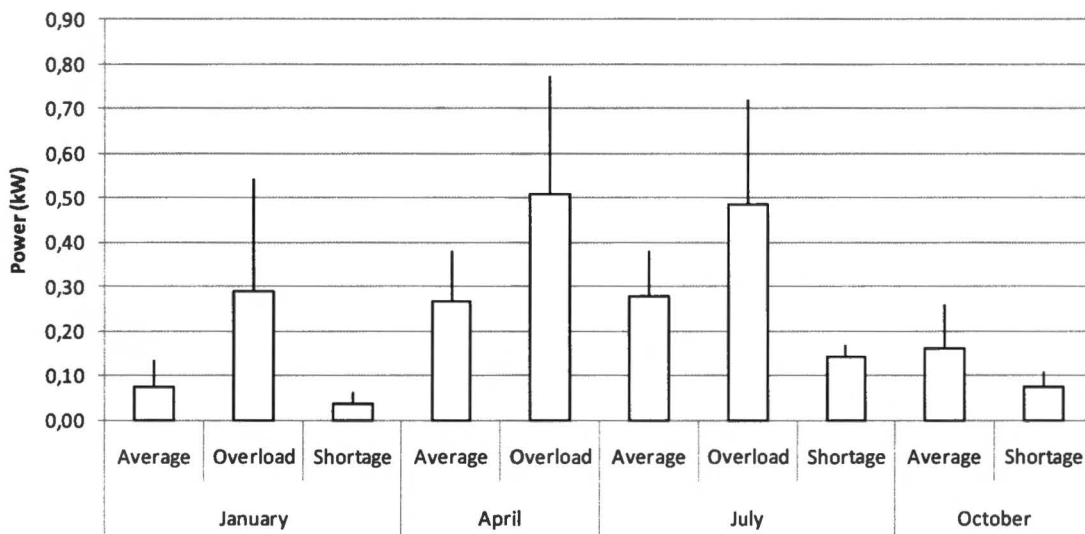


Figure 48: PV power output per household for every scenario (the same for detached and terraced house).

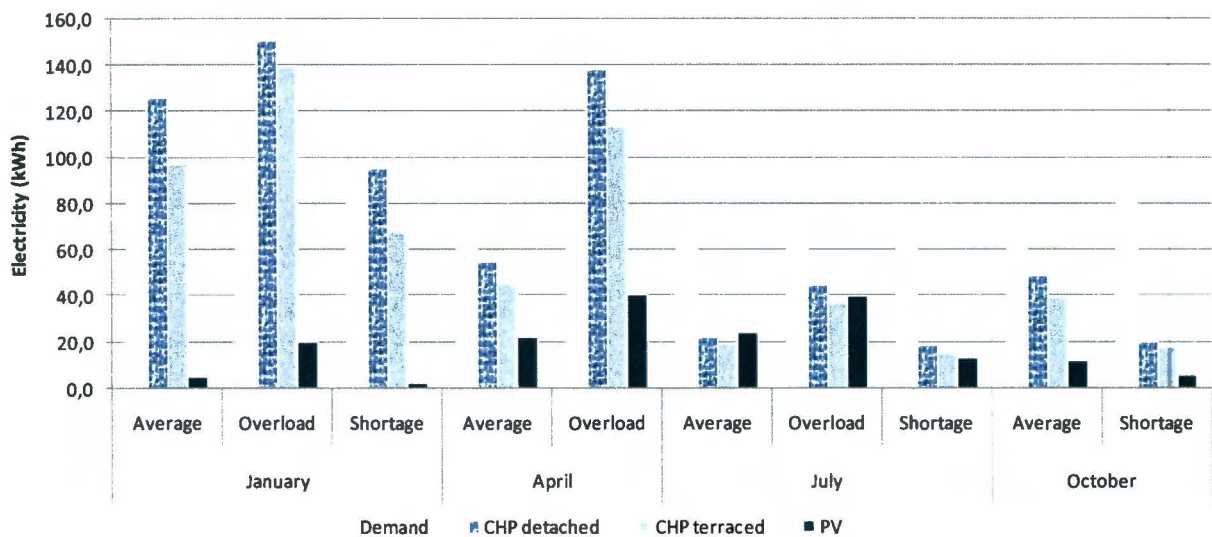


Figure 49: Electricity demand and yield of the detached and terraced houses within a week for different scenarios.

The average scenarios of Figure 49 are reordered in Figure 50 to facilitate the assessment of the proportions between the electricity yields. Every slice contains the electricity yield throughout a week. CHP supplies more than three quarters of the total electricity yield of the total four average weeks. However, only a part of it is consumed by the households in the LV network, shown in Figure 51 and Figure 52.

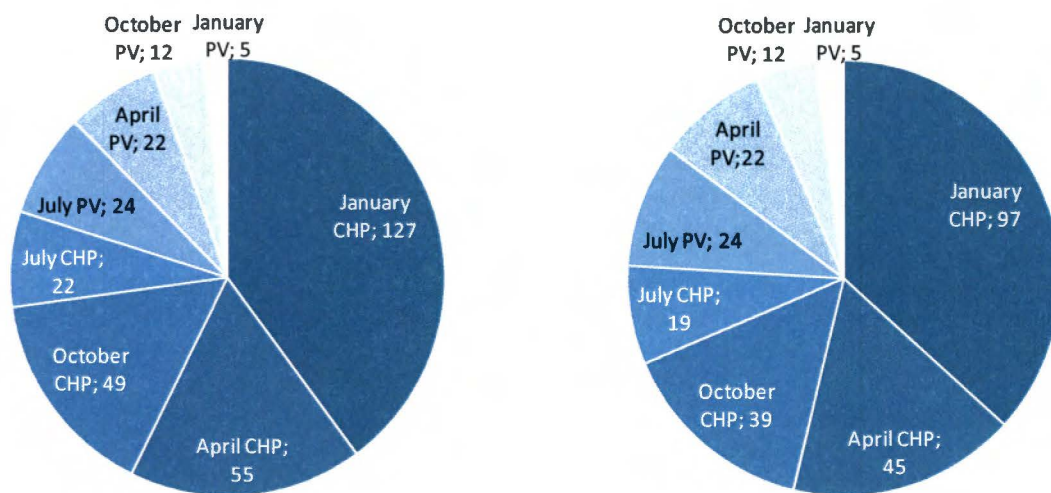


Figure 50: Electricity yields of a detached (left) and terraced (right) house within a week for the average scenarios (kWh).

In Figure 51 and Figure 52 the proportions of the weekly electricity yield to the total weekly electricity demand of the relevant scenarios are shown. For each scenario the hundred percent represents the total electricity demand within a week of the scenario concerned. For the detached house for six out of ten scenarios it is possible to supply the loads when discrepancy between demand and supply is disregarded. For the terraced house it is four out of ten. The lower heat demand of the terraced house has reduced the operation time of the CHP significantly.



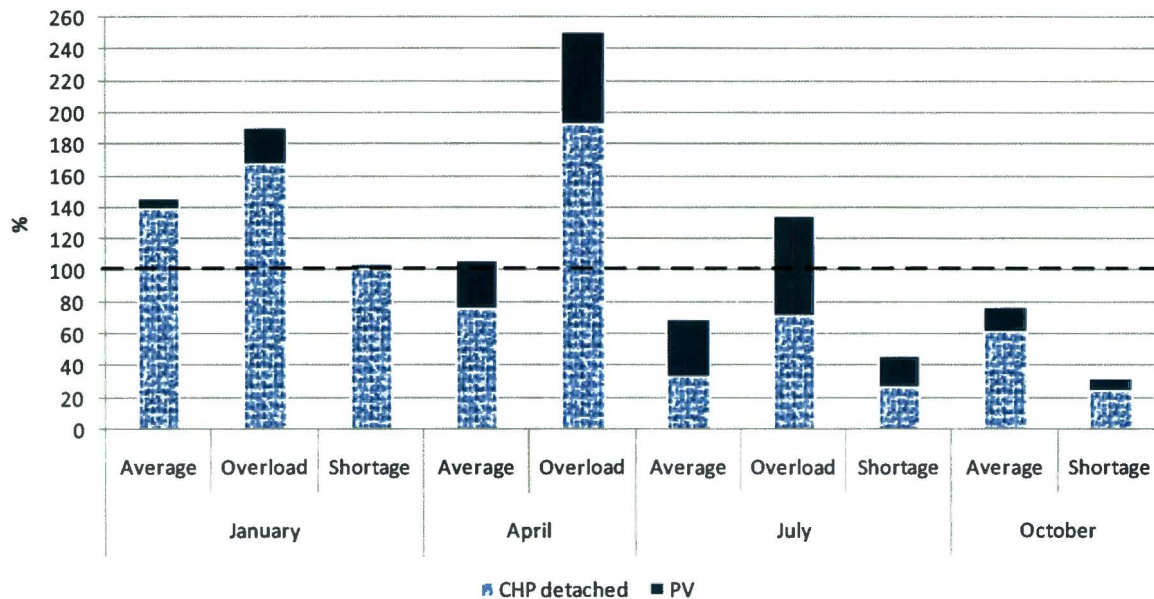


Figure 51: Percentage of the total electricity demand within a week of a detached house for different scenarios.

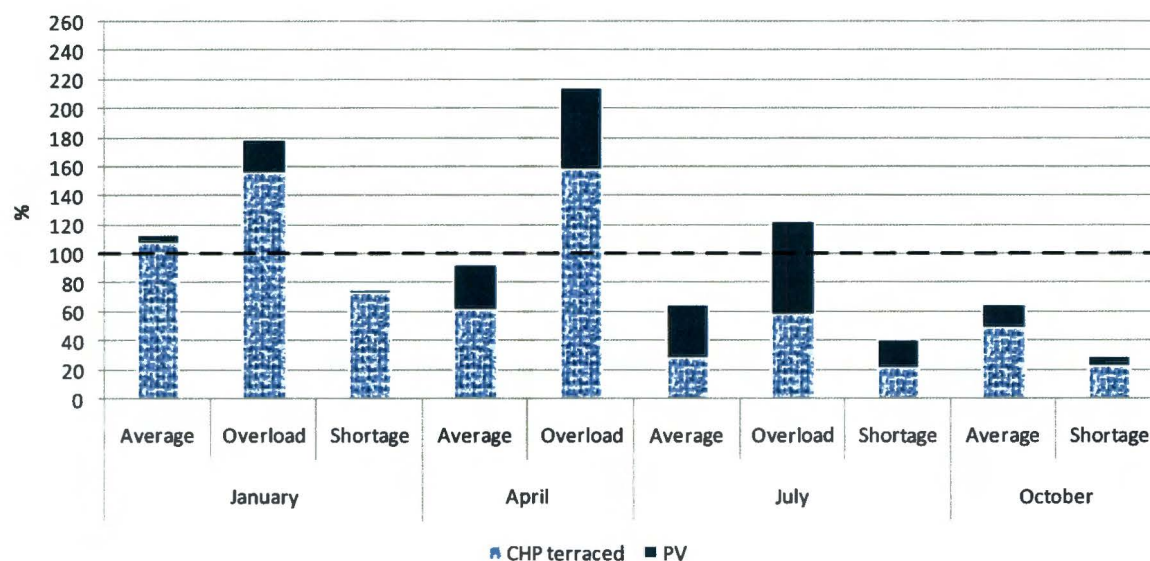


Figure 52: Percentage of the total electricity demand within a week of a terraced house for different scenarios.

### 8.3 Battery Energy Storage

Load-flow calculations of the generated load profiles investigate the peak power and capacity required from the BES devices. Firstly, BES is simulated without limitations to keep the transformer node from transporting power. An islanding mode is imitated by removing the transformer between the swing bus and the LV network. The storage devices operate on the basis of local measures. The storage devices at the end-node of the cables change their power output until a voltage level set-point of that node is reached. The set-point is based on the turning point when supply equals demand. The storage device at the transformer node imitates the active and reactive power flow through the transformer node. The simulation happens in small step changes in rotation, because when the voltage of one node changes it might effect the voltage levels within the entire LV network.

The maximum peak power during the average scenarios occurred in April with a total of 235 kW<sub>e</sub> that is almost 1 kW<sub>e</sub> per household. The required storage capacity is limited. In situations with excess electricity yield, storage has to bridge the moments of shortage. Conversely, the scenarios in which the electricity generation is more scarce, the moments of excess power supply throughout a week determine the storage capacity. The total storage capacity installed in the self-supporting neighbourhood is 937 kWh, almost 4 kWh per household. The capacity and peak power requirement of the transformer node storage device is mainly 4 to 5 times bigger than the requirement of

each end-feeder device. The peak power and capacity limits as well as storage losses (16% [37]) are integrated in the ‘Vision’ macro for further load-flow calculations to assess the design of the power supply and BES.

### 8.3.1 Peak Power

The size of the BES is determined by the average scenarios, because the average scenarios determine the most efficient peak power and capacity of the BES. With the help of load-flow calculations, it is investigated by what amount of power ( $kW_e$ ) and to what extent (kWh) the BES will be charged and discharged. BES is programmed in the ‘Vision’ macro, Appendix D. A flexible solution for integrating BES in the macro requires that each BES operates only on the basis of local measures [23]. At first BES is simulated without storage limitations, to keep the transformer from transporting power and to find out what happens to the BES power flow when it is responsible for the power supply.

The power transport through the transformer shows whether there is an excess power supply or shortage which is decisive for charging or discharging the BES. From the load-flow calculations without BES it is clear that a three phase voltage level below 410 (V) at the end-node of the cables correspond to a power transport from the upper grid into the LV network. This points to a lack of electricity supply from the distributed generators at that time. The power flow is reversed when the end-node voltage level comes above 410 three phase (V), when the distributed generators clearly supply excess power. It is desirable that BES is only charged by the distributed generators within the LV network and BES discharges before the upper grid takes action. For this to happen the voltage set-point of the BES connected at the end-node of the cables is set at 410 three phase (V). The BES has a different voltage setting in island mode, because the transformer does not join in anymore. The turning-point of the reverse power flow and therefore the BES voltage set-point must be 400 three phase (V) in island mode instead.

The BES format (exclusive of the power and capacity limits) of Figure 54 is programmed in the ‘Vision’ macro. The difference in the current end-node voltage level ( $UBES1$ ) and the set-point of the BES voltage level ( $Uset$ ) is multiplied by a factor C and then added to the initial BES power output (or input). Because of problems in stability and effectiveness of this regulation system, a fictitious time integration is included. The C is multiplied by the number of steps (i) with which the BES power is changed. The next load-flow calculation has an end-node voltage level closer to the set point as a result. This happens in rotation from BES 1 to BES 7, because when the voltage of one node changes it might effect the voltage levels within the entire LV network. Figure 53 demonstrates the course of the BES 1 voltage level of one macro load-flow calculation. One should take note of the fact that the x-axis is fictive and that the final 15-minute-mean voltage level is the voltage level after 100 step-changes (i). Another BES is placed at the transformer, called BES7 in Figure 53. BES7 makes sure that the remainder of the required real and reactive power through the transformer-node is assumed by BES7 itself.

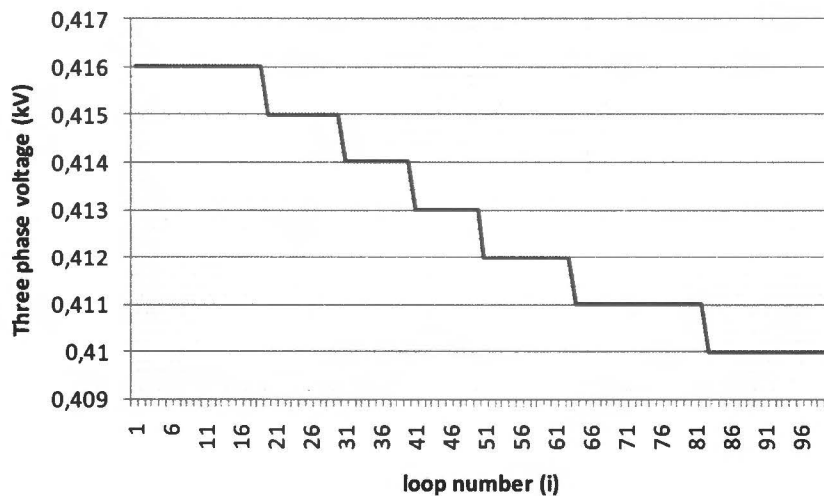


Figure 53: BES voltage regulation.



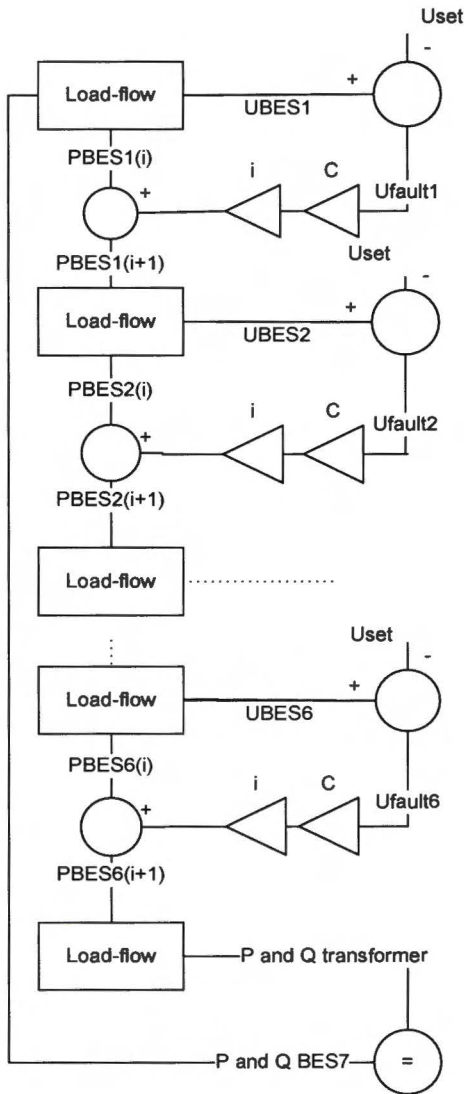


Figure 54: BES model without limits in 'Vision'

From the resulting BES power profile the maximum real-time power output ( $\text{kW}_e$ ) and the required storage capacity ( $\text{kWh}$ ) is determined, Table 7. The largest absolute value of the BES power output is set as the maximum BES power output in its discharging and reloading mode. The absolute maximum BES power at the end-node of the cables occurred during the average scenario in April, with a 15-minute-mean of  $24 \text{ kW}_e$ . The BES at the transformer required a maximum power of  $91 \text{ kW}_e$ . Both values are set as BES limits in the 'Vision' macro for further load-flow calculations. With a total of  $235 \text{ kW}_e^{10}$  BES within the self-supporting residential area, the BES devices are able to supply almost  $1 \text{ kW}_e$  per household.

BES	January		April		July		October		BES size
	Connected	Islanded	Connected	Islanded	Connected	Islanded	Connected	Islanded	
Power at feeder (kW)	18,5	19,0	23,4	24,0	21,5	22,1	20,4	21,1	24
Capacity at feeder (kWh)	86,6	82,0	82,0	84,4	40,5	41,6	57,1	58,9	87
Power at transformer (kW)	77,0	79,1	90,3	85,5	84,7	79,3	87,4	86,0	91
Capacity at transformer (kWh)	414,5	377,8	323,8	303,0	160,8	150,4	229,3	213,5	415

Table 7: Needed BES capacity and maximum power at a voltage set point of 410 V three phase.

### 8.3.2 Capacity

The determination of the required BES capacity needs considerable more effort. The BES capacity is the intermediary between demand and supply and therefore subject to the balance between demand and supply throughout the week. If in a week total electricity demand is larger than electricity yield, excess power that reloads

<sup>10</sup>  $6 \text{ end-node BES devices} \times 24 \text{ kW}_e + 1 \text{ transformer-node BES device} \times 91 \text{ kW}_e = 235 \text{ kW}_e$

the BES system is the limiting factor for the BES capacity. Bigger storage capacities may remain unused, since there is not enough excess power throughout the week to supply the local loads at times of shortage. The power of the generators within the LV network will never be sufficient to fully reload the BES. In this case the amount of excess power supply determines the storage capacity of the BES devices.

If throughout a week total electricity demand is less than the electricity supplied by the distributed generators, an excess electricity yield is created. In that case the electricity shortage that discharges the BES system is the limiting factor for the BES capacity instead. The energy that is expected to be consumed within a week is stored including the expected storage losses and the rest is transported to the upper grid. If more electricity could be stored while not needed, unnecessary storage losses will incur.

Concluding, the required BES capacity is limited. At average scenarios with general excess electricity yield, the BES has to bridge the moments of shortage. Conversely, the scenarios in which the electricity generation is more scarce, the moments of excess power supply during the average scenarios throughout a week determine the size of the BES. Take an average week in July for example. From the required power supplied by the BES it is concluded that an overall shortage is created, Figure 55. Since BES can only supply what is taken in, the maximum capacity needed in this scenario is the energy content during reload, Figure 56.

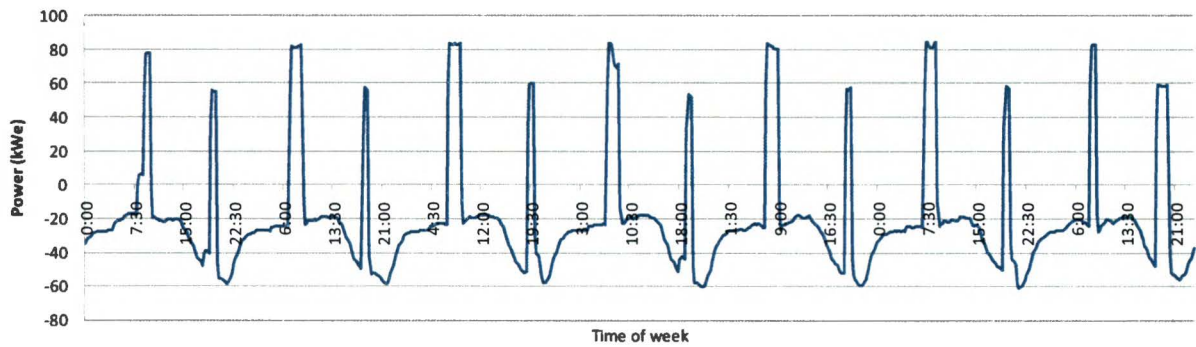


Figure 55: BES power profile at the transformer. No BES limits. Average scenario in July.

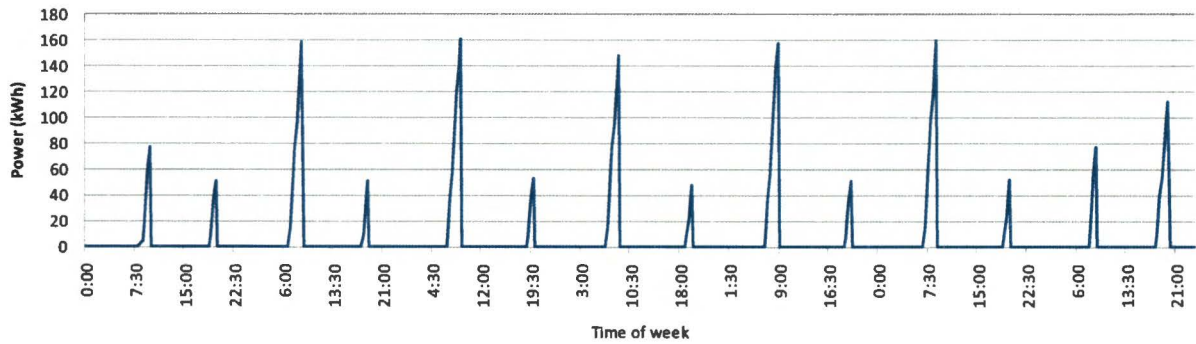


Figure 56: Required BES capacity at the transformer. Average scenario in July.

Between the peaks in Figure 56 the BES is fully discharged. Because the BES will be completely discharged between the reloading peaks, the cumulative stored electricity does not cross the 160 kWh in July. The same approach is used for every BES in the average scenarios shown in Appendix E. Appendix E clearly shows that January sets the required capacity of the BES near the transformer (415 kWh) and at the end of the feeder (87 kWh). Times of shortage and excess power supply are very close together in this month, that is probably the reason January required the highest BES capacity. The total storage capacity installed in the self-supporting neighbourhood is 937 kWh<sup>11</sup>, almost 4 kWh per household.

The largest values presented in Table 7 are set as limits. These limits are implemented in the ‘Vision’ macro, in Appendix D for the final load-flow calculations that investigate the eventual effect of BES on the LV network. Figure 57 illustrates the control mechanism of one BES device at the end of a feeder. The BES power output (or input), called PBES, is limited by the maximum power output (or input) and the electricity extractable from the

<sup>11</sup> 6 end-node BES devices x 87 kWh + 1 transformer-node BES device x 415 kWh = 937 kWh



BES, called the capacity CBES. A negative PBES value points at a discharge of the battery that feeds the network, as the positive PBES value designates the reload of the battery extracting power from the LV network. Total transport and storage losses of the BES are around 17%, Figure 58 [37]. To keep the capacity of the BES up to date, the 'Vision' macro subtracts 8% when it is reloading and 8% when it is discharging. When the BES reloads, the power input (PBES > 0) is multiplied by 0.92, so only a part of the power is stored while the full 100% is extracted from LV network. A BES power output (PBES < 0) indicates that the BES is discharging. This power output is needed by the LV network, exclusive of the BES losses. The capacity loss is 8% more than the load-flow calculations indicate and therefore the capacity of the BES decreases with the power output divided by 0.92. If eventually the capacity appears not sufficient, the BES power including the step change (PBES(i+1)) is set back to the initial power (PBES(i)). BES7 deviates from the last step, since BES7 is able to calculate the exact extractable or obtainable active and reactive power.

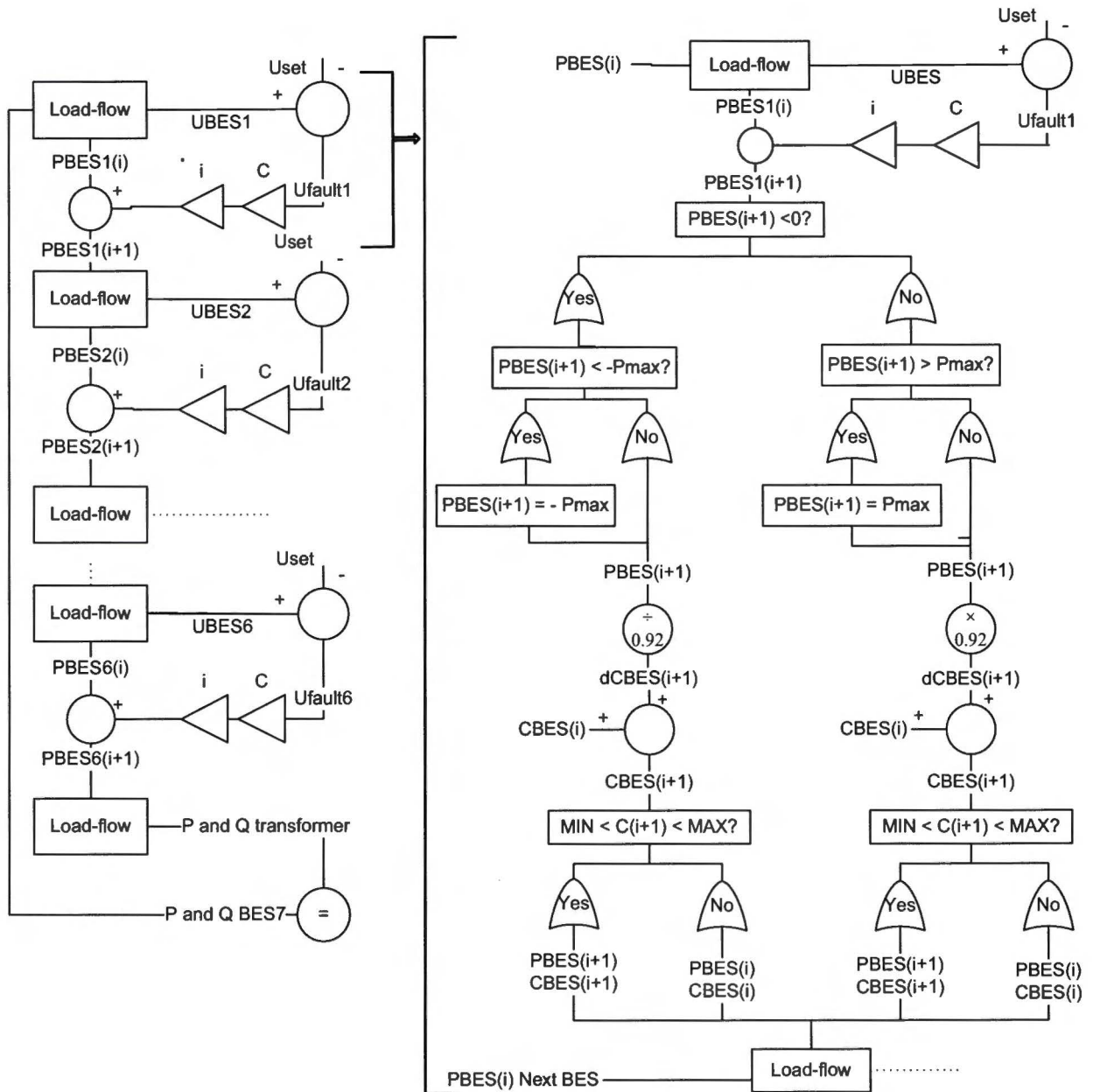


Figure 57: BES model with limits in 'Vision'.

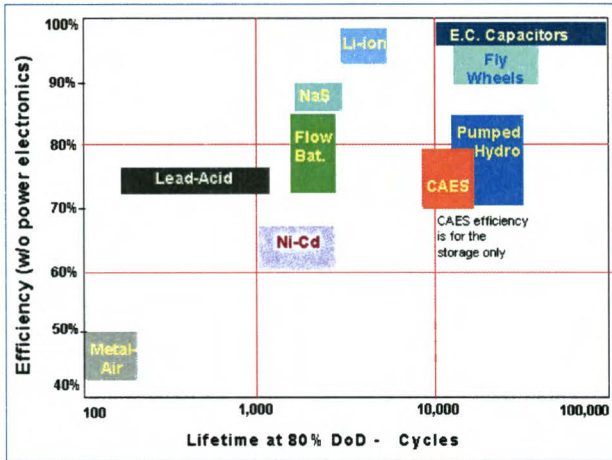


Figure 58: BES efficiencies [37]

## 9. The Assessment

The case study objective proposed in this report is to verify statements about the alternative operational approach by calculating reverse power flow, voltage levels, system losses, cable and transformer loads with the simulation program 'Vision Network Analysis'. The characteristics of the low voltage (LV) network and generators (section 4), the scenarios that have to be assessed (section 5) and the optimized design (section 8) are already specified. The main conclusions from these sections that enable the load-flow calculations are:

- the 15-minute-mean electricity demand profiles (Appendix C) throughout a week for the 10 scenarios (Table 1 page 52),
- the optimized installed photovoltaic (PV) power of  $1 \text{ kW}_{\text{peak}}$  per household,
- the 15-minute-mean constant power output profiles of the generators throughout a week for the 10 scenarios (Appendix C),
- the total peak power ( $235 \text{ kW}_e$ ) and capacity ( $937 \text{ kWh}$ ) of the battery energy storage (BES) devices (Table 7 page 49),
- the operating characteristics of the BES devices programmed in the Vision macro (Figure 57, page 51)
- and the characteristics of the LV network configuration (Figure 5 on page 16):
  - 150 Al cables and 400 kVA transformer (10.25kV:400V)
  - Cable lengths
  - Placement of the generators and BES devices.

Figure 4 on page 15 indicates that the self-supporting residential area is ready to be evaluated. The results of the load-flow calculations are summarized in this section. It should be noted that the results are based on 15-minute-means throughout a week. Section 9.1 outlines the reverse power flow. The reverse power flow is limited. Distributed generation reduces power extracted from the grid. During the overload scenarios the reverse power flow *to* the upper grid did not exceed the average power flow without distributed generation *from* the upper grid. The maximum effect of the BES is achieved, although this is very little in January/April overload scenarios and July/October shortage scenarios.

Section 9.2 delineates the system losses. The LV network losses of the self-supporting residential area include LV cable and transformer losses calculated with the 'Vision' macro. The transport losses over the rest of the medium voltage (MV) and high voltage (HV) network are estimated by the network operator. A considerable amount of the transport losses is reduced when distributed generators and BES are implemented, except for the overload scenarios. Unfortunately, storage losses are bigger than the reduced transport losses. Putting more effort in the placement of the storage devices is useless, since the LV network losses are minimal.

The third parameter, voltage levels is assessed in section 9.2. Distributed generation increases the 15-minute-mean voltage levels but they stay within the range of +9% and -2% of the nominal 230 (V) voltage level. At scenarios with a good energy balance, storage converges the voltage levels. At shortage scenarios BES covers the peaks while during overload scenarios the minima instead.



Cable loads do not reach 32%, whereas the transformer loads reach 78%. The transformer is therefore further specified in section 9.4. On overall the transformer loads decrease by distributed generation, though the times of excess power supply have much effect on the transformer loads. At the lowest amount of 15-minute-mean power demand of 200 W per household and the highest 15-minute-mean power output of 1.8 kW, the transformer-load increases to 99% and the voltage level would increase to 252 V. Just below the upper limit of 100% and 253 V respectively.

## 9.1 Reversed power flow

From Figure 59 it is seen that the inclusion of distributed generation reduces the power extracted from the grid especially in January. From the average scenarios without BES, January is the only month in which the power transport to the upper grid is higher than the power transport from the upper grid. In July and October the electricity shortage is considerable. The effect of the total installed BES of 235 kW<sub>e</sub> and 937 kWh, i.e. 1 kW<sub>e</sub> and 4 kWh per household spread out in the LV network, is the highest achievable, since in every scenario which includes BES either one of the bars (from/to the grid) is reduced to zero. In the overload and shortage scenarios the imbalance between demand and supply is often too big, so BES can only make a small difference. To reduce the power transport to or from the upper grid in these scenarios, one should look for another solution than BES. Appendix F shows the real-time power flow over the transformer.

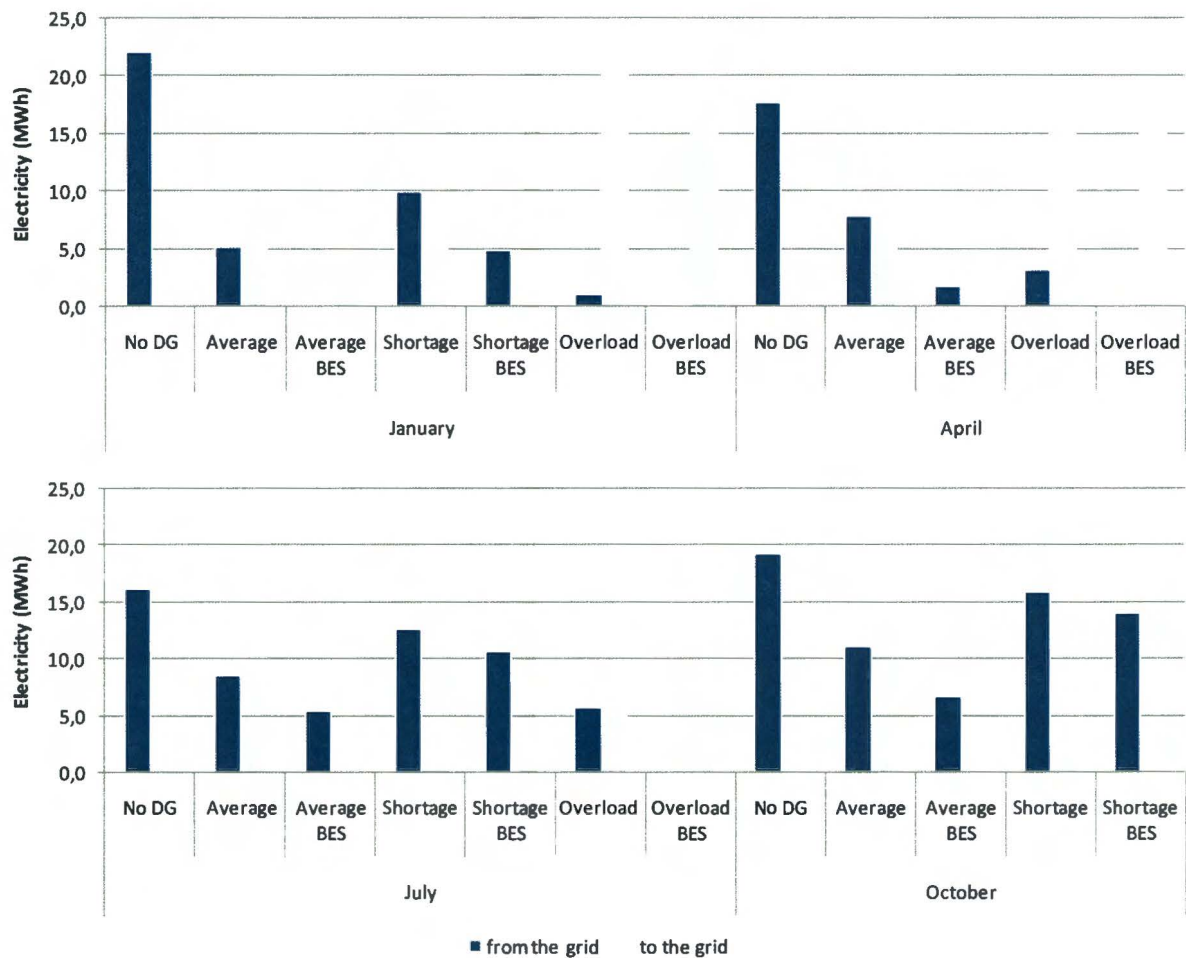


Figure 59: Electricity transport within a week in January and April (above) and July and October (below) for different scenarios.

## 9.2 System Losses

The LV network losses of the self-supporting residential area include the LV cable and transformer losses that calculated by the 'Vision' macro. The transport losses over the rest of the MV and HV network are estimated by the network operator:

- A. LV network losses: 1.24%
- B. MV/LV transformer losses: 0.5%
- C. MV transport losses: 1.43%
- D. MV/HV transformer losses: 0.4%
- E. HV transport losses: 0.84%

So, the MV and HV transport losses account for about 2,67%<sup>12</sup> with respect to the electricity production at the central power plants. This percentage of MV and HV losses is converted to 2.74%<sup>13</sup> with respect to the electricity consumption of the self-supporting residential area (including the cable and transformer losses). The estimated HV and MV network losses in Figure 60 will be 2.74% of the power transported over the LV transformer to or from the upper grid (calculated in section 9.1).

Following Figure 60, a considerable amount of the transport losses is reduced in the average scenarios when distributed generators are implemented and BES is added. Nevertheless, storage losses counterbalance transport losses and during the overload scenarios distributed generators increase transport losses because of overproduction. Storage losses are the highest during scenarios at which BES matters the most, i.e. at a good electricity balance.

Not much effort has been put to placing the BES devices in the self-supporting residential area. The maximum result of putting more effort to optimise the BES placing is the disappearance of the LV network losses in the average scenarios, i.e. the small dark blue parts of the bars.

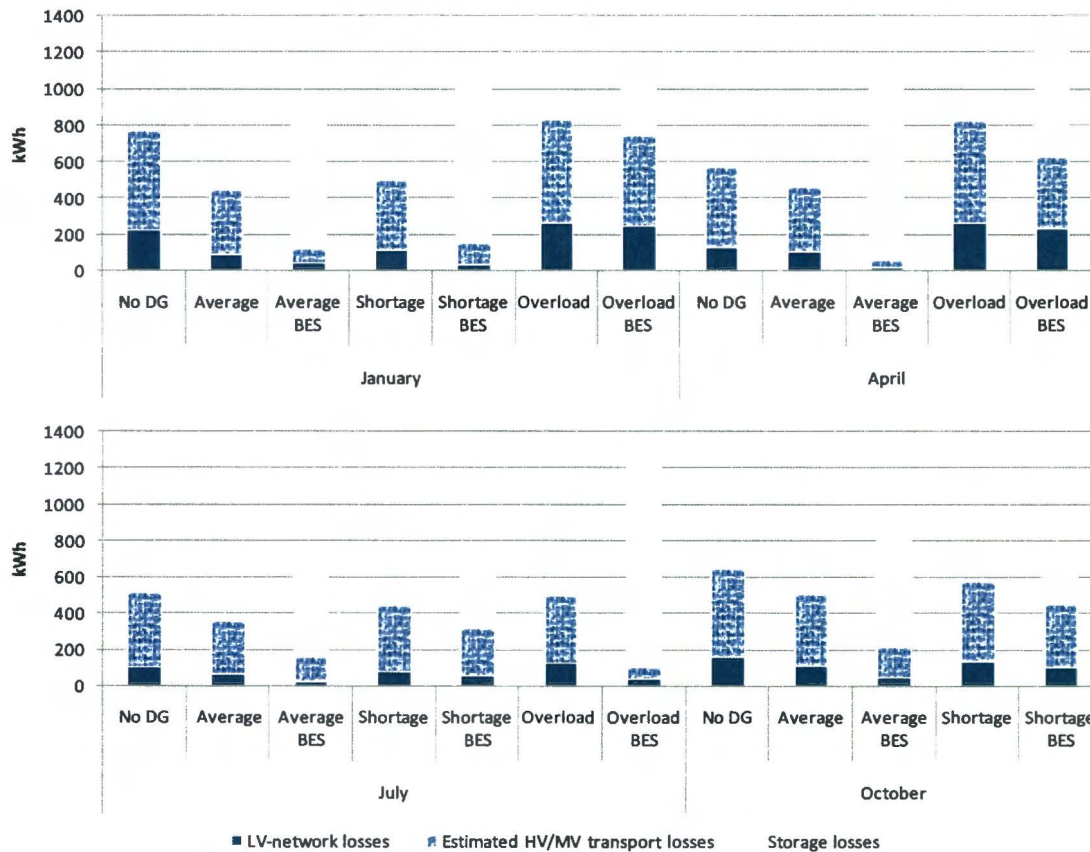


Figure 60: System losses within a week for different scenarios in January and April (above) and July and October (below) when grid-connected.

<sup>12</sup> Estimated MV/HV transport losses = C + D + E  
 $1.43\% + 0.4\% + 0.84\% = 2.67\%$

<sup>13</sup>  $2.67 / (100 - 2.67) * 100\% = 2.74\%$



### 9.3 Voltage levels

In January, April, July and October the average scenarios are calculated in five situations, Figure 61 and Figure 63; without distributed generators ‘No DG’ (1), with distributed generation and unity power factor ‘*pf 1*’ (2), with distributed generation and a 0.95 power factor ‘*pf 0.95*’ (3), with distributed generation (power factor 0.95) and BES in grid-connection ‘*Grid BES*’ (4) and with distributed generation (power factor 0.95) and inexhaustible BES ‘*Islanded BES*’ (5). The top of the white boxes represent the mean voltage level plus the mean deviation, whereas the bottom of the boxes matches the mean voltage level minus the mean deviation. The boxes represent almost 70% of the 15-minute-mean voltage level calculations throughout a week. The projections above and below the boxes reflect the absolute maximum and minimum. The reproduction of the voltage levels into these boxes is to evaluate the steadiness of the voltage level throughout the week. The voltage level of node C is investigated in this section, since during the scenarios without BES the highest as well as the lowest voltage levels take place at node C. Node C is the end-node of the largest cable with most of the loads and generators connected in series.

Following the Netcode 95% of the 10-minute-mean voltage levels are allowed to vary between +/- 10% of the nominal voltage level (230 V). To compensate the 15-minute-means instead of 10-minute-means, it is decided that the +/- 10% of the nominal voltage level should not be crossed at all. It appears that low voltage levels are no issue in this case study, so the range of the y-axis in Figure 61 and Figure 62 measures plus 10% and minus 5% of the nominal voltage. The voltage levels in Figure 61 and Figure 62 are mostly above the nominal voltage level 230 V, but do not cross +10% of the nominal voltage. Because the Netcode in this case study is not violated, it does not mean the voltage levels should be left as they are and no lessons have to be learnt from the figures. It might be practical to know the effects of distributed generators, their power factor and BES on the voltage levels, when self-supporting residential areas extend or new come into existence.

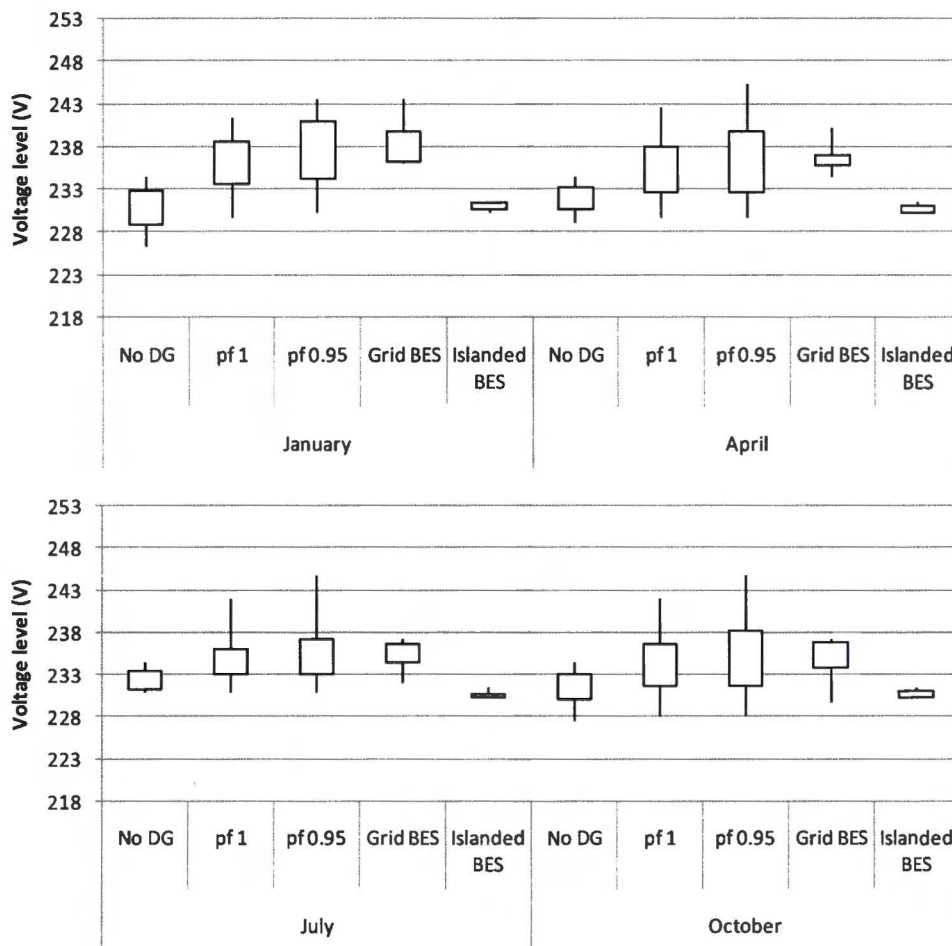


Figure 61: Average scenario voltage levels at node C.

The implementation of distributed generation increases voltage levels in the LV network. Moreover, the smaller the power factor of the generators the higher the absolute and the range of that voltage level. The effect of BES in the average scenarios is positive. Though, the BES has difficulties to reduce voltage level peaks in January and the voltage level pits in October. The fact is, because of the long-term overload in January BES overcomes the moments of shortage only. In October and July this is the other way around. In April the voltage levels are improved on both sides. Because the better energy balance during April the BES can reload and discharge when necessary.

The BES in islanding mode is simulated as an inexhaustible source or load, therefore the range of the voltage level is compact, Figure 61. Because the voltage set-point is diminished with 10 voltage three phase (V) when the transformer falls away, the voltage level is lower in islanding mode than when grid-connected. Unfortunately, inexhaustible BES is not realistic. Therefore, this voltage level is only reached if the demand and supply completely match. For this to happen a control system on the combined heat and power (CHP) systems, demand-side management and/or a synchronous generators with a P/f and U/Q static are necessary.

In January and April of Figure 62, the BES completely fails to reduce the higher voltage levels in the overload scenarios, whereas in these months overloads are prevalent and need to be solved. In October and July it is just the opposite. Yet the higher voltage levels cause the main problems. The minimum voltage level does not cross 227 V one phase in the October shortage scenario, which is 1.3% below nominal voltage. The highest voltage level is 249 (V) in July, which is 8.3% above nominal voltage. If the lowest amount of 15-minute-mean power demand of 200 W per household and the highest 15-minute-mean power output of 1.8 kW is combined, the voltage level at node C would increase to 252 V one phase. Just below the upper limit of 253 V. Appendix G shows some real-time voltage levels of node C as well as the voltage levels along the cable of node C.

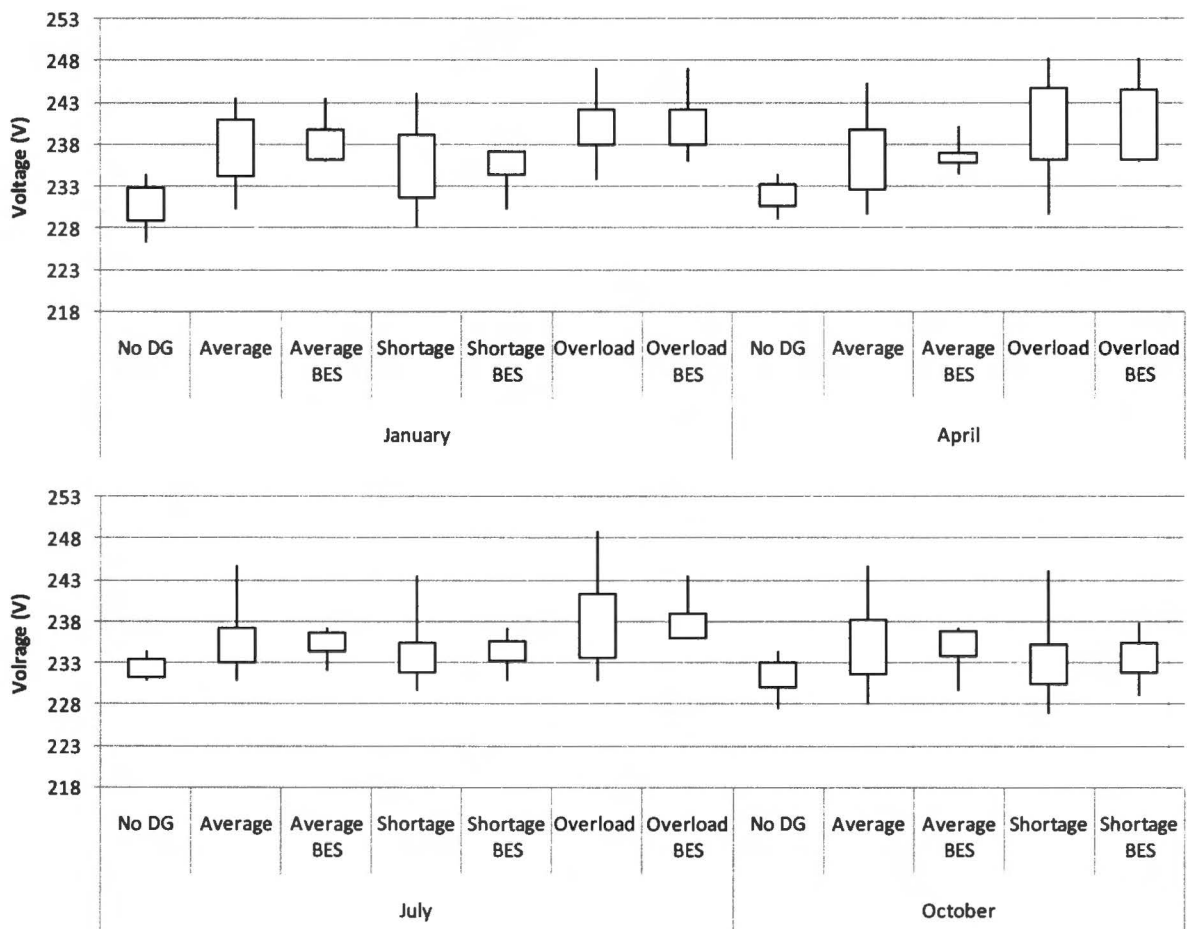


Figure 62: Voltage levels at node C for all scenarios in grid-connection.



## 9.4 Transformer loads

Cable loads do not cross 32%, while the transformer loads reach 78%. Therefore the transformer is regarded as the weakest link and specified in this section. The mean transformer loads decrease when distributed generation is implemented as is seen from the white boxes from Figure 63. Though, according to the projections at the boxes, the maximum transformer loads in April and July increase because of appearing times of overproduction. On overall distributed generation with a power factor of 0.95 decrease the transformer loads, with respect to distributed generation at a power factor of 1, because of the reduction in reactive power transport. BES reduces the transformer loads even further.

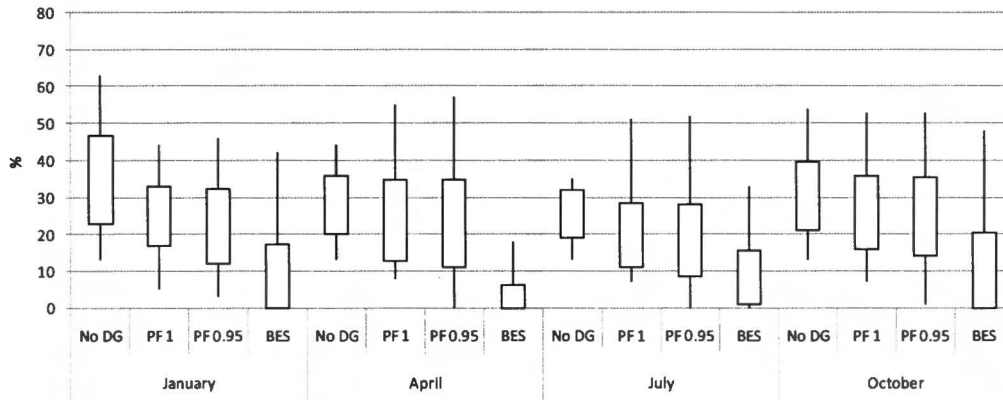


Figure 63: Transformer loads for the average scenarios when grid-connected.

In scenarios where the BES has yet proved its effectiveness on voltage levels and reverse power flow, the effect also becomes visible in the transformer loads of Figure 64. The overall decrease in transformer loads is enough to increase the life expectancy, but it is not recommended to replace the transformer to a smaller one. If the lowest amount of 15-minute-mean power demand of 200 W per household and the highest 15-minute-mean power output of 1.8 kW is combined, the transformer load without BES would increase to 99%. Again, just below the maximum.

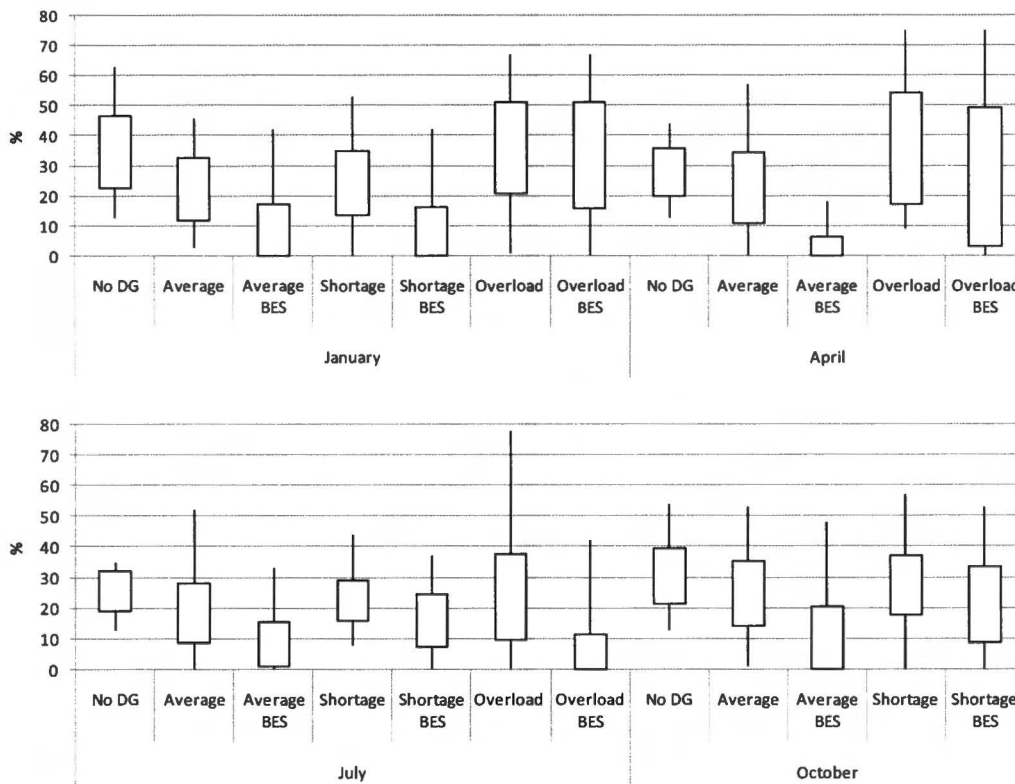


Figure 64: Transformer loads for all scenarios when grid-connected.

## 10. Discussion

This research is only applicable for the assessment of 15-minute-mean steady-state parameters, that have averaged out the demand profiles. To obtain the peaks the simultaneity of all profiles are kept 100% during the load-flow calculations. The main problems are caused by overproduction of the distributed generators. For that reason the question remains whether more specific demand profiles are valuable for steady-state calculations when the low voltage (LV) network has trouble with the higher voltage levels and transformer loads caused by distributed generators. After all, the generator's (maximum) power output is limited and occurs also during the 15-minute-mean profiles.

Two problems have occurred that are difficult to resolve at the same time. The self-supporting residential area needs an extension of the power supply system, but at the same time the current power supply system calls for peak load shaving. The peak power, capacity and operational control of the storage devices succeeded in minimizing the reverse power flow and transport losses. Unfortunately, storage losses have counterbalanced the effects on transport losses. At scenarios that contend with general excess electricity yield, storage devices are on overall fully charged and fail to serve peak load shaving, i.e. limit voltage peaks and transformer loads. This indicates the need for a different solution. A different operational control on the storage devices, such as a higher voltage set-point, increases the charge-limit, but will decrease storage efficiency. Shutting down the generators is also an option, though it would be a shame not to take advantage of the generator's power output since three out of four average scenarios are not completely self-supporting yet.

### 10.1 Generator Control

The reason that the energy balance in January and April results in an excess electricity yield is because the CHP is heat driven and the photovoltaic (PV) power output (once installed) is uncontrollable. The heat control makes sure that the combined heat and power (CHP) supplies the heat demand irrespective of the electricity demand. An additional electricity control may turn off the CHP even when heat is required. The supplementary heater can easily take over the heat supply decreasing the electrical power supply of the CHP.

The excess power supply in January and April can damage the efficacy of the power supply system within the self-supporting residential area, namely by increasing voltage levels, transport losses, cable and transformer loads, but also by decreasing the cost-effectiveness of the power supply within the self-supporting residential area. The PV power output does not include any variable costs in contrast with the CHP. CHP still consumes fuel when it is operating. When the PV produces enough electricity to supply the loads or when CHP power output itself creates a prolonged excess electricity yield, it might be better to include an electricity control that deactivates the CHP and let the supplementary heater take over instead.

When one searches for the most economical or efficient electricity control, the conversion efficiencies, storage efficiencies and costs of the total heat system and PV arrays have to be known. In this case study, a pilot study is done that starts with deactivating the CHP only if the PV power output is big enough to supply the loads per 15 minutes. This control system does not jeopardize the main topic in this case study, i.e. the self-sufficiency of the residential area. The results of this alternative operational approach during the April overload scenario are shown in Figure 65 and Figure 66. The figures both show a small improvement of the voltage levels (namely node C) and the transformer loads. Moreover, 42% less power is transported back to the upper grid causing a 28% reduction on cable and transformer losses. Though, with this controller the CHP has to cope with an increased number of switches.



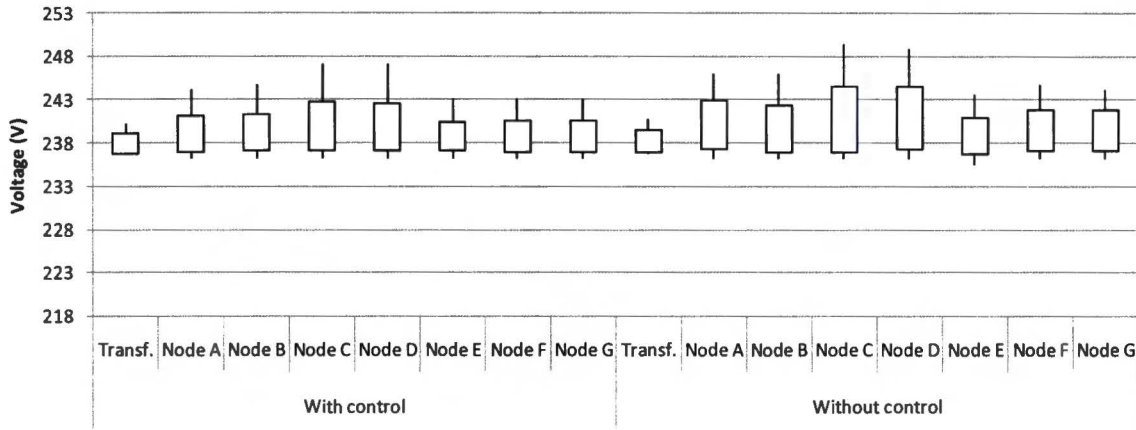


Figure 65: Effect of the generator control on the voltage levels in the April overload scenario.

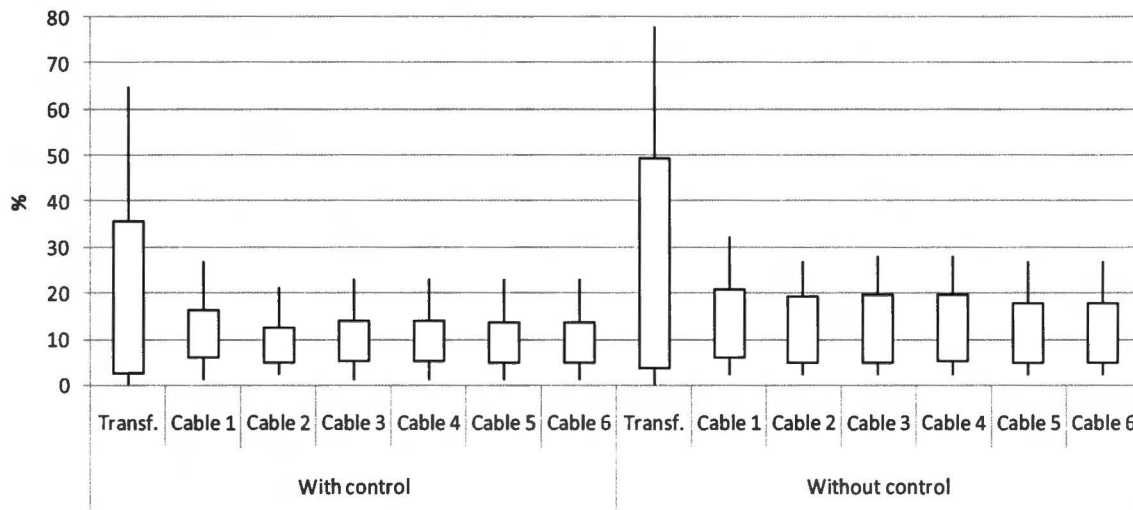


Figure 66: Effect of the generator control on the transformer and cable loads in the April overload scenario.

## 10.2 Storage Control

In a long-lasting overload scenario with a low contribution of PV, like the overload scenario in January, the control of section 10.1 is ineffective, unless there is a communication between the households to turn off only half of the CHP systems which needs an agreement to share the CHP profits. For the scenarios that deal with excess power (overload scenarios), another possibility is to control the storage devices by changing the voltage set-point of the battery energy storage (BES). This may decrease the transformer loads and voltage levels. An increased set-point voltage level makes sure that the excess power flow transported back to the grid will be distributed over a longer time-scale. The reloading of the BES is delayed to capture excess power at times it is most essential. Until the excess power supply is less BES discharges again.

Figure 67 and Figure 68 are the results of a second pilot study with load-flow calculations at a BES voltage set-point of 419 V three phase (242 V 1-phase) during the January overload scenario. When the voltage level on the BES connection node is below 419 V three phase, the BES discharges to make room for the moments of high storage necessity when the voltage level of the connection node is above 419 V three phase. In other words, the power is transported to the different BES devices at high voltage levels above 419 V and is then transported back to the grid when the voltage level decreases below 419 V three phase. Figure 67 demonstrates an overall reduction on the average voltage level. Though, the ultimate maximum voltage levels are still not removed, indicating the need of an even higher BES voltage level set-point. Figure 68 proves the effectiveness on cable and transformer loads. Nevertheless, the positions of the BES cause a back and forth transport of power, therefore increasing cable losses with 82%. Concluding, the BES devices act as a buffer spreading the reverse power flow over a longer time-scale, which decreases voltage levels and transformer loads. A side effect is that the reverse power flow takes a long route with extra storage losses before it is rejected to the upper grid.

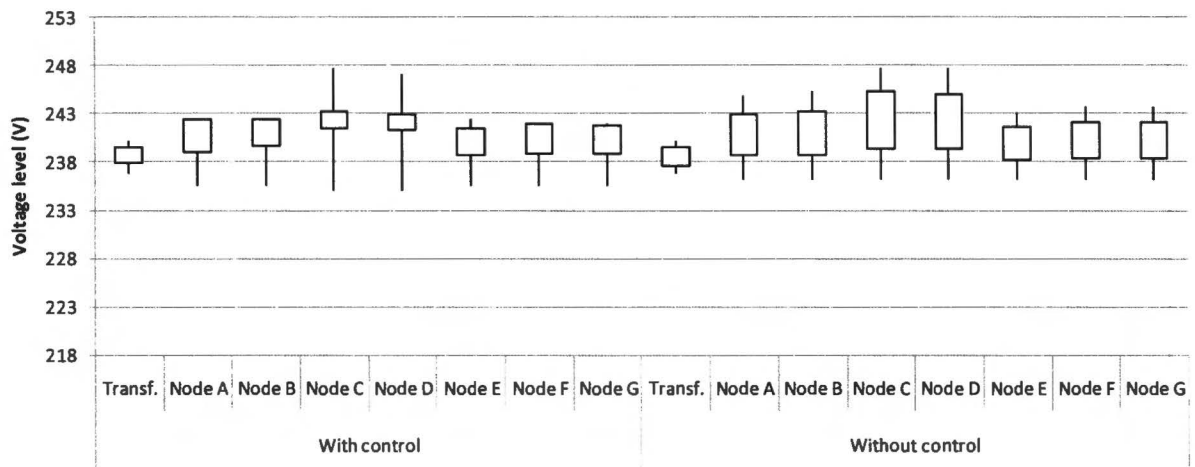


Figure 67: Node C voltage level during an overload scenario in January for different BES voltage settings.

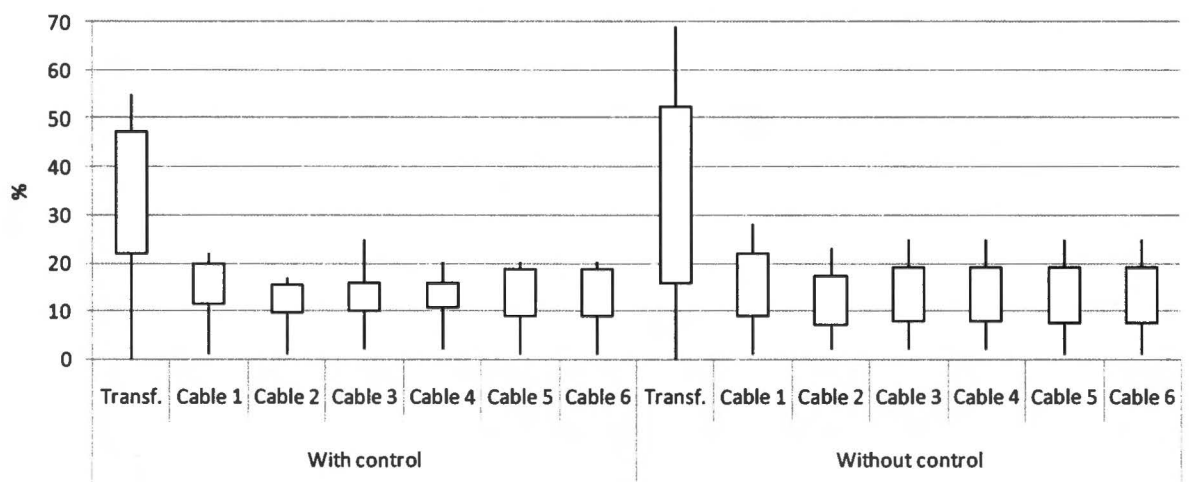


Figure 68: Transformer and cable loads during an overload scenario in January for different BES voltage settings.

### 10.3 Increase photovoltaic power

With an electricity control on the CHP, the amount of PV can be increased, provided that the roof is big enough, to supply more power in July and October, while it will not induce any problems in January and April. Another way to increase the energy yield in especially July and October, is to install a two way tracking PV system, i.e. a PV system that has two fixed optimal inclination angles instead of only one that is optimised for a whole year. The two inclination angles are optimised for the months that require highest PV power, October and July respectively. The best inclination angle is 22° in July and 53° in October. The changes with respect to the angle of 36° are put in Table 8. January and April have higher PV electricity yield at an inclination angle of 53° than at an angle of 22°, and are therefore set at 53°. In January the new PV electricity yield is higher than during the initial design, which might be undesirable. Though, 8.8% of the total PV electricity yield in January is still negligible compared to the electricity overproduction of the CHP systems.

The optimal installed PV peak power might increase as well, due to the 2-way tracking PV power output, which is not taken in table 7 yet.

Monthly radiation (Wh/m <sup>2</sup> )	January	April	July	October
Inclination angle 22°	-	-	4920	-
Inclination angle 53°	1040	4010	4340	2410
Inclination angle 36°	956	4170	-	2300
Difference (Wh/m <sup>2</sup> )	84	-60	160	110
Difference (%)	+8.8%	-1.4%	+3.4%	+4.8%

Table 8: Monthly radiation for different inclination angles for 1 kW<sub>peak</sub> installed.



## 10.4 Question Marks

- A self-supporting residential area will be designed, installed, and operated by a customer, group of customers, network operator or energy company [19]. This case study remains ambiguous who designs, installs or operates the different elements of the integrated system. The generators in this case study are suitable to be private owned by the consumers. If the operational and regulatory environment does not change, the same private owners will design and operate the generators. The BES devices are operated in a way it maximizes its efficiency. Who will own or operate the BES devices is yet left in the middle.
- The research question at the current state is therefore: Will the power supply, *owned by the customers*, meet *network operators' challenges* such as reliability, safety, voltage levels, system losses and cable and transformer loads? Of course customers and network operators have the same interests, since the goal of the network operators is to preserve customers' power supply. Though, the research question as it is stated in this case study puts things on their heads, since private owned generators do not aim at serving network operator's challenges.
- If the generators are private owned by the consumers, the consumers are the ones to decide whether they take part of the self-supporting residential area. In that case the residential area becomes self-supporting until every household in the LV network participates.
- The owners of the power supply system will design, install and operate the generators for their own, mostly economical, benefit. Though, participants may be concerned about the environmental effects of their energy supply system as well, or other social effects as safety, reliability and power quality. So, after it is known who designs, installs or operates the generators (and BES devices), the second question concerns the operational mode of the power supply system. Either way, the coordination of investment and operating decisions are mixed up [19].
- If the self-supporting residential area is designed to operate independently, not only the generators but also the connection-mode to the grid must be managed. The same questions as above arise, as to what criteria the grid-connection will be controlled, for example, to cost effectiveness or to the necessity to maintain performance [19].
- If the self-supporting residential area is to become an intelligent entity, that presents itself to the upper grid as a single controlled unit, many more variables have to be dealt with, such as short-circuit current, islanding, protection, stability and reliability indices. Every kind of distributed generator has either adverse or advantageous effects concerning these variables. When transforming the self-supporting residential area into an autonomous network these characteristics can make or brake the self-support of the power supply system. It is currently investigated in what degree the generators used in this self-supporting residential area are able to serve in island mode. The present characteristics of especially micro-CHPs (not only the Microgen) are not suitable for island mode. The key features that makes this aggregate system possible are power electronics, control, and communication capabilities for each generator as well as the overall operation [19]. Concluding, there is still a long way to go. This case study was only a small step to a semi-autonomous system, e.g. 'Virtual power plant', 'Microgrid' or 'Smartgrid'.
- The self-supporting residential area in this case study gives a false impression, since the CHP is still connected to the gas network and will not operate when disconnected. Because of the CHP system, the term 'self-supporting' is falsely assigned to the power supply described in this research.
- This case study treats just one self-supporting residential area. It is uncertain what happens if hundreds or thousands of these self-supporting residential areas are implemented in the distribution system. Will the strong upper grid still exist.
- BES has also the ability to control reactive power. The effect of this ability of the BES systems at the end of the feeders is not yet investigated.
- The power demand of public goods, like streetlights, is lacking in this case study. Also developments in future electricity demand is left out, like the increased use of air-conditioning and low-energy light bulbs
- In the future the Microgen CHP might have the possibility to operate in part load. In this case not only the operation time is designable, but also the power output which makes the determination of the operational control far more complicated.

## 11. Conclusion

The case study objective proposed in this report is to verify statements about the alternative operational approach by calculating reverse power flow, voltage levels, system losses, cable and transformer loads of a well-designed self-supporting residential area in the low voltage (LV) network containing combined heat and power (CHP), photovoltaic (PV) arrays and battery energy storage (BES) devices. The conclusions drawn from this case study are only applicable to self-supporting residential areas that are situated in the same environmental conditions and have a comparable integrated system, such as the LV network, power supply system, BES devices and loads. This case study is also restricted to 15-minute-mean load-flow calculations in steady-state. The load-flow calculations of 'Vision Network Analysis' make use of the Newton-Raphson method, that involve a swing bus representing the upper grid and cables represented by the pi-model.

Extra effort is done to check the validity of the demand data that are used. The yearly electricity demand of 4084 kWh, the yearly heat demand of 47.3 GJ for the detached house and 38.6 GJ for the terraced house are in line with other heat demand surveys and seem good matches with the demand fractions [41]. Though, the 15-minute-mean steady-state parameters have averaged out the electricity demand profiles. Nevertheless, the main problems are caused by overproduction of the distributed generators. Therefore, and because of the 100% simultaneity of the peak loads, it is not expected that more specific demand profiles are valuable for the steady-state calculations in this case study. Moreover, the generators' (maximum) power output is limited and occurs also during the 15-minute-mean profiles.

Previous to the assessment of the self-supporting residential area, the characteristics of the generators, battery energy storage (BES) devices and the LV network are defined and faced with a design methodology. The LV network consists of 6 feeders (150 Al cables) subdivided from a 400 kVA transformer (10.25kV : 400V). The integrated system includes 200 terraced and 40 detached houses that are equipped with 1 kW<sub>peak</sub> polycrystalline PV power and a free-piston Stirling CHP with a linear generator balanced at 50 Hz with a fixed 1 kW<sub>e</sub> and 4 kW<sub>th</sub> power. A supplementary heater and 200 litre heat storage vessel extends the heat supply system. The PV arrays and micro-combined heat and power (CHP) with linear generators as well as the loads are simulated as constant powers. A constant power load will have maximum effect on the LV-network. It is suitable to consider the generators as constant powers, too, since this case study calculates the steady-state conditions. In steady-state the CHP can be considered as a balanced constant power of 1 kW<sub>e</sub> at 50 Hz and the inverter and the sun power define the PV power output regardless of the network conditions. The PV arrays are grid-connected through power electronic inverters whereas the CHP is direct grid-connected. Both have a fixed power factor of at least 0.95.

The self-supporting residential area is assessed during 10 scenarios containing a week. Four of them are average scenarios in January, April, July and October. The average scenarios have decided the installed PV power and BES size. Three overload and three shortage scenarios have evaluated the final design in more extreme weather conditions that concern the wind velocity (m/s), outside temperature (°C), sun hours (hr) and solar radiation (W/m<sup>2</sup>). In April low outside temperatures as well as high sun power occur compared to October, so in April it is more convenient to generate an overload scenario than in October. For the same reasons October has a shortage scenario instead.

It is investigated for every hour whether the CHP, storage vessel or supplementary heater supplies the heat. The storage vessel temperature and the switching frequency are the determining factors for the heat controlled operation time. The CHP operation time is very sensitive to the amount of heat it can reject. A low heat to power ratio and the inclusion of a heat storage vessel has the preference. The 200 litre storage vessel has increased the operation time of the CHP considerably, though, in July and October the heat storage vessel (estimated at 2% an hour) causes relatively high storage losses compared to the heat demand. It is worth trying to reduce the heat to power ratio of 1:4 even more. The heat-controlled operation time of the CHP is also applicable to the electrical power output of the CHP but then converted into 15-minute-means with small start and stop adjustments. The start and stops have practically no influence on the hourly heat demand, contributed by the fact that the heat used to warm up the engines is eventually rejected



From the balance between the weekly electricity demand and CHP electricity yield for the predefined average scenarios it is immediately clear that PV power either improves or worsens the situation. In spite that PV and CHP electricity yield are complementary, it is difficult to complete the self-supporting residential area in the average scenarios of July and October without creating a long-term excess electricity yield in the April and January average scenarios. The highest reduction in electricity shortcomings compared to overproduction appear at 1 kW<sub>peak</sub> installed PV power for the detached houses. The detached house becomes self-supporting in the average scenarios of January and April, the terraced houses only in January. Because of the high heat demand of the detached house in January, the CHP even creates an excess electricity yield. The terraced houses has considerable less CHP electricity yield and require significantly more electricity yield to become self-supporting in April. The PV peak power is yet designed for the detached houses, so it is very likely that the terraced houses require higher PV power, if the rooftop area permits it. Eventually only one out of four average scenarios, namely the January average scenario, is completely self-supporting. The April average scenario comes close.

The BES devices operate on the basis of local measures. The BES devices at the end-node of the cables change their power output until the voltage level of the connection node is reached. This set-point is based on the turning point when demand equals supply. The BES device at the LV side of the transformer imitates the active and reactive power through the transformer node. The maximum absolute peak power required from the BES devices during the average scenarios occurred in April with 24 kW<sub>e</sub> at the end of the cables and 91 kW<sub>e</sub> at the transformer. With a total of six end-node BES devices and one BES device at the transformer node the total installed peak power became 235 kW<sub>e</sub> (1 kW<sub>e</sub> per household). The effective storage capacity is the highest in the average scenario of January, 87 kWh at the end-node of each cable and 415 kWh at the transformer. It figures that the BES at the transformer is 4 to 5 times bigger than the BES devices at the end of the cable. The BES peak power and capacity are set as limits for the next load-flow calculations that have assessed the reverse power flow, system losses, voltage levels and transformer loads.

The self-supporting residential area is assessed 4 times for every scenario to evaluate the effects of distributed generation and BES apart from each other:

1. without distributed generation and BES,
2. with distributed generation at a power factor of 1 and without BES,
3. with distributed generation at a power factor of 0.95 and without BES,
4. and with distributed generation at a power factor of 0.95 and with BES.

The generators within the self-supporting residential area did not create problems in the low voltage (LV) network yet, though results imply the need for any peak load shaving. The reverse power flow is limited. During the overload scenarios the reverse power flow *to* the upper grid did not exceed the average power flow without distributed generation *from* the upper grid. Reduction in transport losses and transformer loads are clearly demonstrated except for the overload scenarios where distributed generators bring about overproduction. The implementation of distributed generation increases the voltage levels in the LV network. Moreover, fluctuations of the generator's power output superimpose on already existing fluctuations of the loads causing a widening of voltage levels. Low power factors reinforce the effects of the generators on the voltage level. The highest general voltage levels occur in April as the maximum voltage level occurs in July. The total range of the 15-minute-mean voltage levels is -2% to +9% of the nominal voltage (230V). Departed from the predefined scenarios the lowest amount of 15-minute-mean power demand of 200 W per household and the highest 15-minute-mean power output of 1.8 kW increases the transformer load to 99% and the voltage level to 252 V. This is just below the upper limit of 100% and 253 V respectively. From the network operator's point of view it is not recommended to install more PV power without additional control systems. Since the self-supporting residential area of this case study is not completely self-supporting yet, the network operator might deal with even higher loads and voltage levels caused by self-supporting residential areas in the future.

The peak power, capacity and operational control of the storage devices also succeeded in minimizing the reverse power flow and transport losses. Unfortunately, storage losses have counterbalanced the effects on transport losses. At scenarios that have a distorted electricity balance BES is ineffective. Especially during the scenarios that have to contend with a general excess electricity yield, storage devices are generally fully charged and fail to serve peak load shaving, i.e. limit voltage levels and transformer loads. So, BES converges the voltage level range at scenarios with a relatively good electricity balance. At times of electricity shortage BES covers merely the peaks and during excess power supply BES covers the minima instead.

## 12. Recommendations

Recommendations for further research concern:

- the increased capacity of the power supply system,
- essential reduction of peak power
- and the necessary control mechanisms that keep the self-supporting residential area live in island mode.

The power supply system within the self-supporting residential of this case study does not yet cause trouble for the network operators, but the results indicate that a possible extension of the power supply system in this case study is limited when it increases peak power. One should search for an energy source that supports the power supply system at times the heat demand is relatively low. PV arrays with an optimized inclination angle in July and October are already suggested. Seasonal storage of the CHP electricity yield in winter is also a possibility.

BES devices have only supported the power supply system and LV network when demand and supply were in balance throughout a week. An extended self-supporting residential area requires different operational controls. A higher BES voltage set-point decreased voltage levels and transformer loads, but as a side effect the system losses increased. The control on the CHP, that switched off CHP when PV could supply the loads, lowered the reverse power flow, transformer loads and system losses. This control system can be developed into an intelligent control system that is able to control the CHP systems apart from each other with the aim to adapt supply to demand within the integrated self-supporting residential area. Though, this control increases the number of CHP switches and possible heat and electricity yield is lost. Another possibility is to replace a few of the micro Stirling CHPs by a larger gas engine CHP that is able to control active and reactive power. Moreover, the synchronous generator with P/f and U/Q static of the gas engine CHP fortifies the power supply system in island mode. It might be interesting to deploy demand side management to prevent voltage rise as well.

And at last, most distributed generators are designed for grid-connection. In that case the generators must be adapted with power electronics to control active, reactive power, frequency and voltage level in island mode.



## References

### Heat Demand Data:

- [1]. van der Laag, P.C. en Ruijg G.J. (2002). Micro-warmtekrachtsystemen voor de energievoorziening van Nederlandse huishoudens. ECN-C--02-006.
- [2]. EnergieNed (2004). Energie in Nederland 2004.
- [3]. Turkstra, J.W. (2007). Appendix Six day DC test for micro-CHP. Unpublished.
- [4]. de Jong, A. et al (2006). Technisch energie- en CO<sub>2</sub>- besparingspotentieel van micro-wkk in Nederland (2010-2030). Unpublished.
- [5]. Boerakker, M. et al (2005). Een blik op de toekomst met SAWEC; Een analyse van het woninggebonden energiegebruik voor de periode 2000-2020. ECN-C--05-070.
- [6]. EnergieNed (2004) Basisonderzoek Warmte Kleinverbruik BWK 2003.
- [7]. EnergieNed (2000) Basisonderzoek Aargasverbruik Kleinverbruikers BAK 2000.
- [8]. EnergieNed (2007) Energie in Nederland 2007.
- [9]. Continuon data (2006). Gas-demand. Measurements. Unpublished.
- [10]. EnergieNed (2006). Basisonderzoek Warmte Kleinverbruik BWK 2005.

### Introduction and Background Information:

- [11]. Popović, D.H. et al (2005) Placement of distributed generators and reclosers for distribution network security and reliability, *International Journal of Electrical Power & Energy Systems*, 27 (5-6), 398-408
- [12]. Abu-Sharkh, S. et al (2006). Can microgrids make a major contribution to UK energy supply, *Renewable & Sustainable Energy Reviews*, 10, 78-127
- [13]. Green, T.C. and Prodanović, M. (2007) Control of inverter-based micro-grids, *Electric Power Systems Research*, 77 (9),1204-121
- [14]. Lasseter, R.H. (2002). Microgrids, *IEEE Power Engineering Society Winter Meeting*
- [15]. Zoka, Y. et al (2007). An economic evaluation for an autonomous independent network of distributed energy resources, *Electric Power Systems Research*, 77(7), 831-838
- [16]. Dondi, P. et al (2002). Network integration of distributed power generation, *Journal of Power Sources*, 106 ;1-9
- [17]. Mitra, J. et al (2005). A Dynamic Programming Based Method for Developing Optimal Microgrid Architectures, in *Proc. 15th Power Systems Computational Conference*.
- [18]. Vovos, P.N. et al (2007). Centralized and Distributed Voltage Control: Impact on Distributed Generation Penetration, *IEEE Transactions on Power Systems*, 22 (1): 476
- [19]. Consortium for Electric Reliability Technology Solutions (CERTS) (2002). White Paper on Integration of Distributed Energy Resources The CERTS MicroGrid Concept, LBNL-50829
- [20]. Canadian Renewable Energy Alliance (CanREA) (2006). Distributed Generation in Canada -Maximizing the benefits of renewable resources, Canadian Renewable Energy Alliance.
- [21]. Shafiu, A. et al (2004). Active management and protection of distribution networks with distributed generation, *IEEE Power Engineering Society General Meeting*, 1: 1098- 1103
- [22]. Bocaletti, C, et al (2005). A Dynamical Model of a Gas Microturbine Generator for Distributed Generation, *European Power and Energy Systems (EuroPES) 2005*.
- [23]. Barsali, S. et al (2002). Control techniques of Dispersed Generators to improve the continuity of electricity supply, *IEEE Power Engineering Society Winter Meeting*, 2: 789- 794
- [24]. Woyte, A. et al (2001). Power flow fluctuations in distribution grids with high PV penetration, 17<sup>th</sup> European Photovoltaic Solar Energy Conference and Exhibition
- [25]. Bayegan, M. (2001). A Vision of the Future Grid, *IEEE Power Engineering Review*, 21(12): 10-12
- [26]. Ackermann, T. et al (2001). Distributed generation: a definition, *Electric Power Systems Research*, 57 (3): 195-204
- [27]. Nikkhajoei, H. and Iravani, R. (2007). Steady-State Model and Power Flow Analysis of Electronically-Coupled Distributed Resource Units, *IEEE Transactions on Power Delivery*, Publication, 22 (1): 721-728
- [28]. Deutsch, N. (2006). The Role of MicroGrid incentives in Achieving Sustainable Development - Challenges and Opportunities for Peripheries -, University of Pecs, Hungary.

- [29]. Kema (2002), Betrouwbaarheid elektriciteitsnetten in een geliberaliseerde markt, rapport: 40110117TDC 02-24787A.
- [30]. Seebregts, A.J. and Volkers, C.H. (2005). Monitoring Nederlandse Elektriciteitscentrales 2000-2004, ECN-C—05-090.

Case study:

- [31]. Lumig, van M.J.A (2007). Bepalen en uitwerken van ca. 6 varianten van toekomstige energiesystemen met decentrale opwekkers. prepared by Laborelec for Continuon Netbeheer, Unpublished.
- [32]. Paddocktrial Apeldoorn (2008), Measurement overview Micro Combined Heat and Power, WhisperGen/MicroGen measurements. Unpublished.
- [33]. Lane, N.W. (2005). Commercialization Status of Free-Piston Stirling Machines, Proceedings of the 12<sup>th</sup> International Stirling Engine Conference.
- [34]. Kim, S. et al (2005). Performance Characterization of Sunpower Free-Piston Stirling Engines, 3rd International Energy Conversion Conference.
- [35]. Verhelst, B. (2004). Elektrische aansluiting van kleine WKK's.
- [36]. Morren, J. (2006), Grid support by power electronic converters of Distributed Generation units, proefschrift TUDelft
- [37]. Website Electrical Storage Association (ESA).
- [38]. Myrzik, M.J.A. (2005). 5N510\_week5\_storage, lecture-notes Distributed Generation. Unpublished.
- [39]. KNMI klimatologie (2005). Klimaatatlas van Nederland, de normaalperiode 1971-2000.
- [40]. DTe rapport (200). Maatstafregulering inkoopkosten berekening van de inkoopkosten van elektriciteit voor levering aan beschermde afnemers.
- [41]. Ecofys (2007), Excel spreadsheets of the electricity and gas demand fractions for the year 2007. Unpublished.
- [42]. Platform Versnelling Energieliberalisering, Profielenmethodiek aardgas versie 2.10, rapporten PVE, 2004
- [43]. Platform Versnelling Energieliberalisering, Profielenmethodiek elektriciteit versie 3.20, rapporten PVE, 2005
- [44]. Phase to Phase BV (2007), User manual Vision 6.1, 07-162 PMO
- [45]. Wired-home weblog



## Nomenclature

AC	Alternating Current	
Al	Aluminium	
BES	Battery Energy Storage	
CAES	Compressed Air Energy Storage	
CHP	Combined Heat and Power	
DC	Direct Current	
DG	Distributed Generation	
DNO	Distribution Network Operator	
E.C. caps	Electrochemical capacitors	
HV	High Voltage	
Li-ion	Lithium Ion	
LV	Low Voltage	
MV	Medium Voltage	
NaS	Sodium Sulfur	
Ni-Cd	Nickel Cadmium	
VRB	Vanadium redox flow battery	
PSB	Polysulfide Bromide	
PV	Photovoltaic	
PVGIS	Photovoltaic Information System	
SMES	Superconducting Magnetic Energy Storage	
TDP	Temperature Dependent Profile	
TIP	Temperature Independent Profile	
ZnBr	Zinc Bromine	
CBES	BES capacity	[kWh]
$c_{\text{water}}$	specific heat of water	[J/(kg°C)]
dCBES	Change in BES capacity	[kWh]
E	Electricity generation	[kWh]
$E_{\text{vessel}}$	Energy content vessel	[J]
f	frequency	[Hz]
$H_{h,i}$	Monthly or yearly average daily global irradiation on the (inclined) surface	[W/m <sup>2</sup> ]
I	Sun power on earth	[W/m <sup>2</sup> ]
$I_{3\text{ph}}$	Three phase current	[A]
n	Number of years or months	
P	Active power	[W <sub>e</sub> ]
PBES(i)	Initial power in- or output of the BES	[W]
PBES(i+1)	BES power in- or output after a step change	[W]
$P_k$	Installed peak power	[W <sub>peak</sub> ]
$P_{\text{loss}}$	Active power loss	[W]
Q	Reactive power	[Var]
R	Resistance	[Ohm]
$r_p$	System performance ratio	
S	Apparent power	[VA]
Sl	Storage loss	[J]
T	Temperature	[°C]
$T_{\text{outside}}$	Outside temperature	[°C]
$T_{\text{vessel}}$	Vessel temperature	[°C]
U	Voltage	[V]
UBES	Voltage level at the BES connection-node	[V]
U <sub>fault</sub>	Discrepancy between UBES and U <sub>set</sub>	[V]
U <sub>set</sub>	Voltage level set-point at the BES connection-node	[V]
$V_{\text{vessel}}$	Volume vessel	[m <sup>3</sup> ]
X	Inductive reactance	[Ohm]
$X_C$	Capacitance reactance	[Ohm]

# Appendix

## Appendix A Demand-Side

### Appendix A1 Heat Demand

<b>Heat Demand (GJ)</b>				<b>efficiency</b>		<b>Gas demand (GJ)</b>			
<b>source</b>	<b>Space Heating</b>	<b>Hot Water</b>	<b>Total</b>	<b>SH %</b>	<b>HW %</b>	<b>source</b>	<b>Space Heating</b>	<b>Hot Water</b>	<b>Total</b>
1998 [1]	41,1	7,6	48,7	88,2	45,2	1998 [1]	50,1	11,9	62,0
2000 [4]	36,9	9,0	45,9	82,3	63,9	2000 [4]	44,8	14,1	58,9
2000 [7]	35,7	9,0	44,7	82,3	63,9	2000 [7]	43,4	14,1	57,5
2000 [5]	36,0	8,5	44,5	85,7	66,7	2000 [5]	42,0	13,0	55,0
2002 [1]	48,7	7,9	56,6	82,3	63,9	2002 [1]	59,4	12,3	71,7
2003 [2]	32,0	8,0	40,0	74,9	70,8	2003 [2]	42,7	11,3	54,0
2003 [6]	27,8	7,5	35,3	82,3	63,9	2003 [6]	33,8	11,7	45,5
2005 [10]	27,0	8,0	35,0	82,3	63,9	2005 [10]	32,8	12,5	45,3
2006 [9]	35,7	8,8	44,5	82,3	63,9	2006 [9]	43,4	13,8	57,2
2006 [8]	27,9	6,7	34,6	73,0	54,0	2006 [8]	38,2	12,3	50,5
2010 [4]	31,5	8,6	40,1	82,3	63,9	2010 [4]	38,3	13,5	51,7
2010 [1]	31,8	7,8	39,6	82,3	63,9	2010 [1]	38,7	12,2	50,9
2015 [4]	29,0	8,5	37,5	82,3	63,9	2015 [4]	35,2	13,3	48,5
2020 [5]	26,0	6,7	32,7	89,7	82,7	2020 [5]	29,0	8,1	37,1
2020 [4]	23,9	8,3	32,2	82,3	63,9	2020 [4]	29,0	13,0	42,0
Ratio	0,798	0,202	1	82,3	63,9		0,759	0,241	1

<b>Terraced</b>	<b>Space heating</b>	<b>Hot Water</b>	<b>Total heat</b>	<b>Detached</b>	<b>Space heating</b>	<b>Hot Water</b>	<b>Total heat</b>
1998 [1]	35,9	7,6	43,5	1998 [1]	63,2	7,6	70,8
2000 [4]	35,6	9,0	44,6	2000 [4]	48,1	9,0	57,1
2003 [6]	31,3	7,6	38,9	2003 [6]	47,6	7,6	55,2
2005 [10]	23,4	8,0	31,4	2005 [10]	42,0	8,0	50,0
2010 [4]	30	8,6	38,6	2010 [4]	38,7	8,6	47,3
2015 [4]	28,1	8,5	36,6	2015 [4]	34,4	8,5	42,9
2020 [4]	26	8,3	34,3	2020 [4]	31,2	8,3	39,5

Figure 69: Figure 71: Heat vs. gas demand of an average house (above), terraced and detached house (below). Yellow boxes are copied from literature, the rest is calculated with the data in the table.

### Appendix A2. Electricity Demand

<b>Electricity demand (kWh)</b>	
1998 [1]	3200
2000 [3]	3133
2000 [4]	3352
2002 [1]	3500
2003 [2]	3402
2006 [8]	3402
2006 [9]	3949
2010 [1]	3700
2010 [4]	4084
2015 [4]	4433
2020 [4]	4631

Figure 70: Electricity demand of an average house.



## Appendix A3. Sources Demand Surveys

1. van der Laag, P.C. en Ruijg G.J. (2002). Micro-warmtekrachtsystemen voor de energievoorziening van Nederlandse huishoudens. ECN-C--02-006. *Gas demand. Unclear whether it is corrected for cooking-gas or other heat sources.*
2. EnergieNed (2004). Energie in Nederland 2004. *Gas and heat demand. Unclear whether other heat sources are included. Corrected for cooking gas.*
3. Turkstra, J.W. (2007). Appendix Six day DC test for micro-CHP. By e-mail. *Heat demand, based on measurements of new build houses using residential area heating*
4. de Jong, A. et al (2006). Technisch energie- en CO<sub>2</sub>- besparingspotentieel van micro-wkk in Nederland (2010-2030). By e-mail. *Heat demand, educated guesses. Corrected for other heat sources, conversion losses and future improvements in isolation.*
5. Boerakker, M. et al (2005). Een blik op de toekomst met SAWEC; Een analyse van het woninggebonden energiegebruik voor de periode 2000-2020. ECN-C--05-070 *Heat and gas demand, educated guesses.*
6. EnergieNed (2004) Basisonderzoek Warmte Kleinverbruik BWK 2003. *Heat demand. Survey, new built houses connected to residential area heating.*
7. EnergieNed [2000] Basisonderzoek Aargasverbruik Kleinverbruikers BAK 2000. *Gas demand. Survey. Corrected for cooking gas.*
8. EnergieNed (2007) Energie in Nederland 2007. *Gas and heat demand. Unclear whether other heat sources are included. Corrected for cooking gas.*
9. Continuum data (2006). *Gas-demand. Measurements. Not corrected for anything.*
10. EnergieNed (2006). Basisonderzoek Warmte Kleinverbruik BWK 2005. *Heat demand. Survey, new built houses connected to residential area heating.*

## Appendix B (Heat-)Power Balance

Heat detached House	January			April			July			October	
	Average	Overload	Shortage	Average	Overload	Shortage	Average	Overload	Shortage	Average	Shortage
<b>Heat Demand</b>											
Total MJ	1732	2495	1390	982	1943	225	771	188	850	214	
Max kW	19,1	27,3	15,4	11,1	21,4	3,7	9,0	2,1	9,8	3,5	
Min kW	3,1	4,5	2,5	1,7	3,5	0,4	1,2	0,4	1,4	0,4	
Mean kW	11,5	16,5	9,2	6,5	12,8	1,5	5,1	1,1	5,6	1,4	
Mean deviation kW	4,2	6,0	3,4	2,4	4,7	0,6	1,9	0,4	2,1	0,6	
<b>Heat Supply</b>											
Total CHP output (MJ)	1829	2174	1382	806	2002	331	662	288	720	302	
Direct CHP (MJ)	1558	1915	1039	468	1735	56	316	37	374	48	
Heat Vessel (MJ)	122	136	206	208	130	131	217	109	216	119	
Supplementary heater (MJ)	51	444	145	305	78	39	238	43	261	47	
Storage losses (MJ)	148	123	137	130	137	145	129	142	131	135	
Contribution Direct CHP (%)	90	77	75	48	89	25	41	19	44	22	
Contribution Vessel (%)	7	5	15	21	7	58	28	58	25	56	
Contribution suppl. Heat (%)	3	18	10	31	4	17	31	23	31	22	
Lost CHP output (%)	8	5	10	16	7	44	19	49	18	45	

Figure 71: Heat data average house throughout a week.

Heat Terraced House	January			Maart			July			October	
	Average	Overload	Shortage	Average	Overload	Shortage	Average	Overload	Shortage	Average	Shortage
<b>H demand terraced</b>											
Total MJ	1413	2036	1134	801	1585	184	629	154	694	175	
Max kW	15,6	22,3	12,6	9,1	17,4	3,0	7,3	1,9	8,0	2,8	
Min kW	2,5	3,6	2,0	1,4	2,8	0,3	1,0	0,3	1,2	0,3	
Mean kW	9,3	13,5	7,5	5,3	10,5	1,2	4,2	1,0	4,6	1,2	
Mean deviation kW	3,4	4,9	2,7	2,0	3,8	0,5	1,6	0,3	1,7	0,5	
<b>Terraced</b>											
Total CHP output (MJ)	1411	2016	994	662	1642	288	547	230	576	274	
Direct CHP (MJ)	1073	1781	640	322	1345	41	218	25	251	35	
Heat Vessel (MJ)	198	106	222	213	149	107	202	74	198	102	
Supplementary heater (MJ)	142	150	272	266	91	35	210	55	245	37	
Storage losses (MJ)	140	129	131	127	148	140	128	132	127	136	
Contribution Direct CHP (%)	76	88	64	49	82	14	40	11	44	13	
Contribution Vessel (%)	14	5	22	32	9	37	37	32	34	37	
Contribution suppl. Heat (%)	10	7	27	40	6	12	38	24	43	14	
Lost CHP output (%)	10	6	13	19	9	49	23	57	22	50	

Figure 72: Heat data terraced house.

Electricity/Power	January			April			July			October	
	Average	Overload	Shortage	Average	Overload	Average	Overload	Shortage	Average	Shortage	
Power/Electricity Demand											
Total kWh	90,45	89,44	93,55	72,78	71,61	66,68	63,26	70,28	79,27	80,51	
Max kW	0,96	0,97	1,01	0,69	0,68	0,55	0,54	0,62	0,84	0,88	
Min kW	0,21	0,20	0,21	0,20	0,20	0,20	0,20	0,20	0,21	0,21	
Mean kW	0,54	0,53	0,56	0,43	0,43	0,40	0,38	0,42	0,47	0,48	
Mean deviation	0,18	0,18	0,20	0,12	0,11	0,10	0,09	0,11	0,14	0,15	
PV Power/Electricity Output											
Total kWh	5,31	20,51	2,58	22,04	40,74	24,39	40,35	13,32	12,16	5,60	
Max kW	0,14	0,54	0,06	0,38	0,77	0,38	0,72	0,17	0,26	0,11	
Min kW	0,00	0,00	0,00	0,00	0,00	0,00	0,00	0,00	0,00	0,00	
Mean kW	0,03	0,12	0,02	0,13	0,24	0,15	0,24	0,08	0,07	0,03	
Mean deviation kW	0,04	0,17	0,02	0,13	0,26	0,13	0,25	0,06	0,09	0,04	
CHP Power/Electricity Output (detached)											
Total kWh	126,70	150,70	95,39	55,39	138,70	22,39	45,39	19,39	49,39	20,39	
CHP Power/Electricity Output (Terraced)											
Total kWh	97,39	139,70	68,39	45,39	113,57	19,39	37,39	15,52	39,39	18,39	

Figure 73: Electricity data detached and terraced house.

Electricity/Power comparison	January			April			July			October	
	Average	Overload	Shortage	Average	Overload	Average	Overload	Shortage	Average	Shortage	
detached House											
kWh overload	53,17	85,88	33,29	33,64	39,74	14,49	45,28	10,50	25,00	8,98	
kWh Shortage	-11,61	-4,10	-28,86	-28,98	-13,39	-34,38	-22,79	-48,06	-42,71	-63,49	
Total Balance	41,56	81,77	4,43	4,66	26,35	-19,89	22,49	-37,57	-17,71	-54,51	
Maximum power overload	0,78	1,04	0,77	0,90	1,34	0,89	1,27	0,69	0,80	0,78	
Maximum power shortage	-0,56	-0,35	-0,82	-0,67	-0,29	-0,55	-0,54	-0,59	-0,81	-0,88	
Terraced House											
kWh overload	37,87	78,03	22,88	28,19	24,77	13,18	38,64	8,31	19,67	7,48	
kWh Shortage	-25,61	-7,26	-45,45	-33,53	-23,55	-36,07	-24,15	-49,75	-47,38	-63,99	
Total Balance	12,25	70,77	-22,57	-5,34	1,22	-22,89	14,49	-41,44	-27,71	-56,51	
Maximum power overload	0,73	1,04	0,74	0,90	1,34	0,89	1,26	0,69	0,80	0,78	
Maximum power shortage	-0,79	-0,42	-0,91	-0,69	-0,64	-0,55	-0,54	-0,59	-0,82	-0,88	

Figure 74: Electricity balance detached and terraced house.

## Appendix C. Electrical Power Profiles Detached House

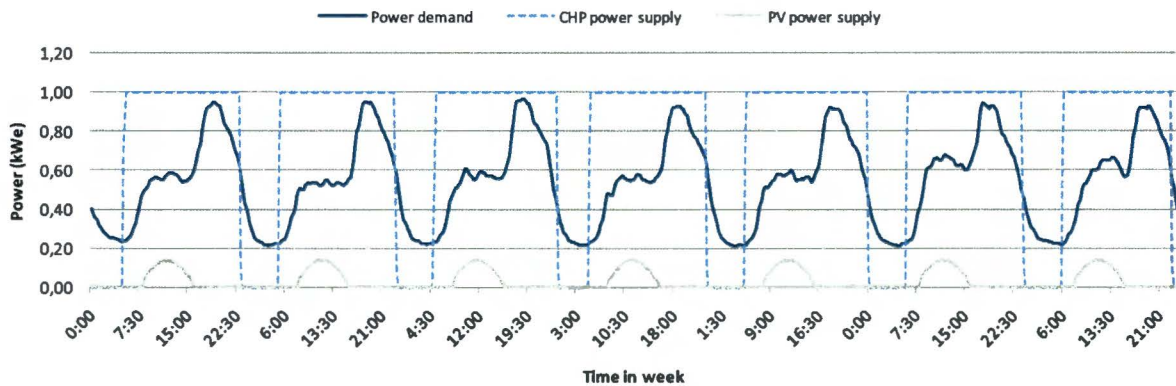


Figure 75: Average scenario power profile of a detached house throughout a week in January.



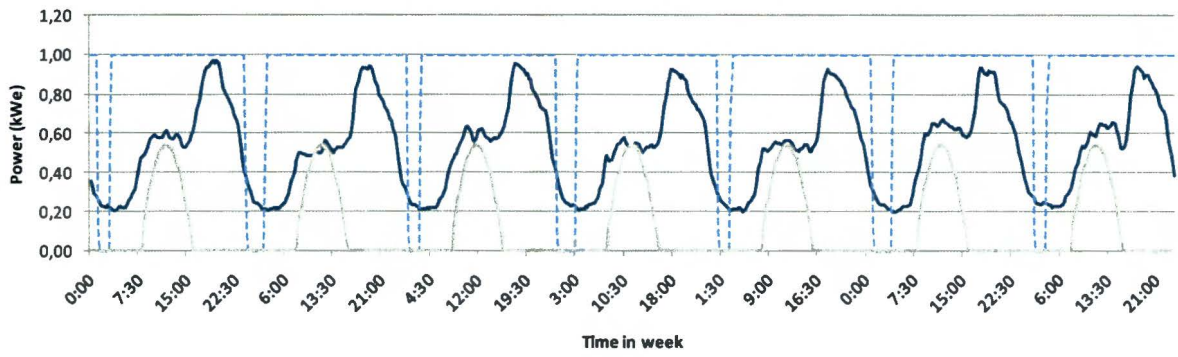


Figure 76: Overload scenario power profile of a detached house throughout a week in January.

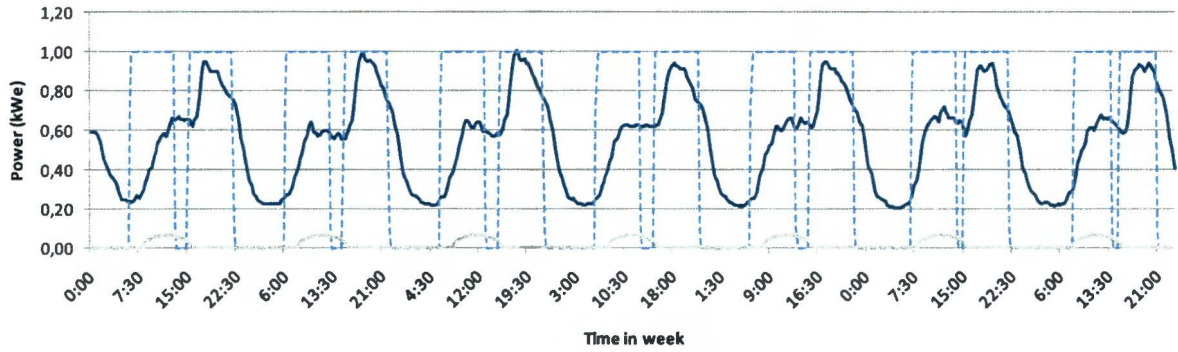


Figure 77: Shortage scenario power profile of a detached house throughout a week in January.

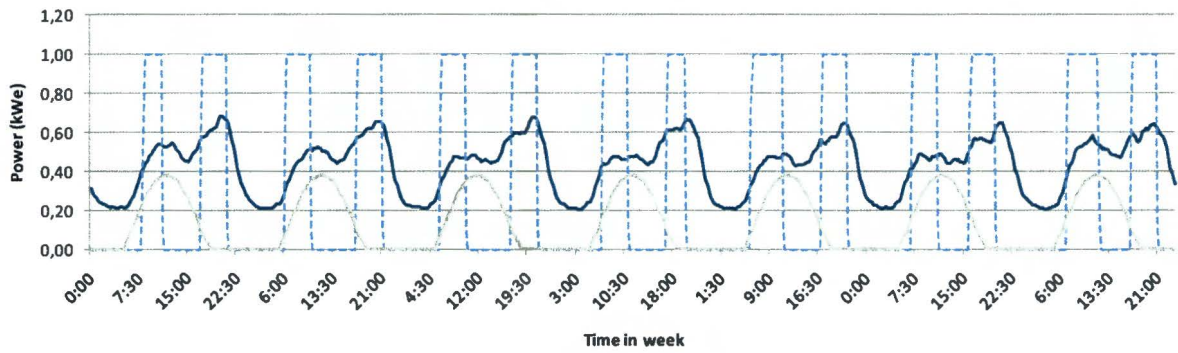


Figure 78: Average scenario power profile of a detached house throughout a week in April

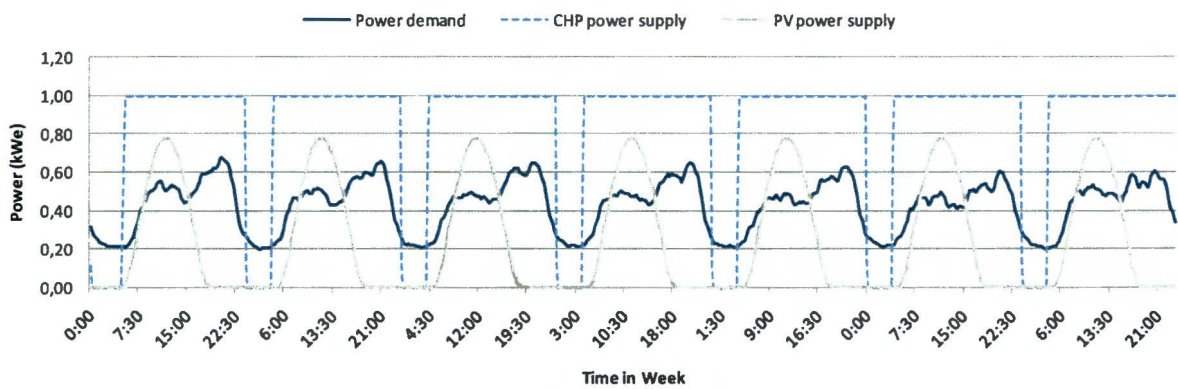


Figure 79: Overload scenario power profile of a detached house throughout a week in April.

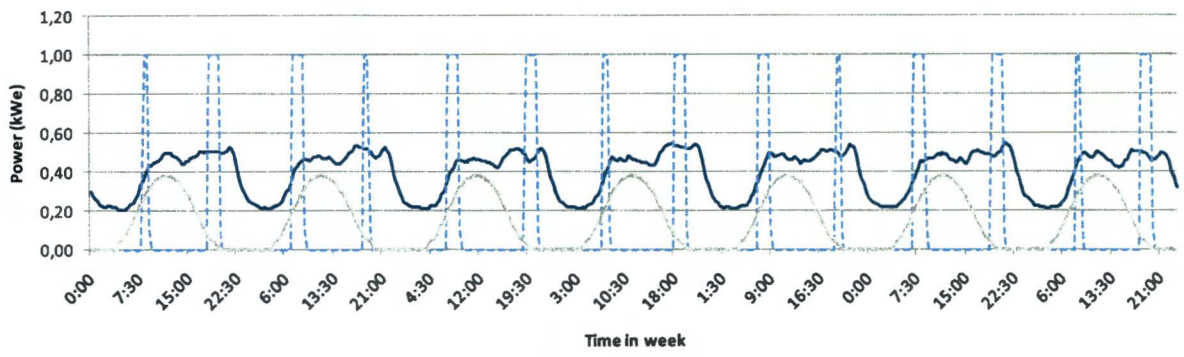


Figure 80: Average scenario power profile of a detached house throughout a week in July

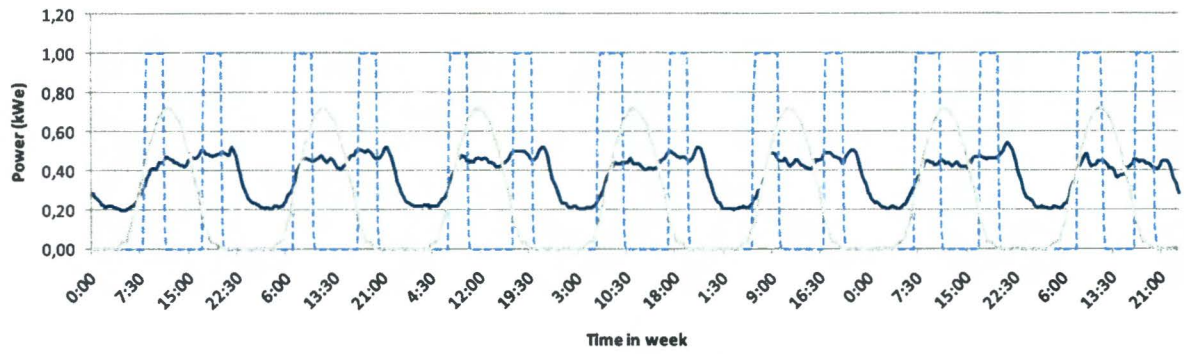


Figure 81: Overload scenario power profile of a detached house throughout a week in July.

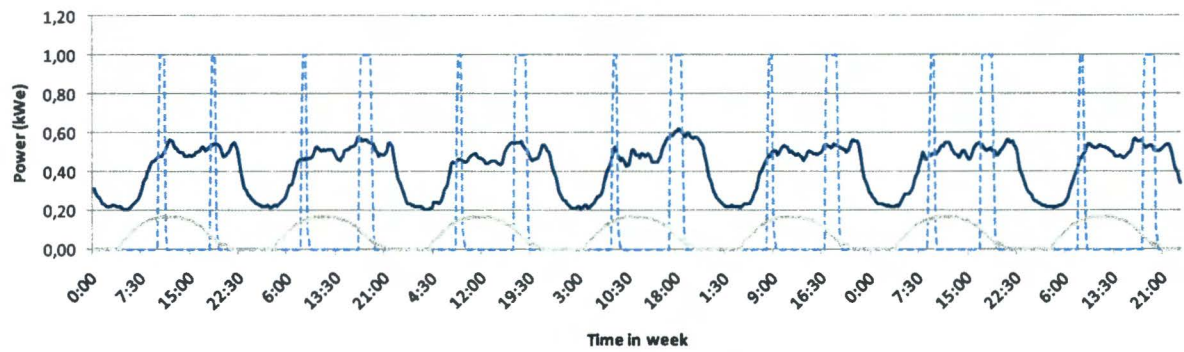


Figure 82: Shortage scenario power profile of a detached house throughout a week in July.

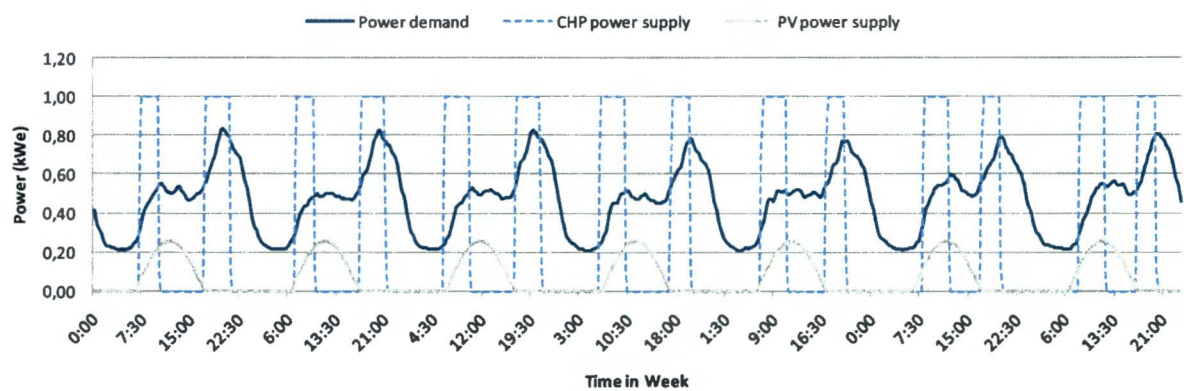


Figure 83: Average scenario power profile of a detached house throughout a week in October.



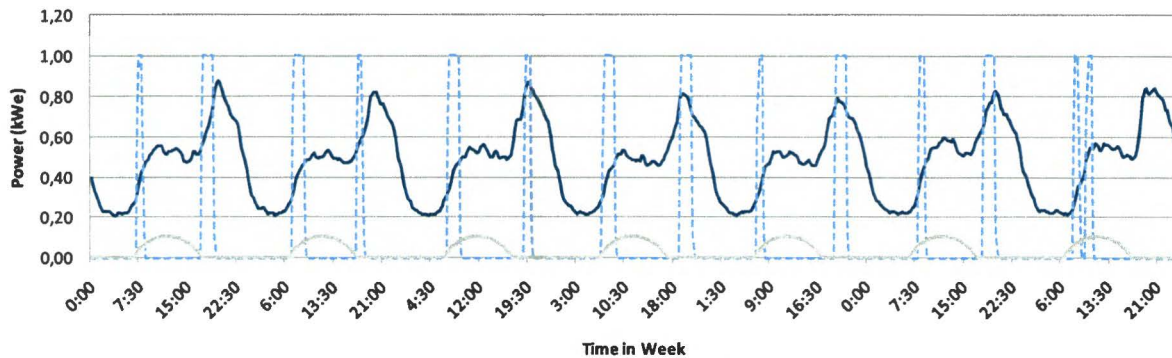


Figure 84: Shortage scenario power profile of a detached house throughout a week in October.

## Appendix D Vision Macro

```
setPQS('_')
```

### //SET LOAD BEHAVIOUR

```
set (loadbehaviour('Frans').ConstantP,100)
set (loadbehaviour('Frans').ConstantQ,100)
set (loadbehaviour('Merel').ConstantP,100)
set (loadbehaviour('Merel').ConstantQ,100)
setselection (Node('Alle knooppunten').Simultaneousness,1)
```

### //CREATE EXCEL SPREADSHEETS

```
Title (1,'Loads')
Write (1,1,1,'Transformer(%)')
Write (1,1,2,'Cable 1 (%)')
Write (1,1,3,'Cable 2 (%)')
...
Write (1,1,7,'Cable 6 (%)')
```

```
Title (2,'Voltages')
Write (2,1,1,'Transformer (V)')
Write (2,1,2,'Node A (V)')
Write (2,1,3,'Node B (V)')
Write (2,1,4,'Node C (V)')
Write (2,1,5,'Node C41 (V)')
Write (2,1,6,'Node D (V)')
Write (2,1,7,'Node E (V)')
Write (2,1,8,'Node F (V)')
Write (2,1,9,'Node G (V)')
Write (2,1,10,'Node X (V)')
```

```
Title (3,'Energybalance')
write (3,1,1,'netverlies (kW)')
write (3,1,2,'netverlies (kVAr)')
Write (3,1,3,'Ploss trafo')
Write (3,1,4,'Qloss trafo')
Write (3,1,6,'P1 from grid')
Write (3,1,7,'Q1 from grid')
Write (3,1,8,'P2 from grid')
Write (3,1,9,'Q2 from grid')
```

```
Title (4,'Voltage Cable3')
Write (4,1,1,'Node C1 (V)')
Write (4,1,2,'Node C5 (V)')
Write (4,1,3,'Node C9 (V)')
Write (4,1,4,'Node C13 (V)')
Write (4,1,5,'Node C17 (V)')
Write (4,1,6,'Node C21 (V)')
Write (4,1,7,'Node C25 (V)')
Write (4,1,8,'Node C29 (V)')
Write (4,1,9,'Node C33 (V)')
Write (4,1,10,'Node C37 (V)')
Write (4,1,11,'Node C (V)')
```

```
Title (5,'zonderBES')
Write (5,1,1,'P1 from grid')
Write (5,1,2,'Q1 from grid')
Write (5,1,3,'P2 from grid')
Write (5,1,4,'Q2 from grid')
```

```
Title (5,'metBES')
Write (5,1,1,'P1 from grid')
Write (5,1,2,'Q1 from grid')
Write (5,1,3,'P2 from grid')
Write (5,1,4,'Q2 from grid')
write (5,1,5,'PI7')
write (5,1,6,'QI7')
write (5,1,7,'Real7')
write (5,1,8,'PI1')
write (5,1,9,'Real1')
write (5,1,10,'PI2')
write (5,1,11,'Real2')
...
write (5,1,18,'PI6')
write (5,1,19,'Real6')
```

### //RECALL EXCEL-FILE INPUT:

```
set (Pad,Network.FilePath)
set (filenaam1, REPLACESTR('MAPWoonhuizen
A.xls','MAP',Pad))
set (filenaam2, REPLACESTR('MAPWoonhuizen
B.xls','MAP',Pad))
open (1, filenaam1)
open (2, filenaam2)
```

```
set(r1j,2)
set(Eopslag1,205000) //watt
set(Eopslag2,205000) //watt
...
set(Eopslag6,205000) //watt
set(Eopslag7,800000) //watt
set(dOpslag1,0)
set(dOpslag2,0)
...
set(dOpslag6,0)
set(dOpslag7,0)
```

```
loop(index, 2,2,1)
```

```
Set(Pnet,0)
Set(Qnet,0)
Set(Load('Opslag1').PI,0)
Set(Load('Opslag2').PI,0)
...
Set(Load('Opslag6').PI,0)
Set(Load('Opslag7').PI,0)
```

```

//READ OUT INFORMATION:
Read (1, 1, rij, 1,PbelastingwoonhuisA)
multiply (PbelastingwoonhuisA,1000)
SetSelection (Load('Woonhuis A').PL,PbelastingwoonhuisA)
Read (1, 2, rij, 1,PopwekwoonhuisA)
multiply (PopwekwoonhuisA,-1000)
SetSelection (Load('Opwek woonhuis A').PL,PopwekwoonhuisA)

```

```

Read (1, 1, rij, 2,QbelastingwoonhuisA)
multiply (QbelastingwoonhuisA,1000)
SetSelection (Load('Woonhuis A').QL,QbelastingwoonhuisA)
Read (1, 2, rij, 2,QopwekwoonhuisA)
multiply (QopwekwoonhuisA,-1000)
SetSelection (Load('Opwek woonhuis A').QL,QopwekwoonhuisA)

```

```

Read (2, 1, rij, 1,PbelastingwoonhuisB)
multiply (PbelastingwoonhuisB,1000)
SetSelection (Load('Woonhuis B').PL,PbelastingwoonhuisB)
Read (2, 2, rij, 1,PopwekwoonhuisB)
multiply (PopwekwoonhuisB,-1000)
SetSelection (Load('Opwek woonhuis B').PL,PopwekwoonhuisB)

```

```

Read (2, 1, rij, 2,QbelastingwoonhuisB)
multiply (QbelastingwoonhuisB,1000)
SetSelection (Load('Woonhuis B').QL,QbelastingwoonhuisB)
Read (2, 2, rij, 2,QopwekwoonhuisB)
multiply (QopwekwoonhuisB,-1000)
SetSelection (Load('Opwek woonhuis B').QL,QopwekwoonhuisB)

```

#### //CALCULATIONS WITHOUT BES

```
Loadflow(0,L,true)
```

#### //CALCULATIONS WITH BES:

```

set(Uset,0.410)
set(C,1500)
set(B1,Node('Checkpoint A').U)
set(B2,Node('Checkpoint B').U)
set(B3,Node('Checkpoint C41').U)
set(B4,Node('Checkpoint X').U)
set(B5,Node('Checkpoint E').U)
set(B6,Node('Checkpoint F').U)
set(Ufout1,Difference(B1,Uset))
set(Ufout2,Difference(B2,Uset))
...
set(Ufout6,Difference(B6,Uset))

```

```
loop(i,1,100,1)
```

#### //BES 1, NODE A:

```

if(Ufout1,<,0)
multiply(Ufout1,C)
multiply(Ufout1,i)
set(dP1,Ufout1)
set(Popslag1,Load('Opslag1').PI)
add(Popslag1,dP1)
//CRITERION 1: Maximum power
if(Popslag1,>,29000)//maximaal vermogen leverbaar.
set(dP1,0)
set(Popslag1,29000)
end
if(Popslag1,<,-29000)
set(dP1,0)
set(Popslag1,-29000)
end
//CRITERION 2: Losses
if (Popslag1,>,0)
set(dOpslag1,product(dP1,0.92))
else
set(dOpslag1,quotient(dP1,0.92))//verliezen
end
add(Eopslag1,dOpslag1)
//CRITERION 3: Maximum Capacity
if(Eopslag1,>,0)
if(Eopslag1,<,410000)
set(Load('Opslag1').PI,Popslag1)
Loadflow(0,L,true)
end
end
if(Eopslag1,<,0)
subtract(Eopslag1,dOpslag1)
subtract(Popslag2,dP2)

```

```

end
if(Eopslag1,>,410000)
subtract(Eopslag1,dOpslag1)
subtract(Popslag2,dP2)
end
//New voltage level:
set(B1,Node('Checkpoint A').U)
set(Ufout1,Difference(B1,Uset))
end

```

#### //BES 2, node B:

```

if(Ufout2,<,0)
multiply(Ufout2,C)
multiply(Ufout2,i)
set(dP2,Ufout2)
set(Popslag2,Load('Opslag2').PI)
add(Popslag2,dP2)
if(Popslag2,>,29000)
set(dP2,0)
set(Popslag2,29000)
end
if(Popslag2,<,-29000)
set(dP2,0)
set(Popslag2,-29000)
end
if (Popslag2,>,0)
set(dOpslag2,product(dP2,0.92))
else
set(dOpslag2,quotient(dP2,0.92))
end
add(Eopslag2,dOpslag2)
if(Eopslag2,>,0)
if(Eopslag2,<,410000)
set(Load('Opslag2').PI,Popslag2)
Loadflow(0,L,true)
end
end
if(Eopslag2,<,0)
subtract(Eopslag2,dOpslag2)
subtract(Popslag2,dP2)
end
if(Eopslag2,>,410000)
subtract(Eopslag2,dOpslag2)
subtract(Popslag2,dP2)
end
set(B2,Node('Checkpoint B').U)
set(Ufout2,Difference(B2,Uset))
end

```

#### //BES 3, node C41:

```
...
```

#### //BES 4, node X:

```
...
```

#### //BES 5, node E:

```
...
```

#### //BES 6, node F:

```

if(Ufout6,<,0)
multiply(Ufout6,C)
multiply(Ufout6,i)
set(dP6,Ufout6)
set(Popslag6,Load('Opslag6').PI)
add(Popslag6,dP6)
if(Popslag6,>,29000)
set(dP6,0)
set(Popslag6,29000)
end
if(Popslag6,<,-29000)
set(dP6,0)
set(Popslag6,-29000)
end
if (Popslag6,>,0)
set(dOpslag6,product(dP6,0.92))
else
set(dOpslag6,quotient(dP6,0.92))
end
add(Eopslag6,dOpslag6)
if(Eopslag6,>,0)
if(Eopslag6,<,410000)

```



```

    set(Load('Opstag6').Pl,Popstag6)
    Loadflow(0,L,true)
end
end

if(Eopstag6,<,0)
    subtract(Eopstag6,dOpstag6)
    subtract(Popstag6,dP6)
end
if(Eopstag6,>,410000)
    subtract(Eopstag6,dOpstag6)
    subtract(Popstag6,dP6)
end
set(B6,Node('Checkpoint F').U)
set(Ufout6,Difference(B6,Uset))
end

//BES 7 at the transformer:
set(Qtrafo,Transformer('Transformer').Q2)
set(Ptrafo,Transformer('Transformer').P2)
add(load('Opstag7').Pl,Ptrafo)
add(load('Opstag7').Ql,Qtrafo)
Loadflow(0,L,true)

//CRITERION 1: LOSSES
if(Load('Opstag7').Pl,>,0)
    multiply(Ptrafo,0.92)
else
    divide(Ptrafo,0.92)
end
add(Eopstag7,Ptrafo)

//CRITERION 2: MAXIMUM POWER
if(Load('Opstag7').Pl,>,91000)
    set(Load('Opstag7').Pl,91000)
    set(Eopstag7,sum(Eopslagoud,83720))
end
if(Load('Opstag7').Pl,<,-91000)
    set(Load('Opstag7').Pl,-91000)
    set(Eopslag7,sum(Eopslagoud,-98913))
end
//CRITERION 3: MAXIMUM CAPACITY
if(Eopslag7,<,0)
    set(Load('Opstag7').Pl,product(Eopslagoud,-1))
    set(Eopslag7,0)
end
if(Eopslag7,>,1700000)
    set(Load('Opstag7').Pl,difference(1700000,Eopslagoud))
    set(Eopslag7,1700000)
end
if(Load('Opstag7').Pl,=,0)
    set(Load('Opstag7').Ql,0)
end
Loadflow(0,L,true)
End

//Check:
if(Network.Result,=,'LF')

//WRITING RESULTS:
for(Cable,k)

```

```

    add(Pnet,k.Ploss)
    add(Qnet,k.Qloss)
end

Write(1,rij,1,transformer('Transformer').Load)
Write(1,rij,2,Cable('Cable 1').Load)
Write(1,rij,3,Cable('Cable 2').Load)
...
Write(1,rij,7,Cable('Cable 6').Load)

Write(2,rij,1,node('Secundair trafo').U)
Write(2,rij,2,node('Checkpoint A').U)
Write(2,rij,3,node('Checkpoint B').U)
Write(2,rij,4,node('Checkpoint C').U)
Write(2,rij,5,node('Checkpoint C41').U)
Write(2,rij,6,node('Checkpoint D').U)
Write(2,rij,7,node('Checkpoint E').U)
Write(2,rij,8,node('Checkpoint F').U)
Write(2,rij,9,node('Checkpoint G').U)
Write(2,rij,10,node('Checkpoint X').U)

write(3,rij,1,Pnet)
write(3,rij,2,Qnet)
Write(3,rij,3,Transformer('Transformer').Ploss)
Write(3,rij,4,Transformer('Transformer').Qloss)
Write(3,rij,6,Transformer('Transformer').P1)
Write(3,rij,7,Transformer('Transformer').Q1)
Write(3,rij,8,Transformer('Transformer').P2)
Write(3,rij,9,Transformer('Transformer').Q2)

Write(4,rij,1,node('Checkpoint C1').U)
Write(4,rij,2,node('Checkpoint C5').U)
Write(4,rij,3,node('Checkpoint C9').U)
Write(4,rij,4,node('Checkpoint C13').U)
Write(4,rij,5,node('Checkpoint C17').U)
Write(4,rij,6,node('Checkpoint C21').U)
Write(4,rij,7,node('Checkpoint C25').U)
Write(4,rij,8,node('Checkpoint C29').U)
Write(4,rij,9,node('Checkpoint C33').U)
Write(4,rij,10,node('Checkpoint C37').U)
Write(4,rij,11,node('Checkpoint C').U)

Write(5,rij,1,Transformer('Transformer').P1)
Write(5,rij,2,Transformer('Transformer').Q2)
Write(5,rij,3,Transformer('Transformer').P2)
Write(5,rij,4,Transformer('Transformer').Q2)
write(5,rij,5,Load('Opstag7').Pl)
write(5,rij,6,Load('Opstag7').Ql)
write(5,rij,7,Eopslag7)
write(5,rij,8,Load('Opstag1').Pl)
write(5,rij,9,Eopslag1)
write(5,rij,10,Load('Opstag2').Pl)
write(5,rij,11,Eopslag2)
...
write(5,rij,18,Load('Opstag6').Pl)
write(5,rij,19,Eopslag6)

End
Add(rij,1)
End

```

# Appendix E Battery Energy Storage

## Appendix E.1 Average scenario in January

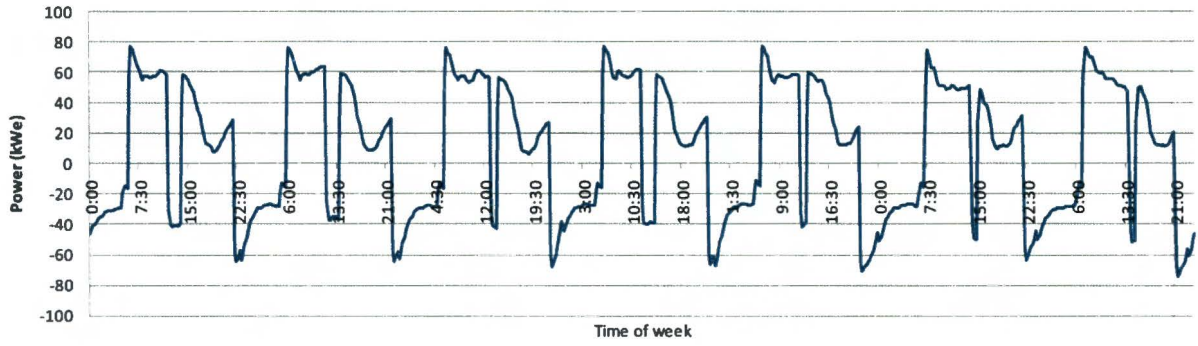


Figure 85: BES power profile at the transformer with no BES limitations throughout an average week in January.

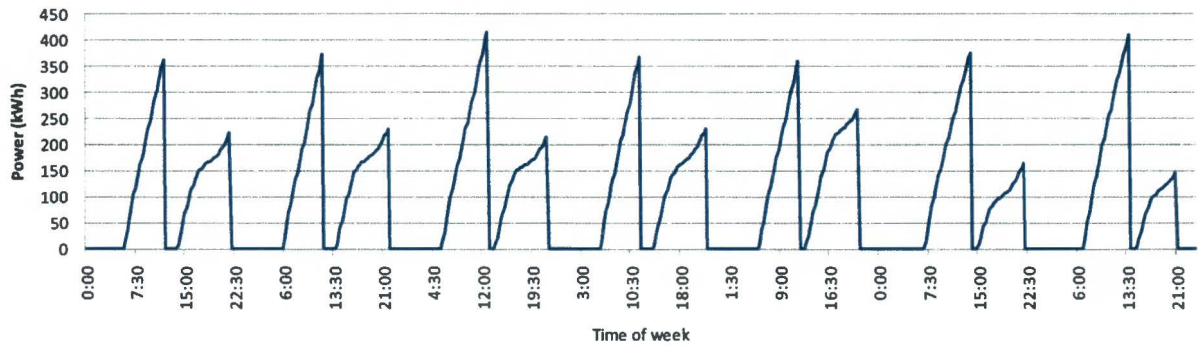


Figure 86: Required BES capacity at the transformer throughout an average week in January (exclusive of storage losses).

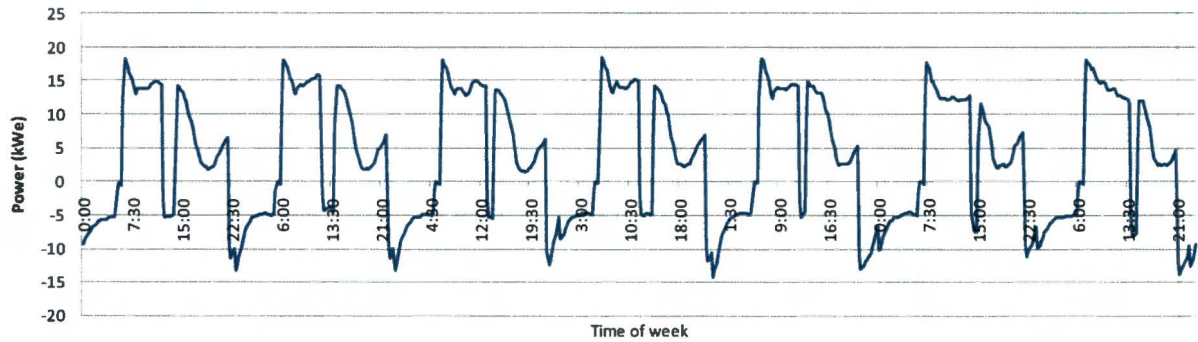


Figure 87: BES power profile at the end of cable three throughout an average week in January.

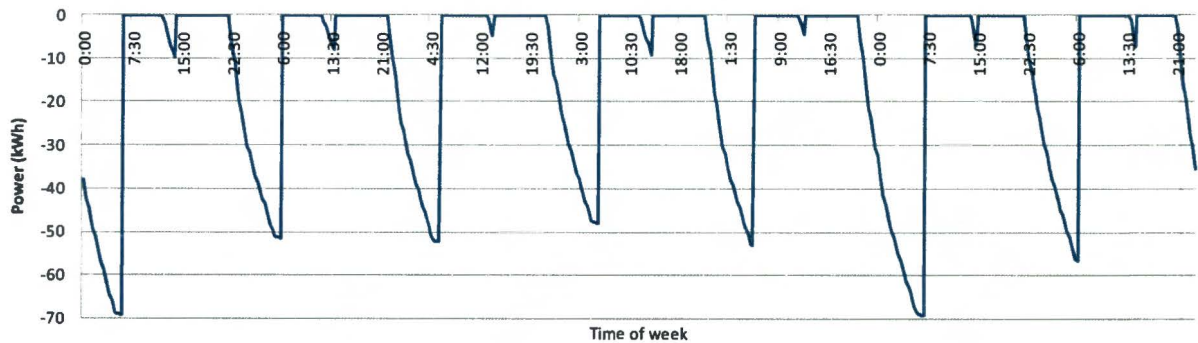


Figure 88: Required BES capacity at Cable three throughout an average week in January.



## Appendix E2 Average scenario in April

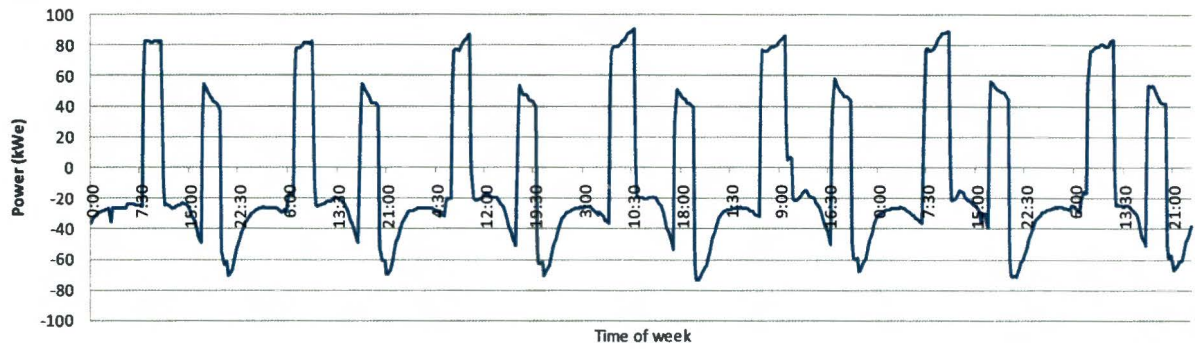


Figure 89: BES power profile at the transformer with no BES limitations throughout an average week in April.

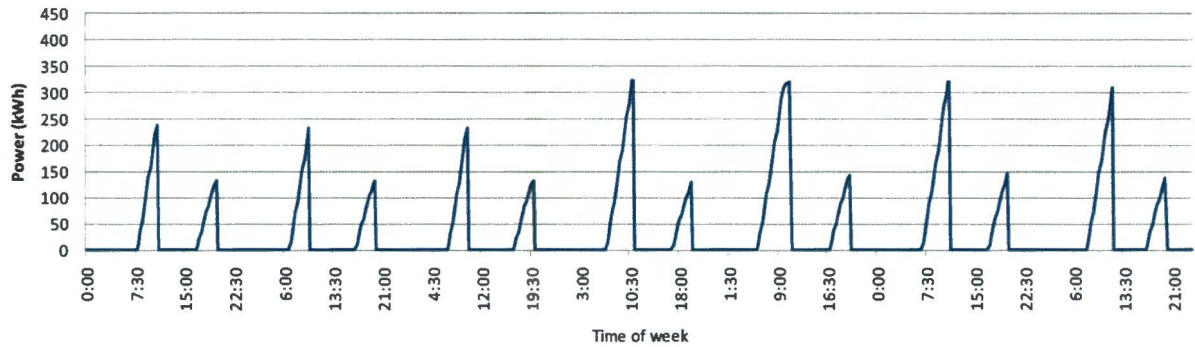


Figure 90: Required BES capacity at the transformer throughout an average week in April.

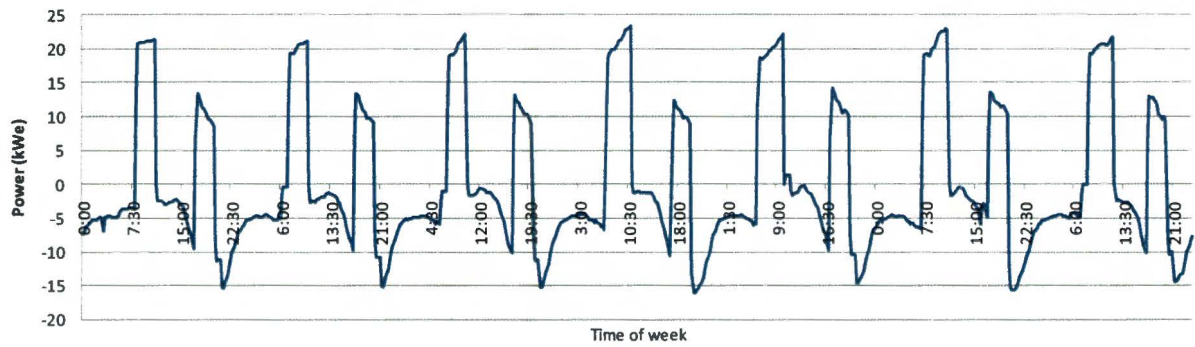


Figure 91: BES power profile at the end of cable three throughout an average week in April.

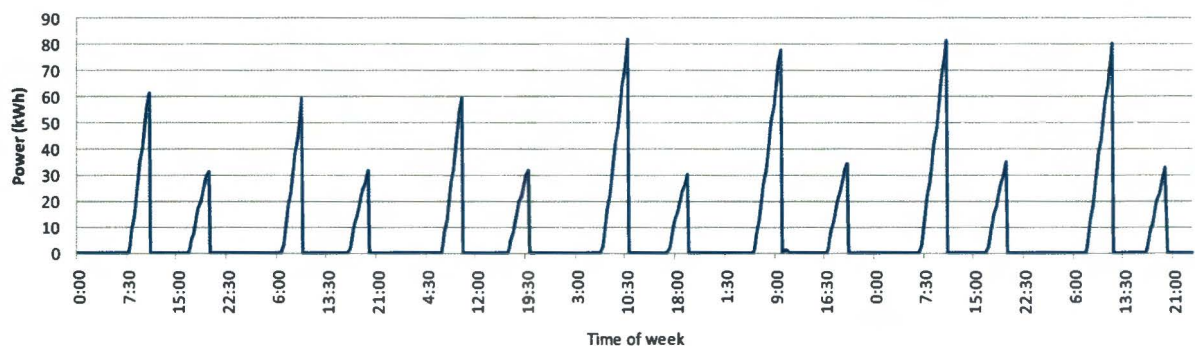


Figure 92: Required BES capacity at Cable three throughout an average week in April.

## Appendix E3 Average scenario in July

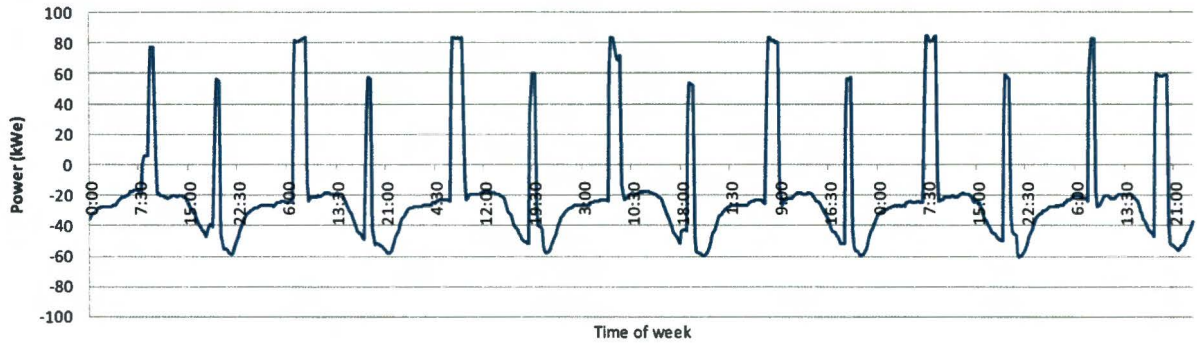


Figure 93: BES power profile at the transformer with no BES limitations throughout an average week in July.

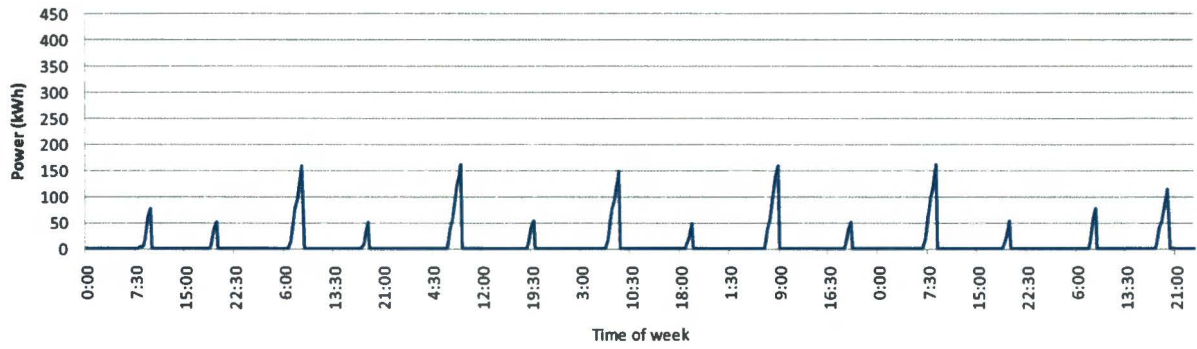


Figure 94: Required BES capacity at the transformer throughout an average week in July.

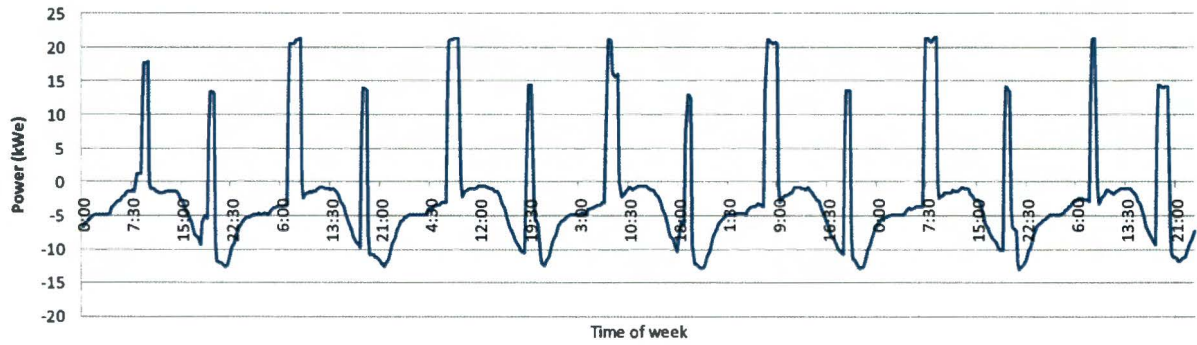


Figure 95: BES power profile at the end of cable three throughout an average week in July.

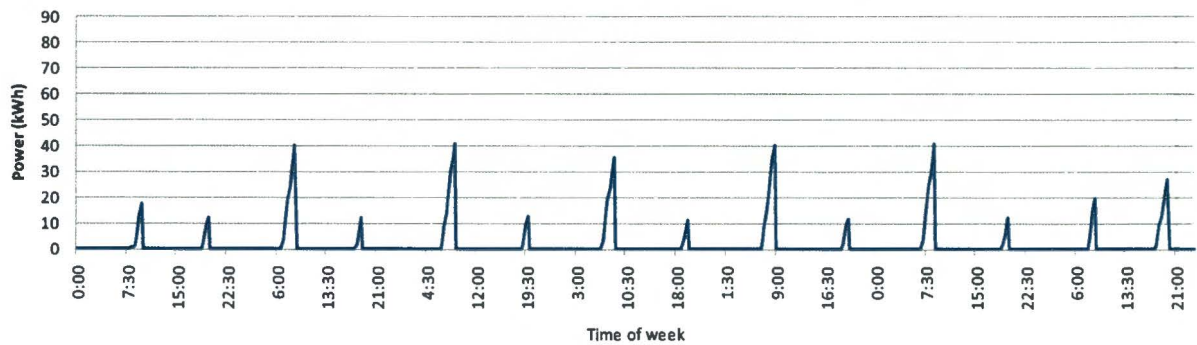


Figure 96: Required BES capacity at Cable three throughout an average week in July.



# Appendix E4 Average scenario in October

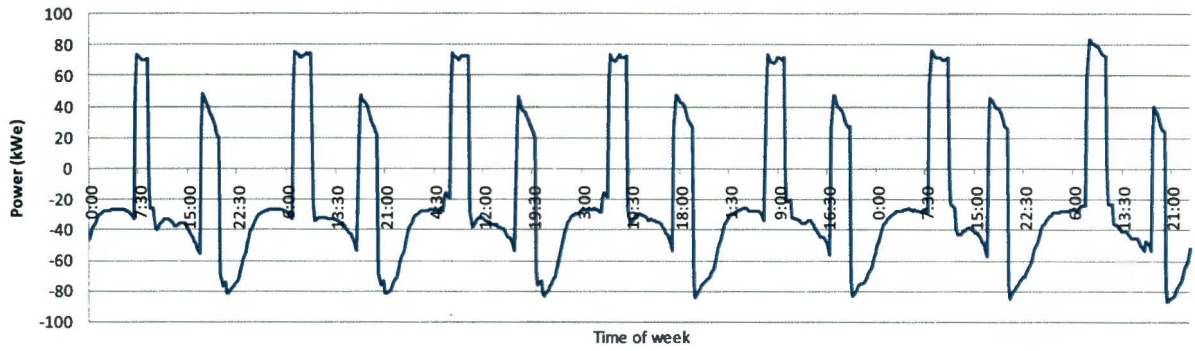


Figure 97: BES power profile at the transformer with no BES limitations throughout an average week in October.

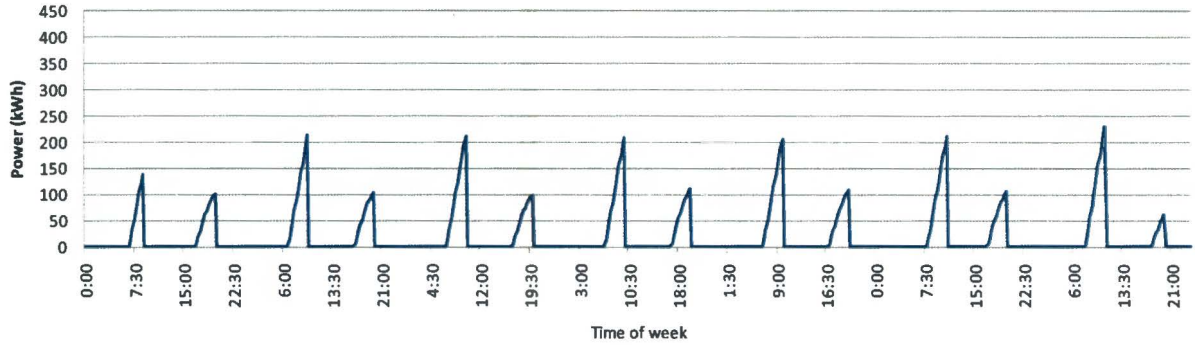


Figure 98: Required BES capacity at the transformer throughout an average week in October.

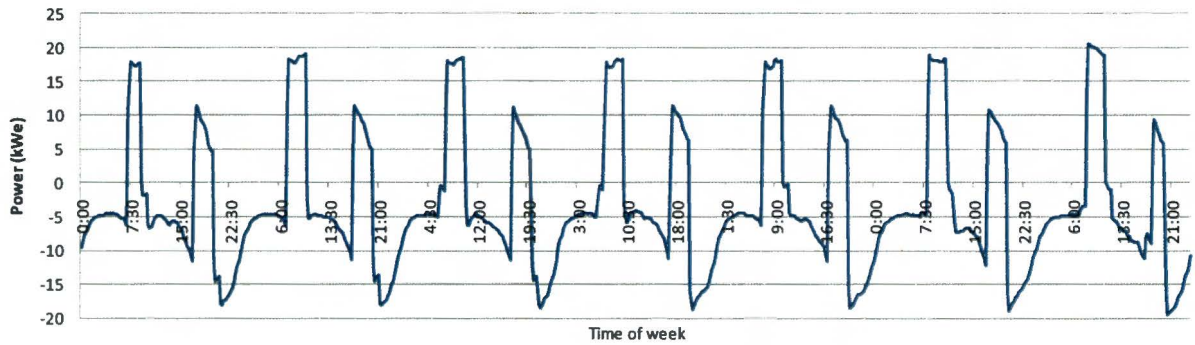
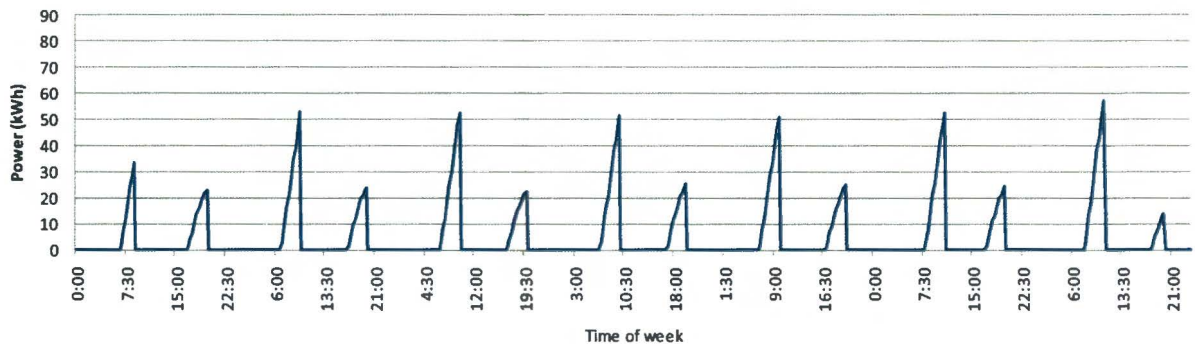


Figure 99: BES power profile at the end of cable three throughout an average week in October.



100: Required BES capacity at Cable three throughout an average week in October.

## Appendix F Reverse Power flow

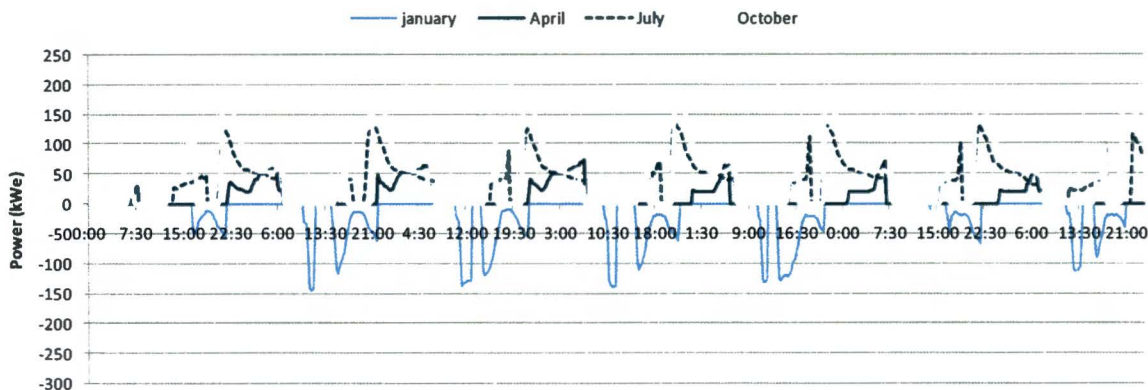


Figure 101: Power flow from the upper grid to the LV network at the average scenarios throughout a week.

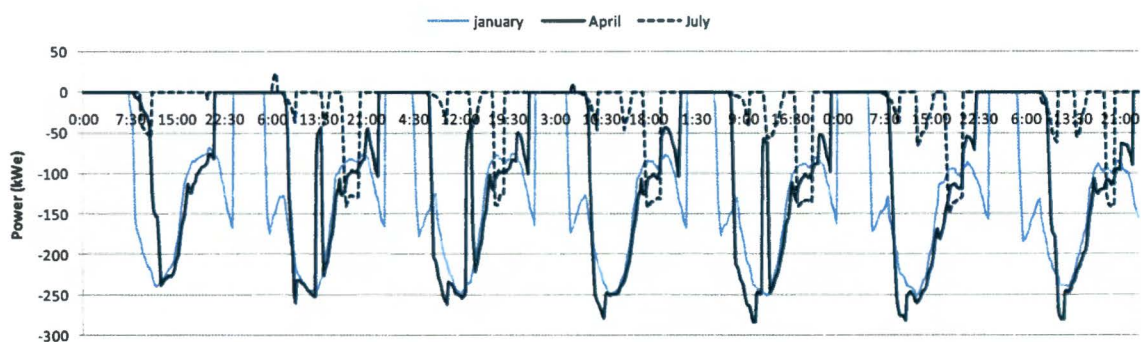


Figure 102: Power flow from the upper grid to the LV network at the overload scenarios throughout a week.

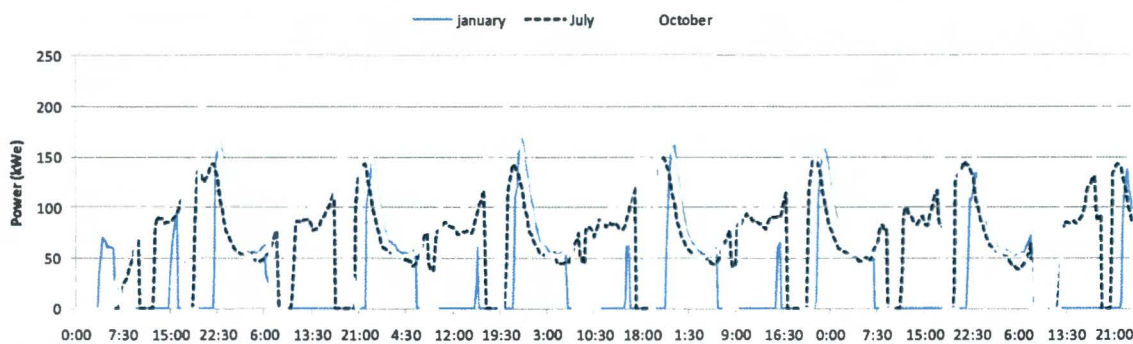


Figure 103: Power flow from the upper grid to the LV network at the shortage scenarios throughout a week.

## Appendix G Voltage levels

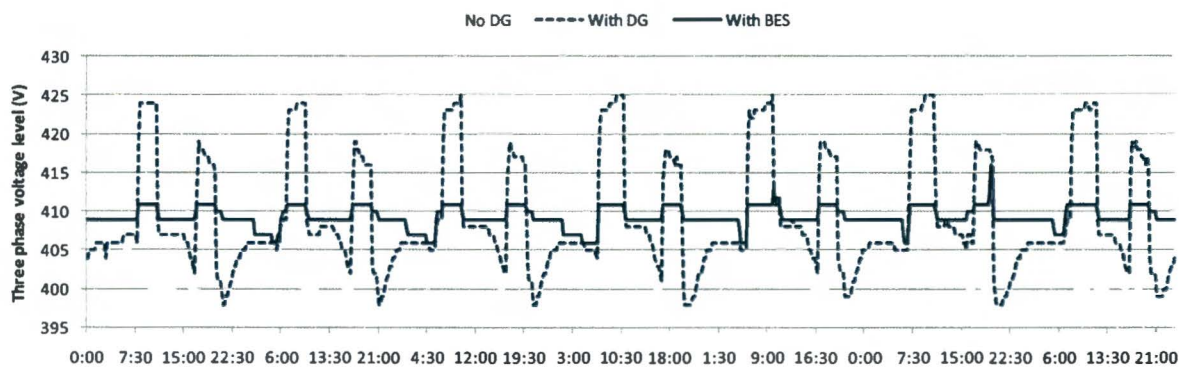


Figure 104: Voltage level of node C throughout a week during the average scenario in April.



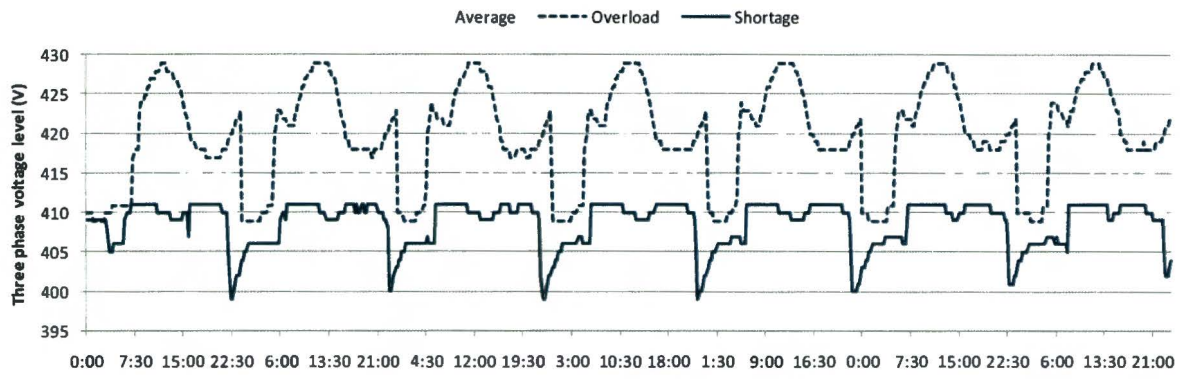


Figure 105: Voltage level of node C throughout a week in January with BES.

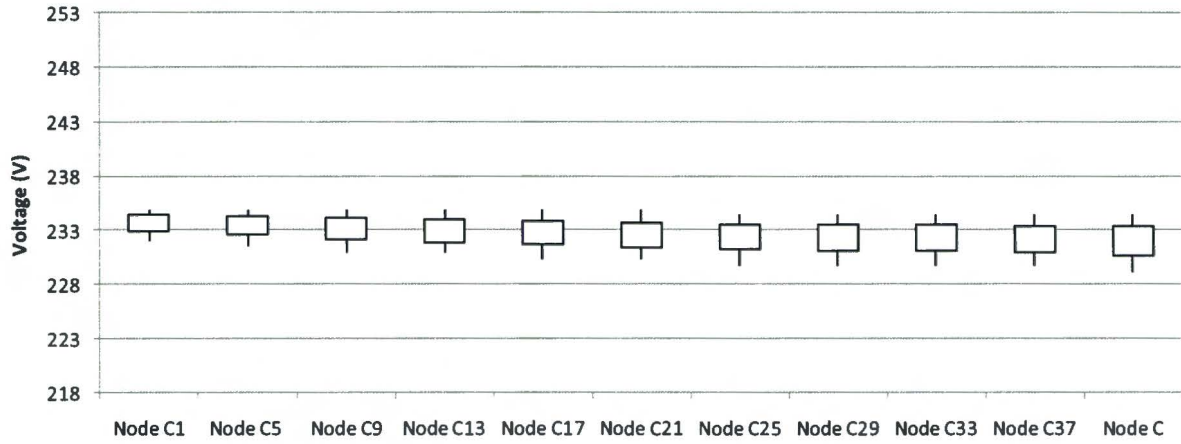


Figure 106: Voltage level along a cable during the April average scenario without distributed generation.

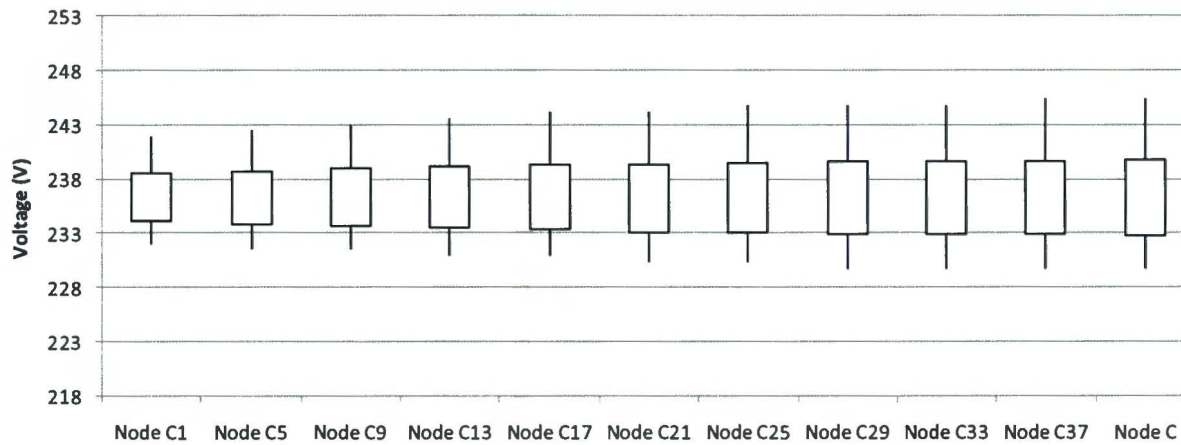


Figure 107: Voltage level along a cable during the April average scenario with distributed generation.

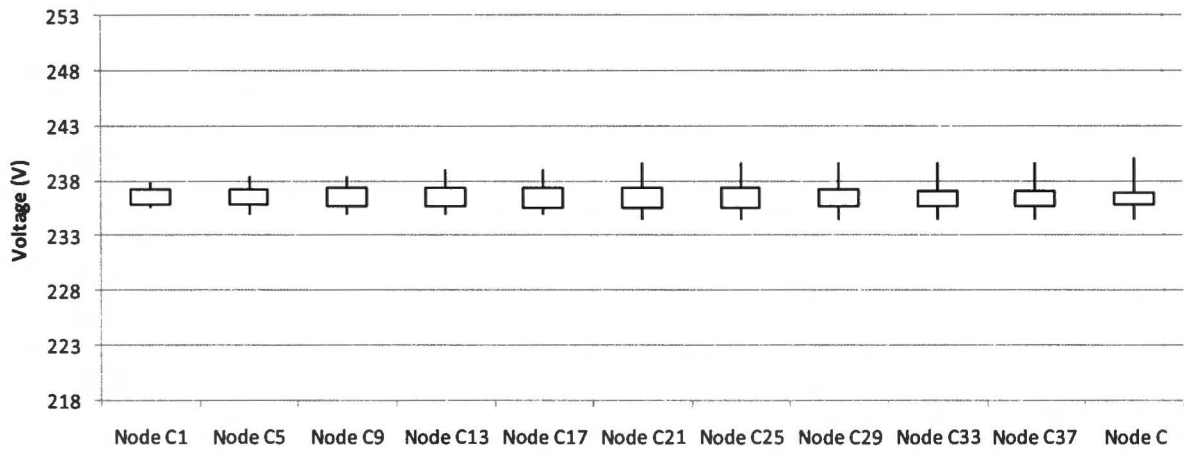


Figure 108: Voltage level along a cable during the April average scenario with battery energy storage.

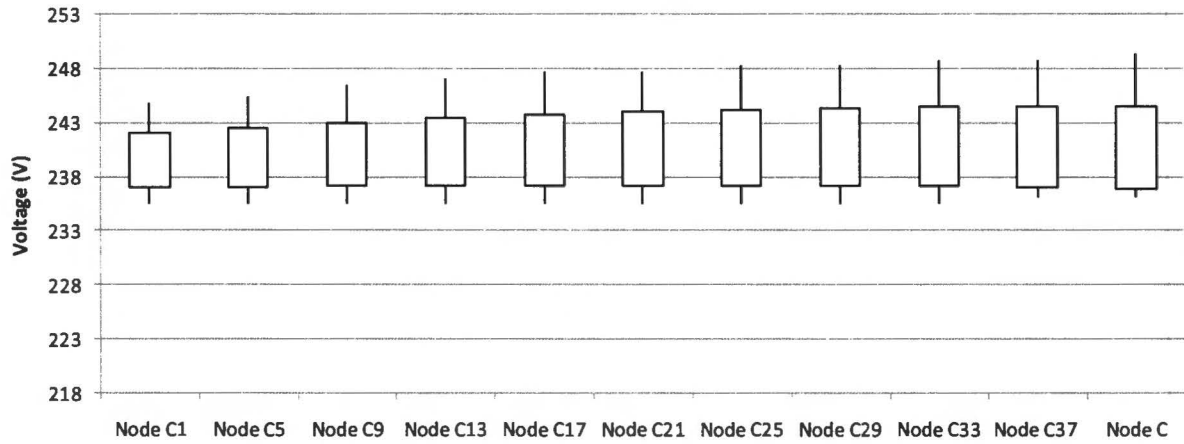


Figure 109: Voltage level along a cable during the April overload scenario with battery energy storage.